Degradation of physical-mechanical properties of materials under irradiation

O.V. Borodin, V.V. Bryk, A.S. Kalchenko, G.D. Tolstolutskaya, V.N. Voyevodin

Department of Radiation Damage and Material Science
National Science Center
"Kharkov Institute of Physics and Technology"

(voyev@kipt.kharkov.ua)

Metals do a lot of strange things when irradiated at elevated temperatures

New mechanisms of dimensional distortion occur as a result of the displacement of atoms, their subsequent migration and segregation, and interactions with transmutants.

- Lattice parameter changes arising from redistribution of solutes, especially by changes in precipitate phases.
- Transmutation induces additional complexity.
- Irradiation growth (volume conservative)
- Irradiation creep (volume conservative)
- Void swelling (non-conservative)
- Gas bubble swelling (non-conservative)

Ageing of RPV & RVI

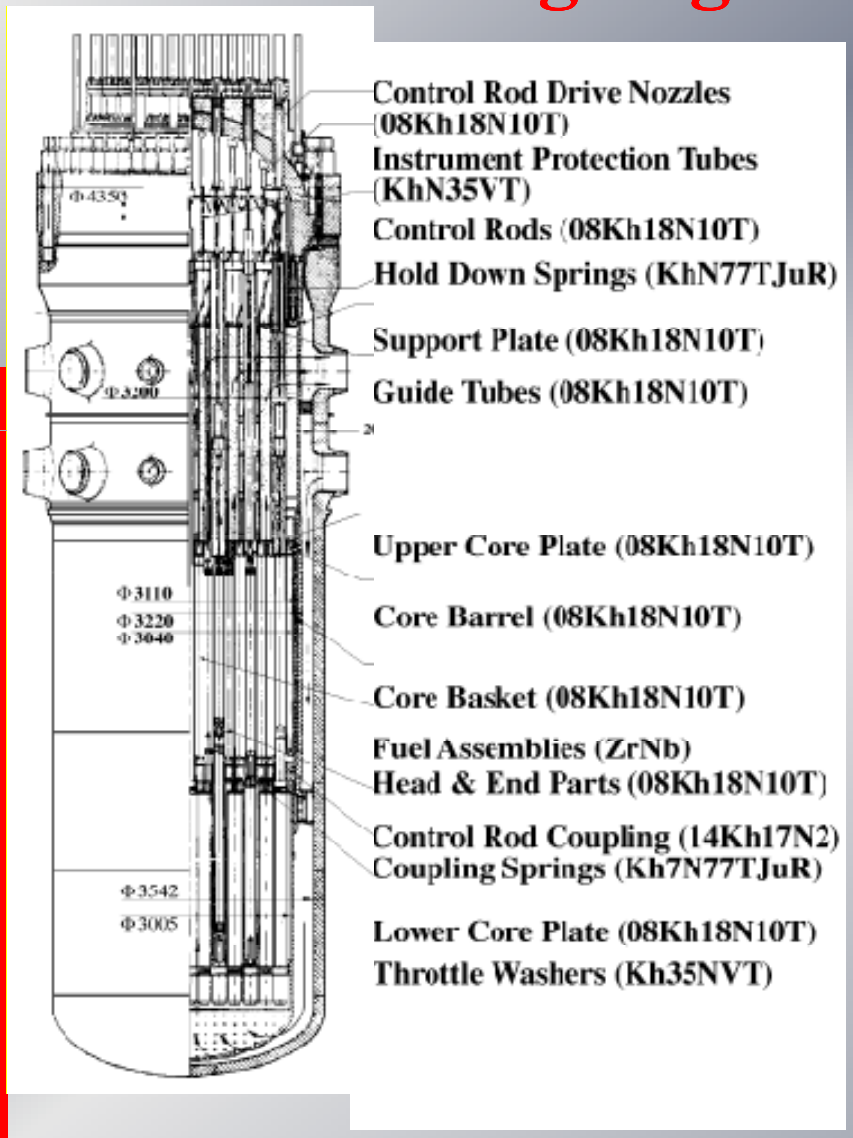

Irradiation hardening

Irradiation embrittlement

- loss of work hardening capability

Thermal embrittlement

Swelling

- incl. void induced embrittlement

Irradiation creep

- incl. creep-swelling interaction

Stress relaxation

- thermal
- radiation assisted

Fatigue (vibration or/and environment)

Corrosion: SCC & IASCC

Pitting, Wear

Synergisms

RADIATION DAMAGE IN RPV MATERIALS DEPENDS, IN PRINCIPLE, ON:

- MATERIAL CHARACTERISTICS
  – MATERIAL PRINCIPAL CHEMICAL COMPOSITION (CONTENT OF ALLOYING ELEMENTS – Cr,Mo, Ni,Mn) AND THUS ALSO ITS MICROSTRUCTURE
  – IMPURITIES CONTAINED IN MATERIAL – PHOSPHORUS, COPPER – MOST DETRIMENTAL, As, Sb, Sn–MINOR EFFEC
  – KILLING/DESOXYDIZING etc. ELEMENTS –Si, V
  – INITIAL MECHANICAL PROPERTIES –SLIGHT EFFECT
- NEUTRON FLUENCE and NEUTRON FLUX
- IRRADIATION TEMPERATURE
- STRESS CONDITIONS DURING IRRADIATION
  – NOT YET CONFIRMED

(M. Brumovský, 2008)

NEUTRON FLUENCE

OPERATING LIFETIME FLUENCE FOR WWERs, PWRs AND THE BWR

REACTOR TYPE	FLUX, $n.m^{-2}.sec^{-1}$ (E>1MeV)	LIFETIME* FLUENCE, $n.m^{-2}$ (E>1MeV)
WWER-440 core weld	1.2×10^{15}	1.1×10^{24}
WWER-440 maximum	1.5×10^{15}	1.6×10^{24}
WWER-1000	$3\text{-}4 \times 10^{14}$	3.7×10^{23}
PWR (W)	4×10^{14}	4×10^{23}
PWR (B&W)	1.2×10^{14}	1.2×10^{23}
BWR	4×10^{13}	4×10^{22}

MOSTLY MUCH HIGHER THAN IN PWR RPVsAS WWER RPVs MUST BE TRANSPORTABLE BY LAND (TRAIN, TRUCK)

10ChGNMAA Weld Irradiation Embrittlement Extended Analysis of Surveillance Results

- No significant role of P and Cu due to low contents P=0.005-0.010 wt%, Cu=0.03-0.08 wt%

- High Ni alone does not always explain different observed shifts (Ni>1.55 wt%)
- Mn level > 0.85 wt% seems to be a key factor

- Other elements could play a role: C, Si, S, etc

- *Mn and Ni are the elements to become non randomly distributed and co-segregated in welds with high Ni & low Cu.*

WWER-1000 RADIATION EMBRITTLEMENT

1. For WWER-1000 welds RE depends on Ni, Mn and Si contents.
2. New models for WWER-1000 steels should be specified.
3. Since RE of WWER-1000 welds is much higher, than for base metal, it can be supposed that the lifetime of VVER-1000 RPV is defined by radiation embrittlement of the core welds.
4. Final solution could be given only from testing specimens from Modified Surveillance Programmes with specimens located near RPV wall in beltline region.

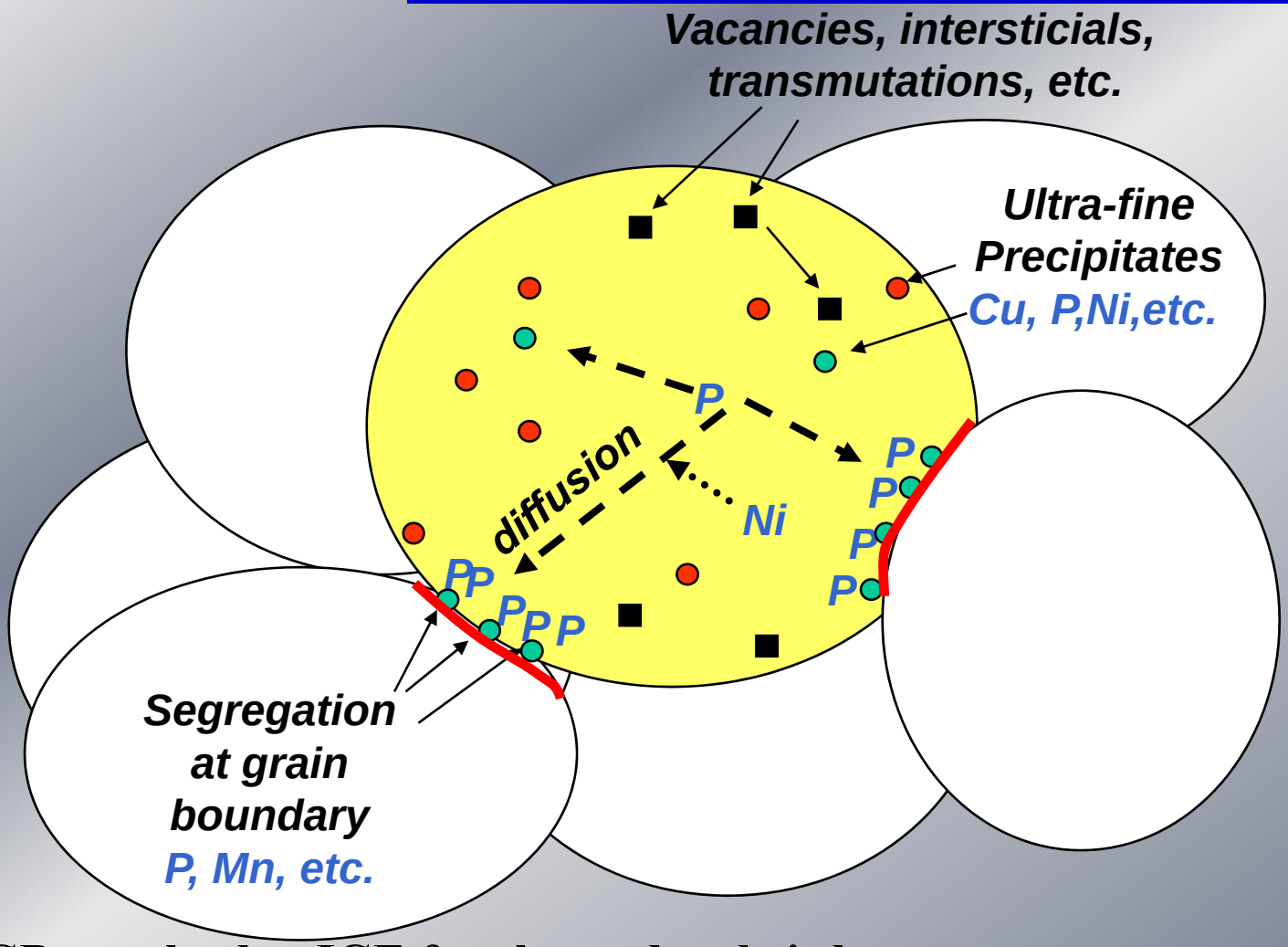

- P to GB may lead to IGF & enhanced embrittlement
- Need to predict P segregation under irradiation
- Need of reliable indicator for non-hardening embrittlement
- Reduce uncertainties on RPV properties (EOL)

(L. Debarberis, 2007)

Late blooming phases ?

Representative U.B. fluences of EU LWRs, specific issues, e.g.:

- **Late Blooming Phases** (high Ni/Mn, Mn, Mn-Si, Cr stability, etc.)
- **Dose Rate effects/Use of accelerated data – Irr. temperature/conditions**
- **Understanding for 60 y extension!**
- **Annealing** efficiency and effectiveness **- New RPVs**

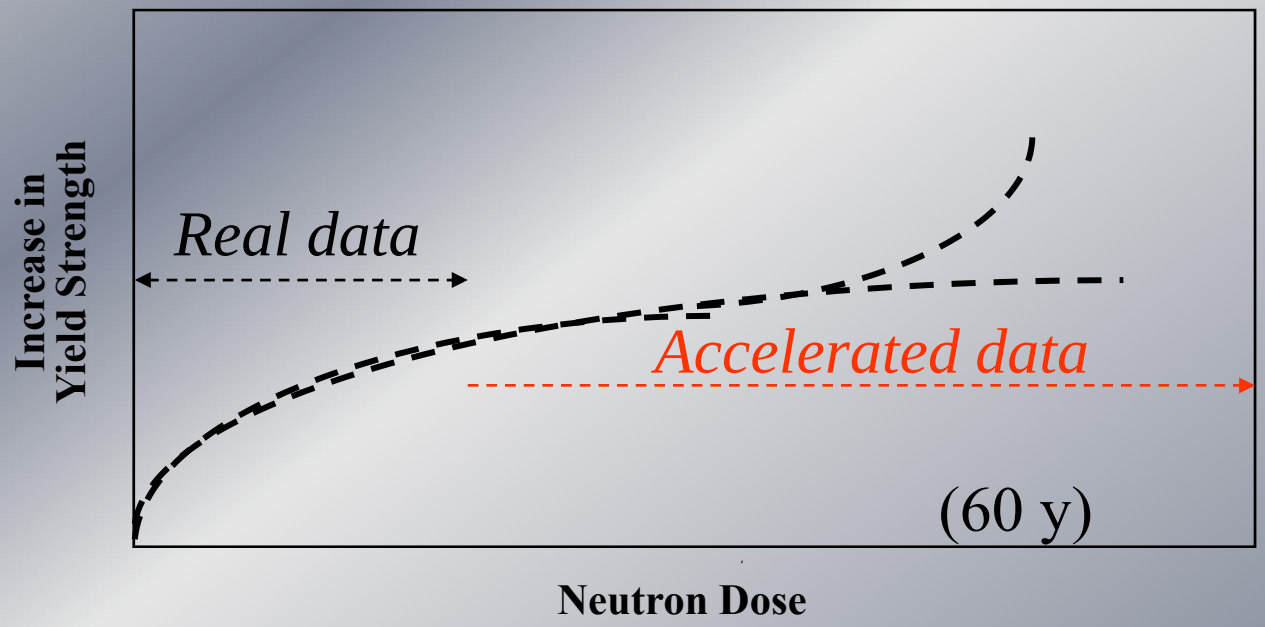

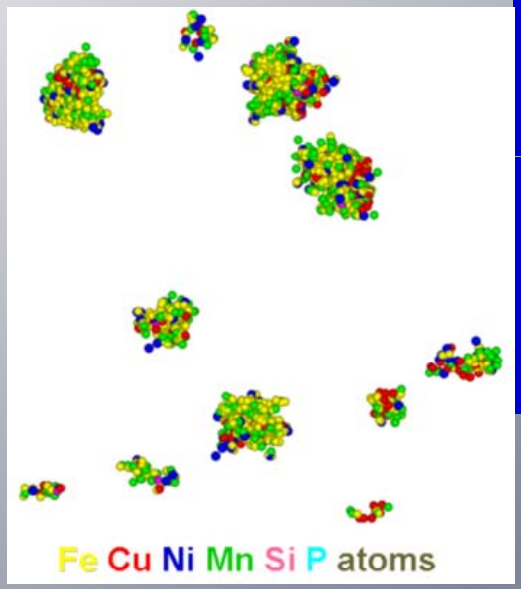

JRC's Model Steels & Realistic Welds

- "Possibility that a significantly detrimental Mn-Ni-Si phase can form, even in low Cu/P materials, at high dose/irradiation time" (Ref. Odette)

Dependence of radiating hardening of specimen-surveillance irradiated fluence of fast neutrons of $1 \cdot 10^{20}$ cm^{-2} at T=270 °C from content of phosphorus in steel (Yu. Nikolayev, 2001)

Material	impurity content, %		R_P 0,2, MPa
	P	Cu	
Base metal (steel 15X2MΦA)	0,006 0,011 0,012	0,01 0,09 0,11	120 160 165
weld metal	0,010 0,023	0,03 0,03	130 170

WWER-1000 Radiation embritlement)
(Y.Schtrombach.2004)

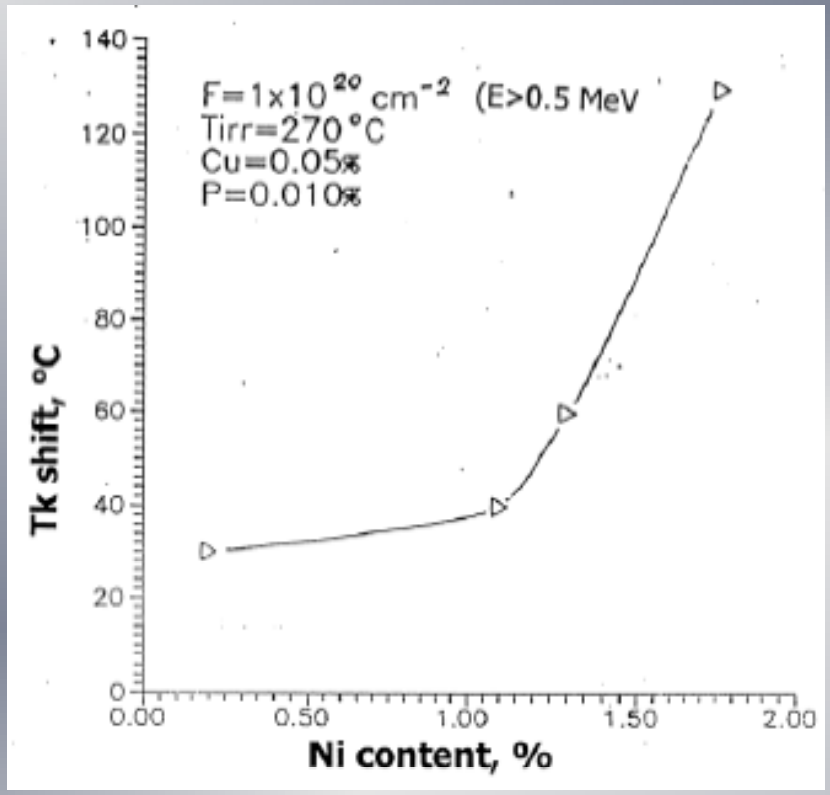

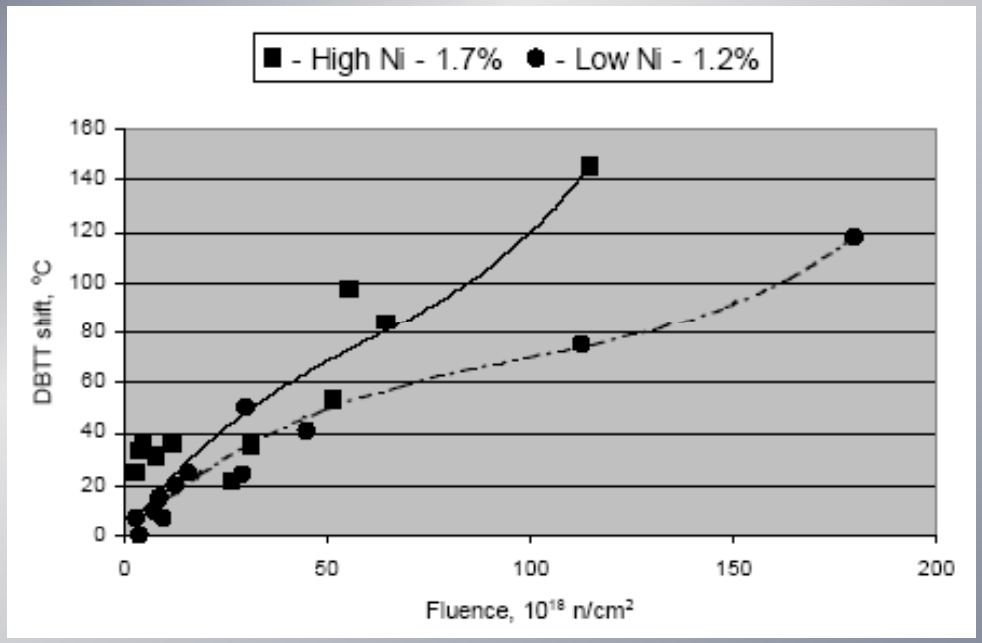

1986 T_k dependence on Nickel content

Radiation embrittlement of WWER-1000 welds with different Ni content

Microstructure of 15Kh2MΦA steel (Cr^{3+}, E=1.8MeV, T= 400°C, D=0.2 dpa)

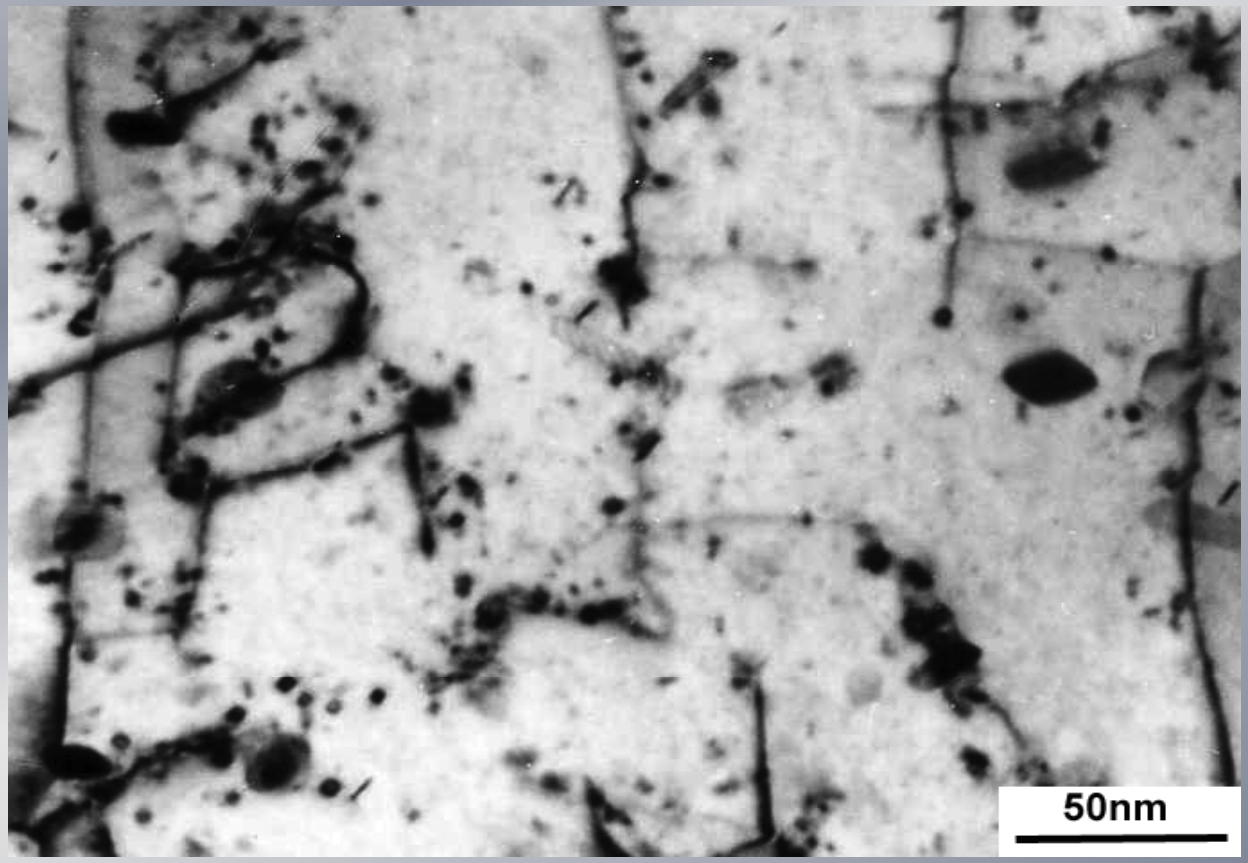

Average loops diameter 6nm, number density $20*10^{21}$ m^{-3}

Parameters of dislocation loops of 15Kh2MΦA steel (Cr^{3+}, E=1.8MeV, T= 400°C)

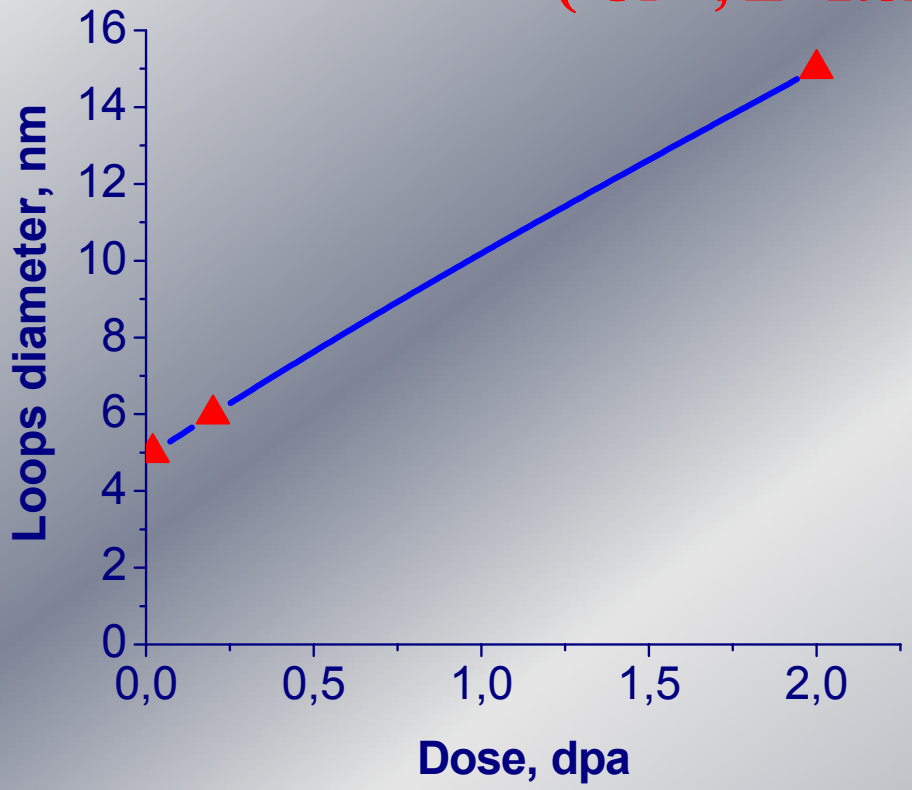

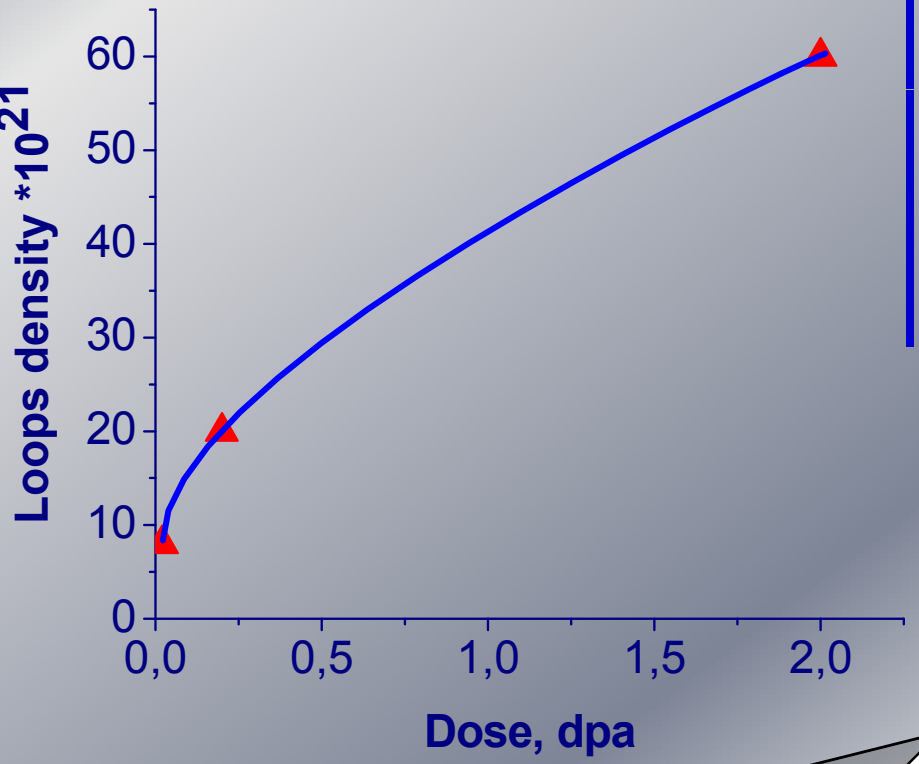

Strengthening mechanism of 15Kh2MΦA steel

Value of variation of yield strength Δσ at the expense of dislocation loops was determined by following formula:

$$\Delta\sigma = \alpha\mu b(Nd)^{1/2}$$

where α-parameter characterizing interaction of moving dislocation with dislocation loops (α ≈0,7);
μ – modulus of elasticity equal to 80 for steel 15Kh2MFA;
b-Burgers vector (a<100>,
N – density of dislocation loops

At experimentally measured values of density and dimension of dislocation loops equal to $3.10^{15}cm^{-3}$ and 21.4 nm respectively the increment of yield strength is 128 MPa.

Strengthening by Irradiation CHR vs. JMTR

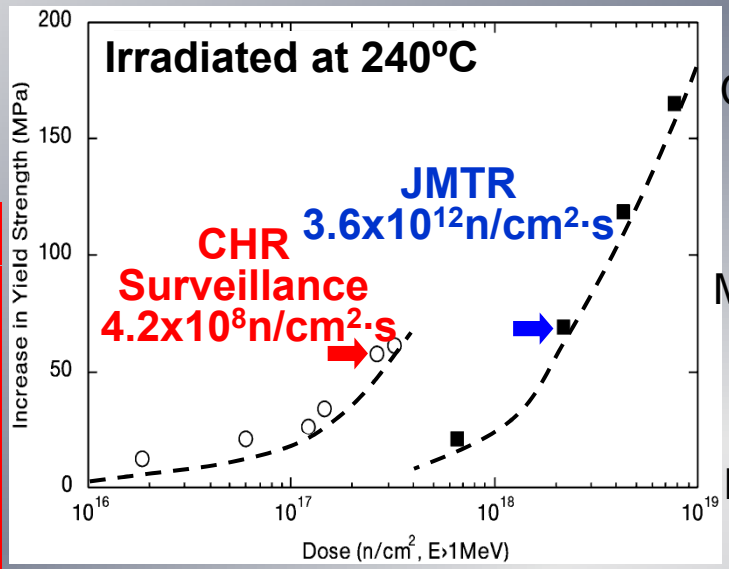

3D-AP Mapping : As-irrad

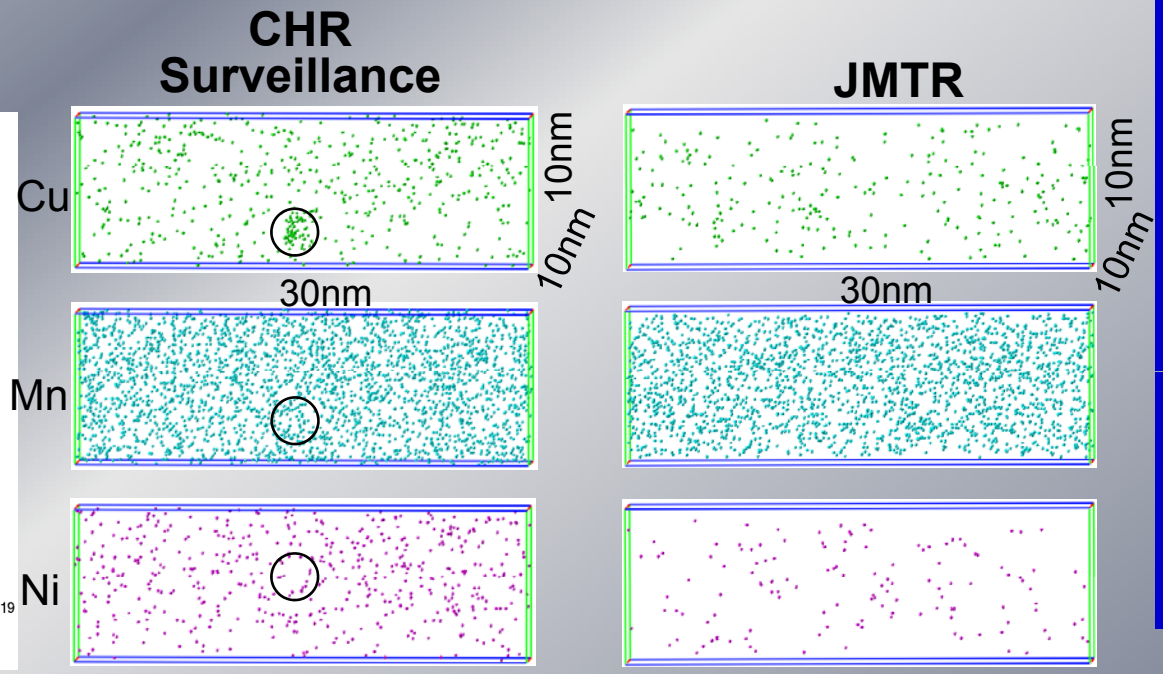

CHR – Calder Hall-Type Reactor

Marked Flux Effects

Low flux irradiation in CHR :
Strengthening is caused by enhanced Cu precipitation at very low doses.

High flux irradiation in JMTR :
Almost the same strengthening is due to matrix defects but not to Cu precipitates. (M. Hasegawa, 2005)

Three main micromechanisms of radiation embrittlement in in pressure vessel steels

Damage of matrix because of radiation-produced clusters of point defects and dislocation loops

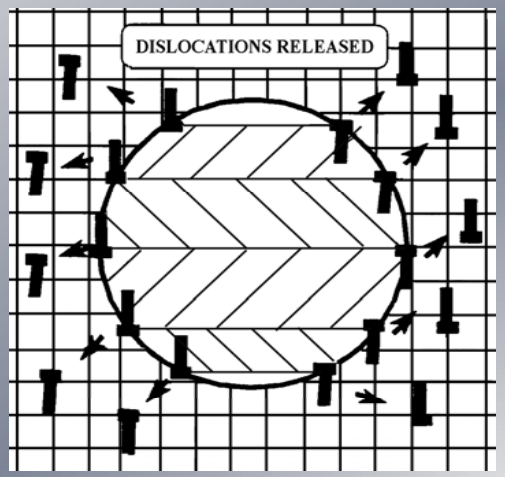

R = 40 Å

Misfits and dislocations of the lattice Di

Semi coherent precipitation
9R (R3m) twinning

Irradiation accelerates the formation of clusters enriched by copper

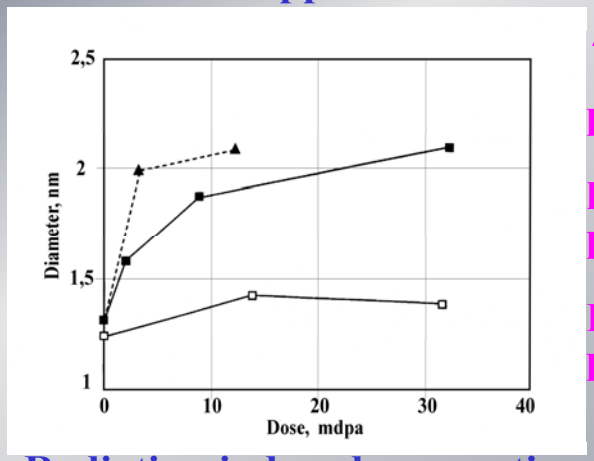

▲ -High content of Cu:
-mean rate of damage production
- High content of Cu: high rate of damage production.
-Low content of Cu: High rate of damage production

Radiation-induced segregation on grain boundaries of embrittling elements such as P.

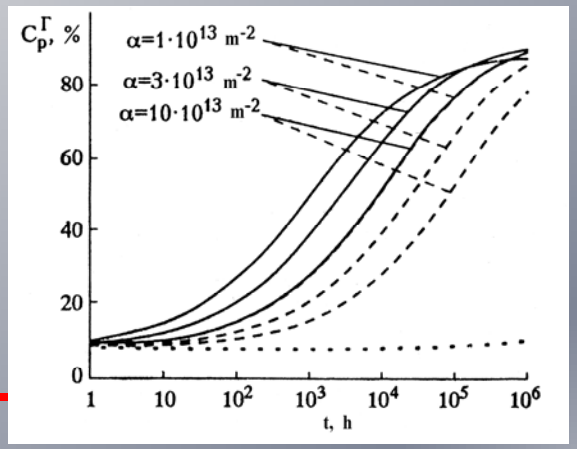

Irradiation grows of Zr alloys at 290-350^{O}C as a function neutron fluence and damage dose

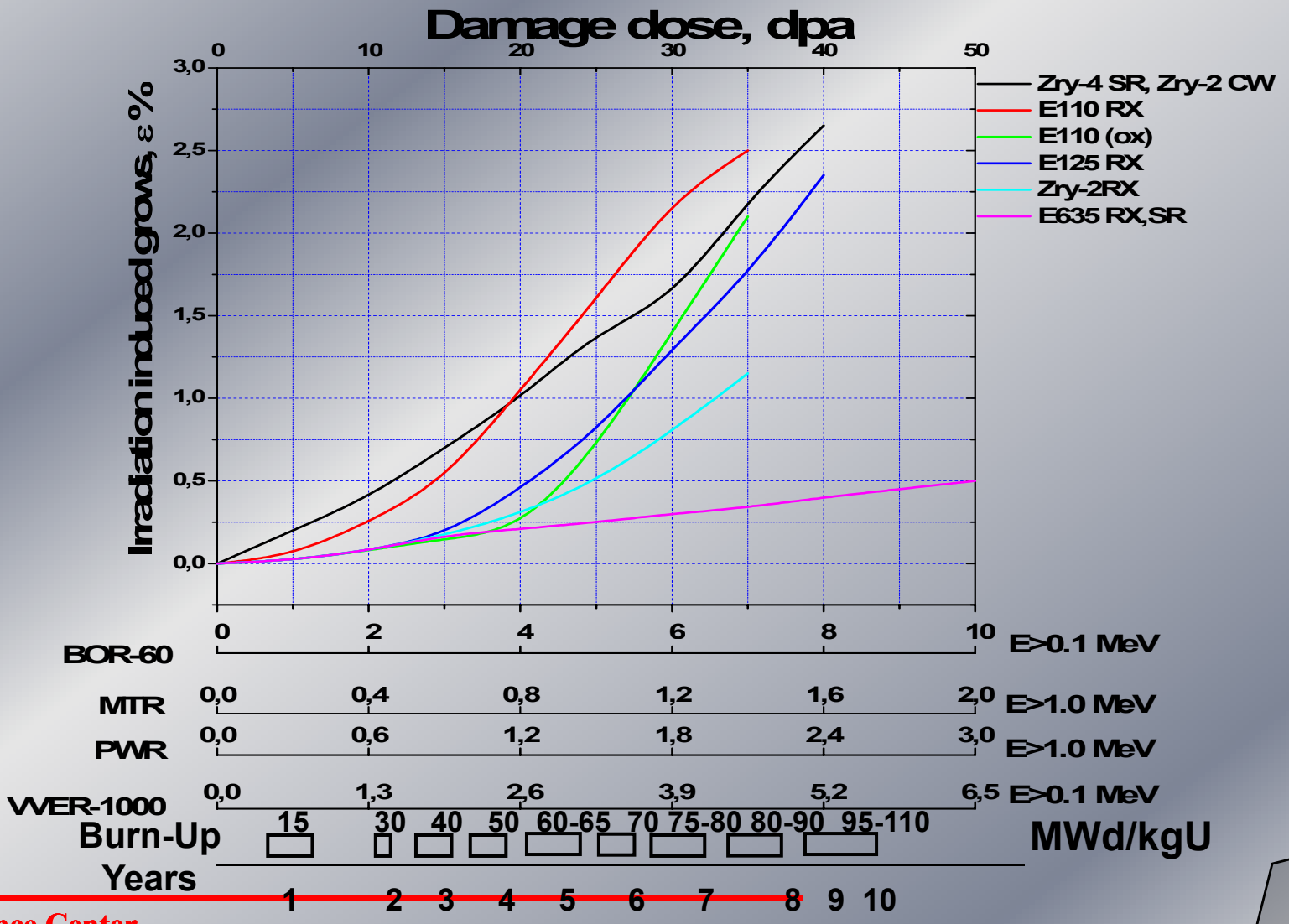

Dose dependence of the <c> -component of dislocation loops density and irradiation growth

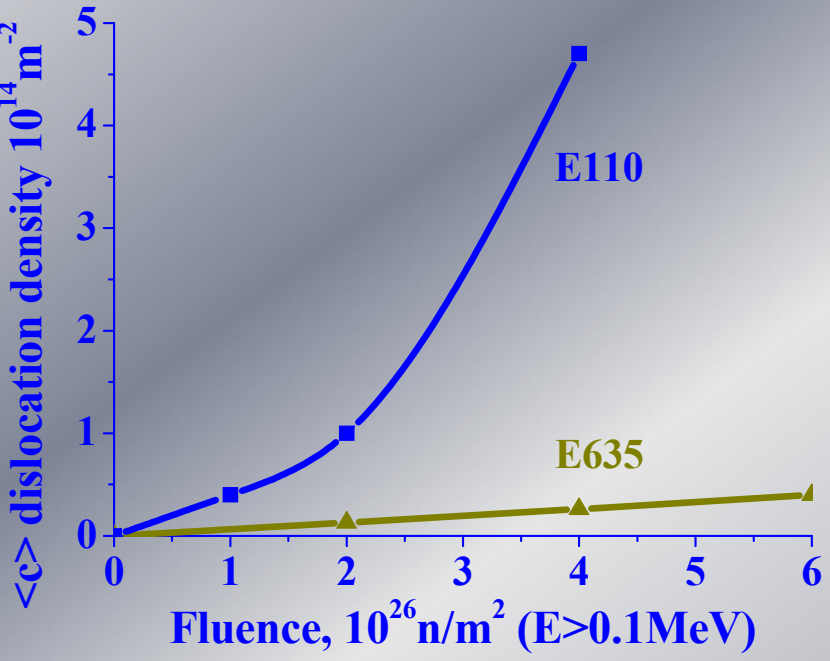

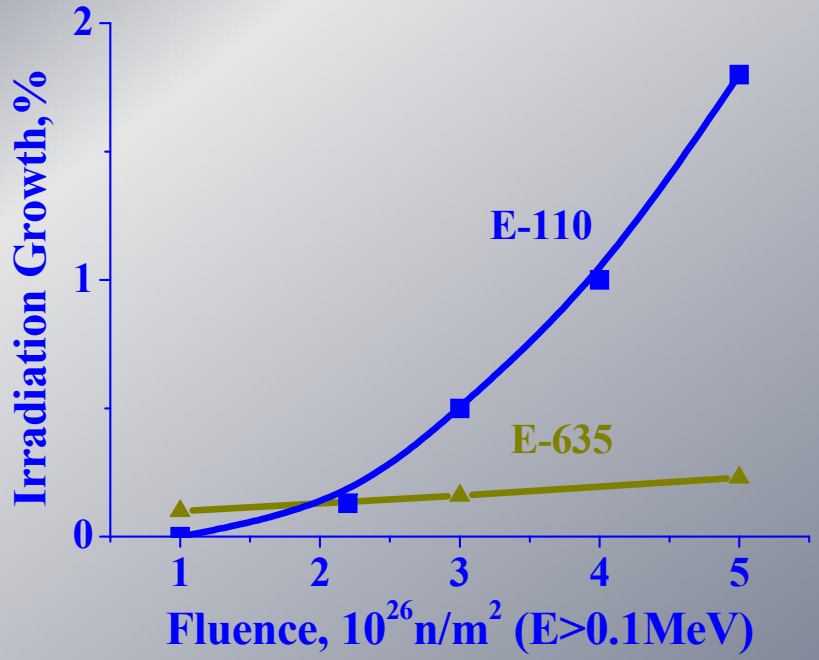

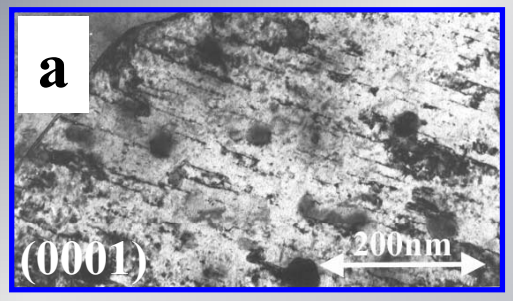

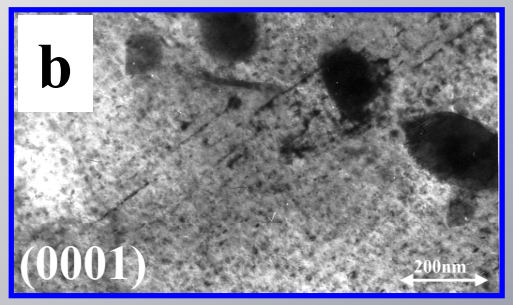

Dislocation structure c-type in E-110 (a) and E-635 (b), D=30 dpa, T=300°C (BOR-60)

Microstructure of E635 alloy (irradiation at T=300^{0}C, to D≈25 dpa, BOR-60)

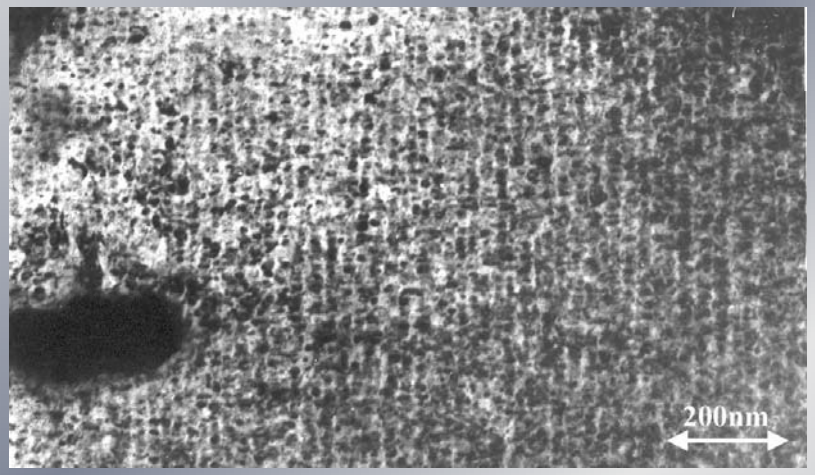

Alignment of dislocation loops <a> -type,

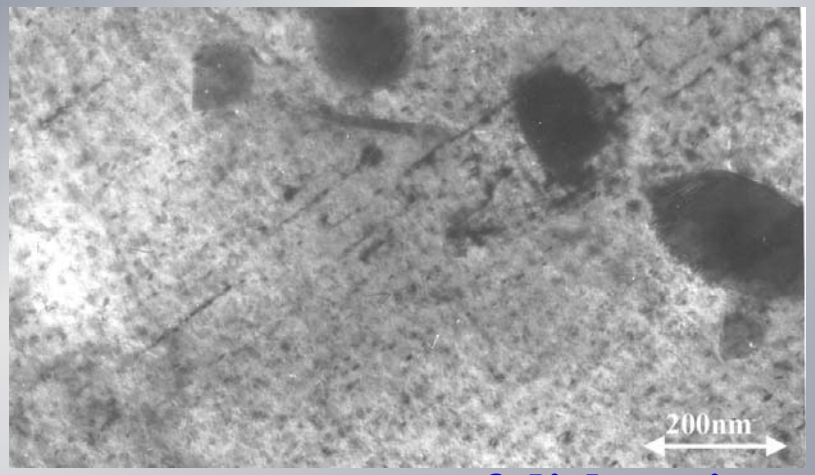

<c> -component of dislocation structure

Average size of dislocation loops <a> -type ~ 12 nm, and concentration $6*10^{15}cm^{-3}$. Alignment of dislocation loops in the plane {0001} are observed. Concentration of <c> -component of dislocation loops is about ~ $6*10^{14}cm^{-3}$. In the E635 alloy take place phase transition $(Zr,Nb)_3Fe \rightarrow \beta$-Zr

Variables that affect swelling

- Major and minor element composition
- Transmutation-induced changes in composition
- Often minor details in heat treatment
- Cold-working or warm-working
- Temperature and temperature history
- Atomic displacement rate
- Total number of displacements
- Helium and hydrogen generation and retention
- Internal or externally applied stresses
- Constraints associated with interacting components
- Gradients in temperature and displacement rate leading to gradients in stress
- Swelling and creep interactions

Main relations in structure and composition of SS under irradiation

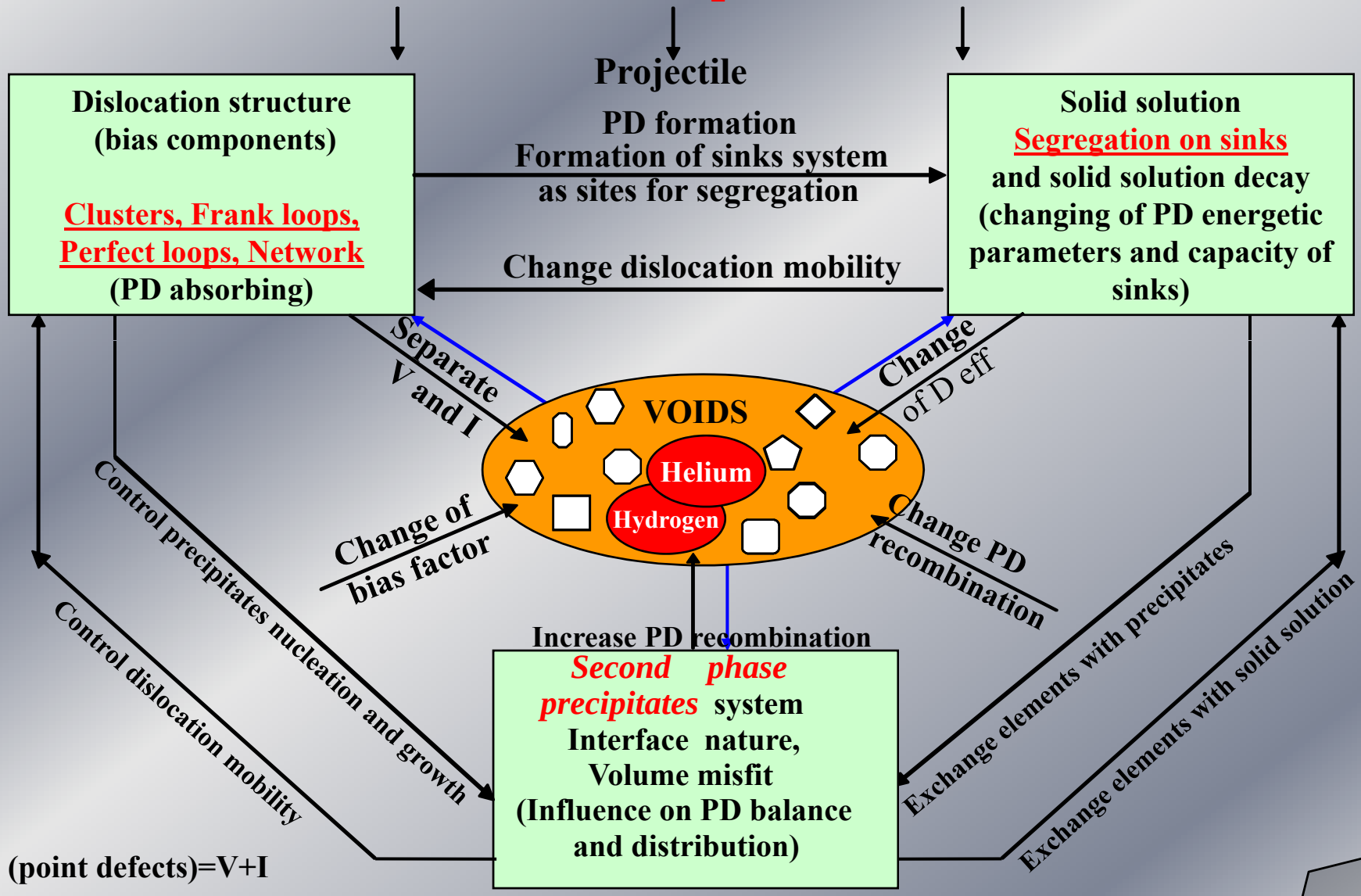

Void swelling is a universal irradiation phenomenon

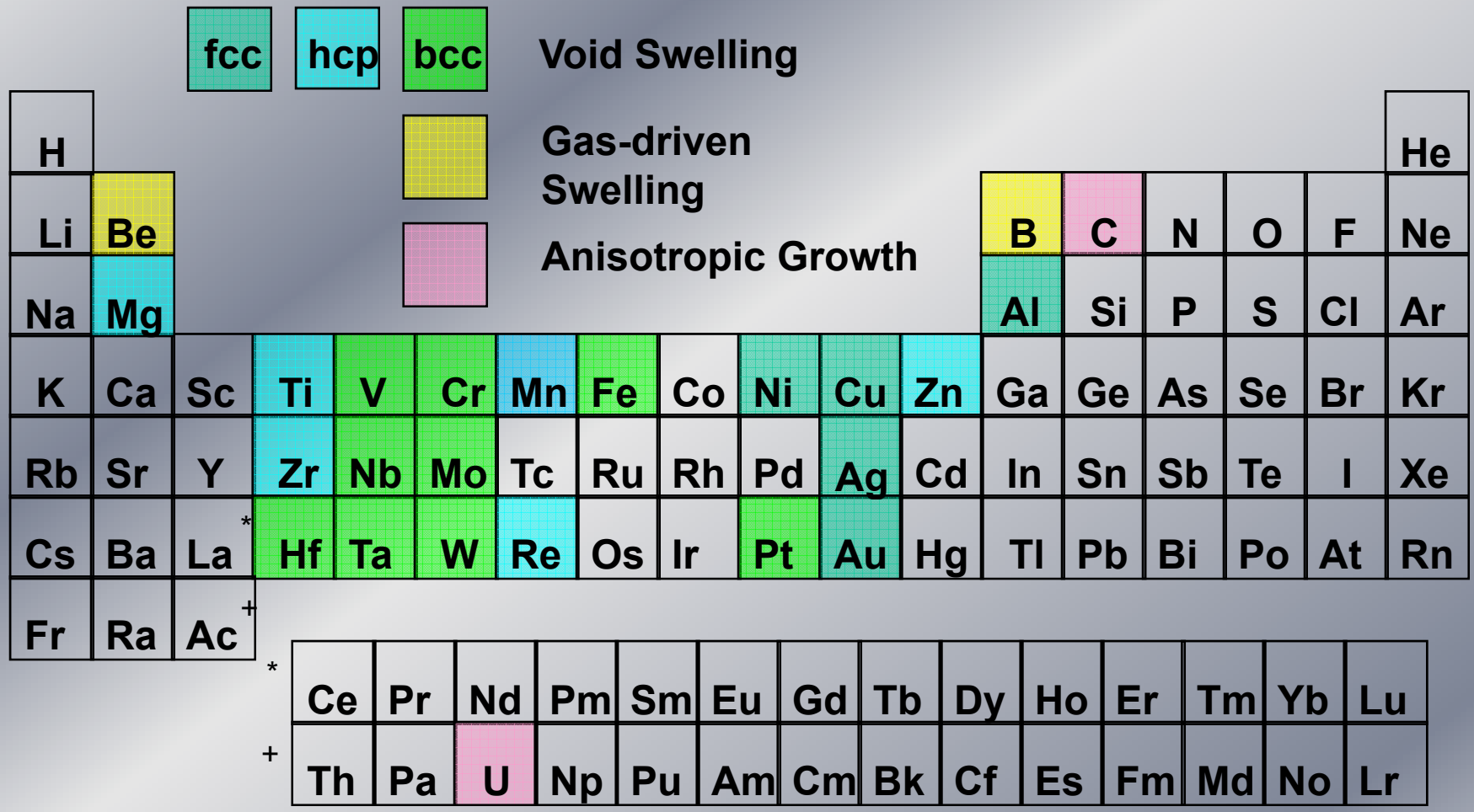

Example of embrittlement arising from void swelling in AISI 321* in BOR-60

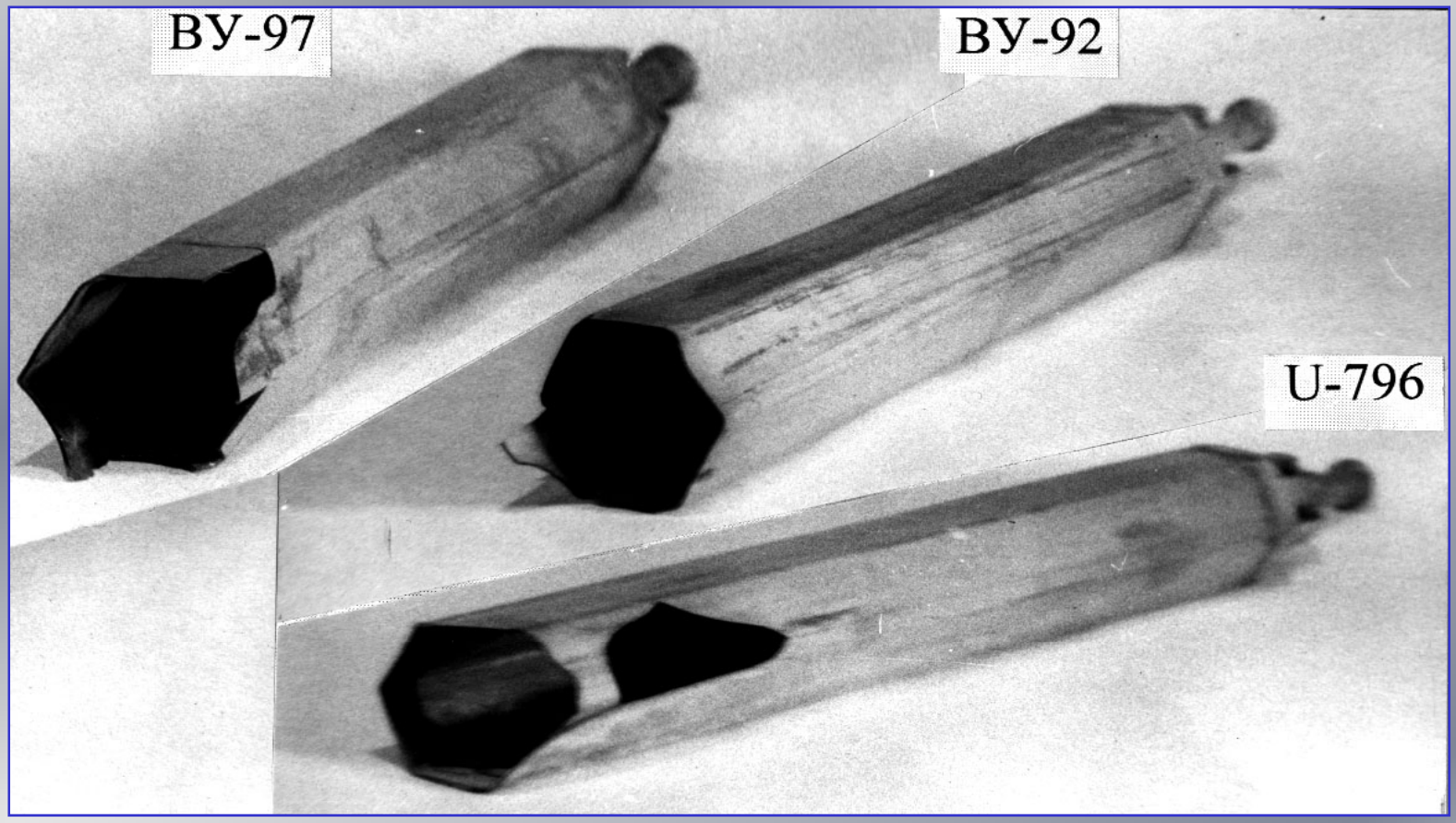

All broken during refueling operations

Examples of swelling and irradiation creep to produce distortion of reactor components at ~75 dpa

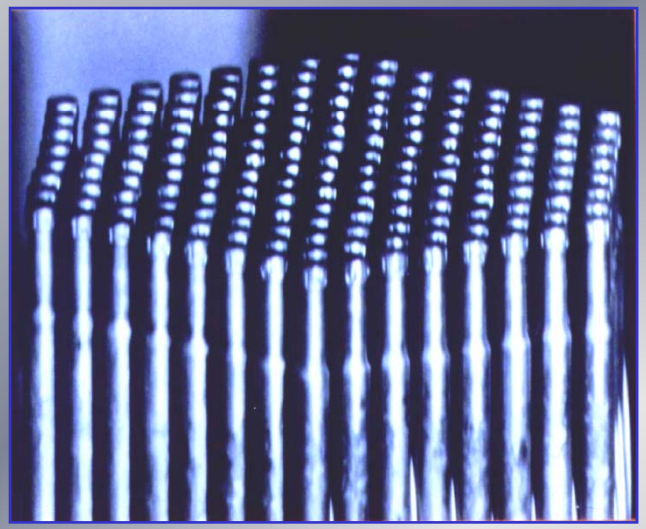

HT9 - no swelling

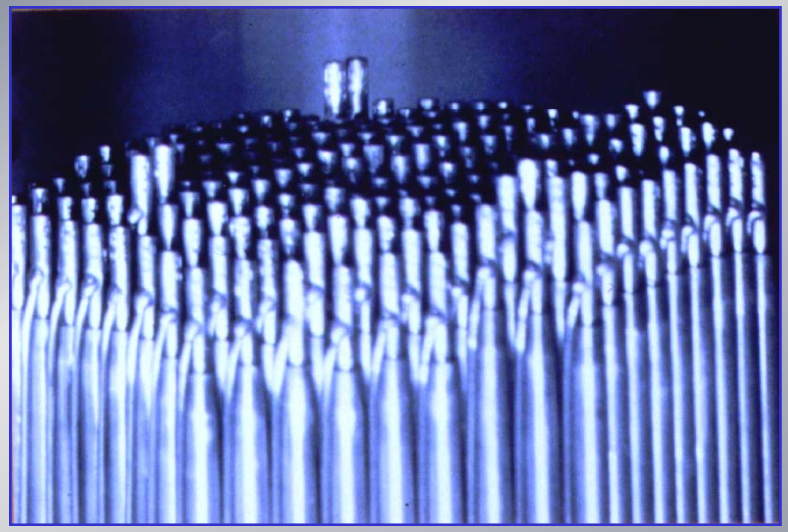

Stainless steel - swelling

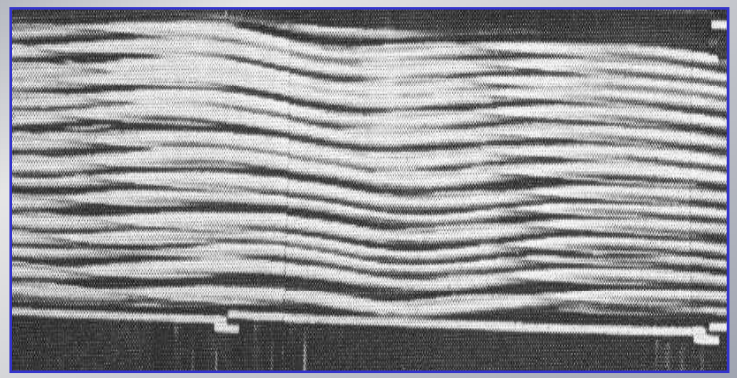

Swelling-creep interaction with wire wrap to produce spiral pins in FFTF, but without direct failures.

Consequence of wire swelling more than cladding

Chuev, Lanskykh, Ogorodov, Sheikmann, Sergeev, 2004

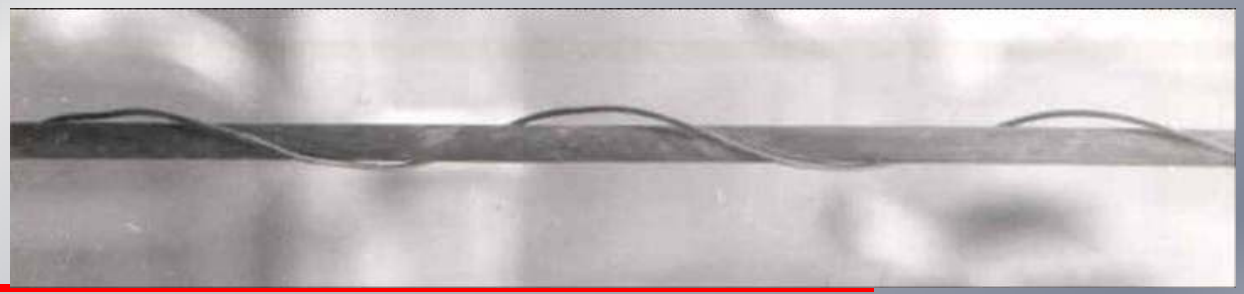

Swelling of cladding and wrapper along active zone

● - data of TEM investigation

○ - data of diameter measurement

| | - data of density change

18Cr-10Ni-Ti: S=32%, D = 66 dpa, T_{max}=480°C

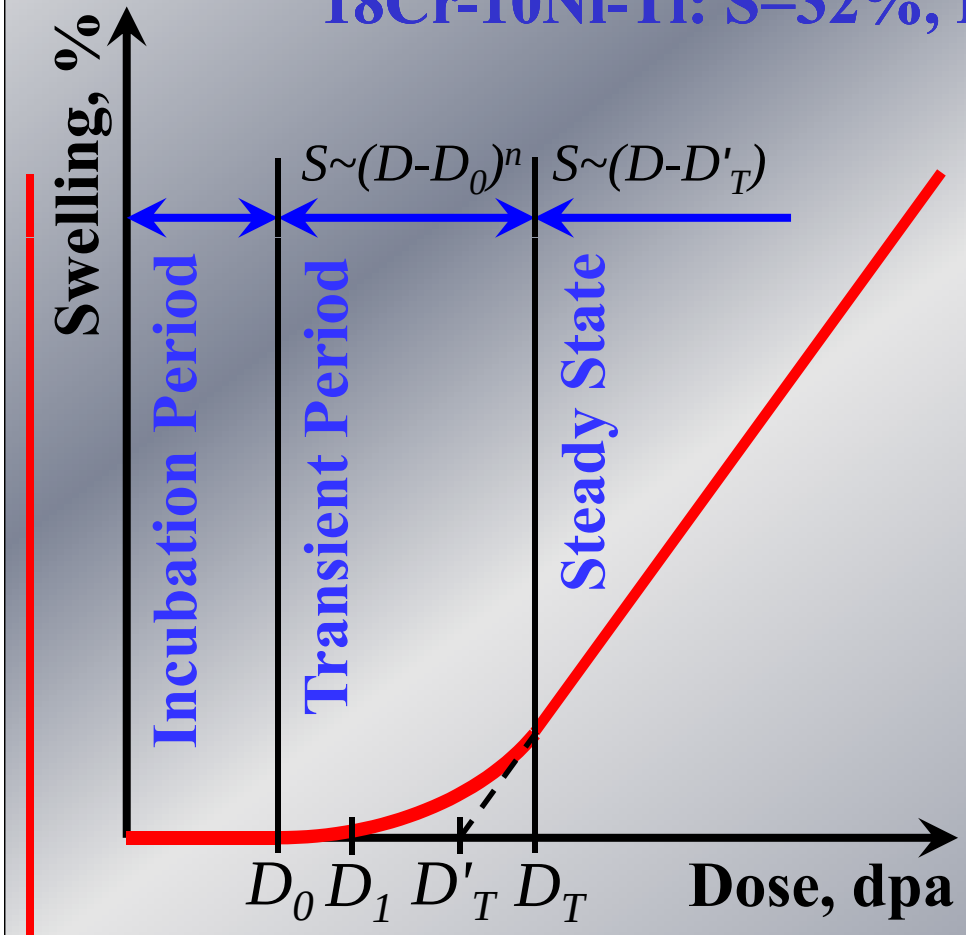

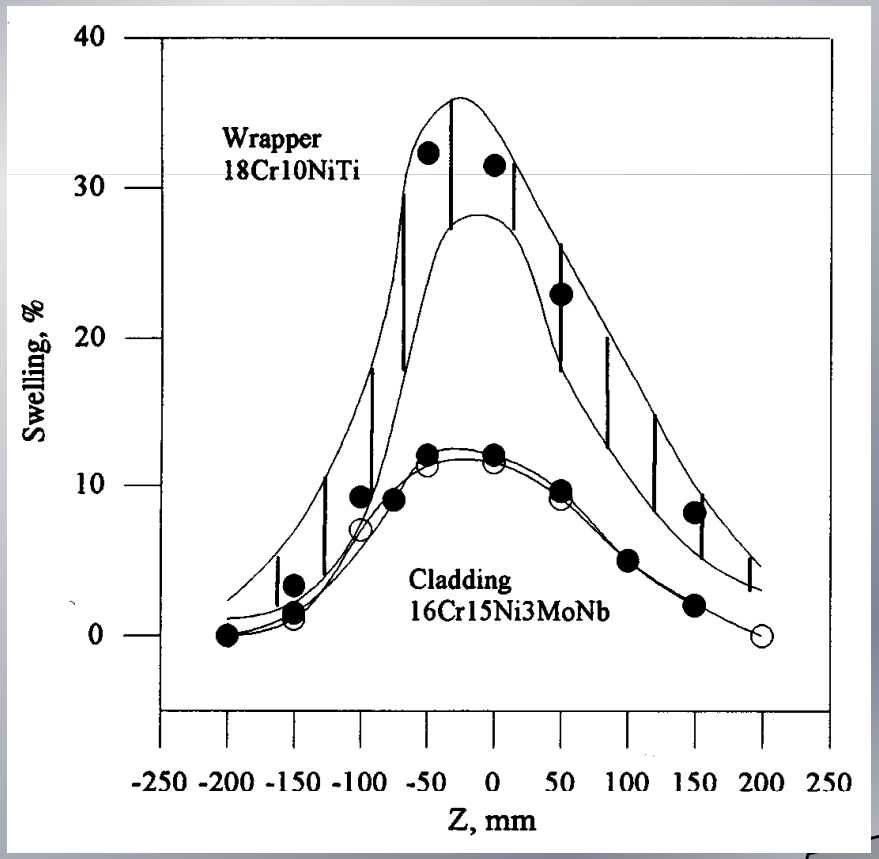

Microstructures devevoped in 20%CW 316 stainless steel and HT9 after side-by-side irradiation in EBR-II at 535^{O}C to 14×10^{22} n·cm-2 (E>0.1 MeV), showing ≈13% and 0% swelling respectively.

(D. Gelles, 1999)

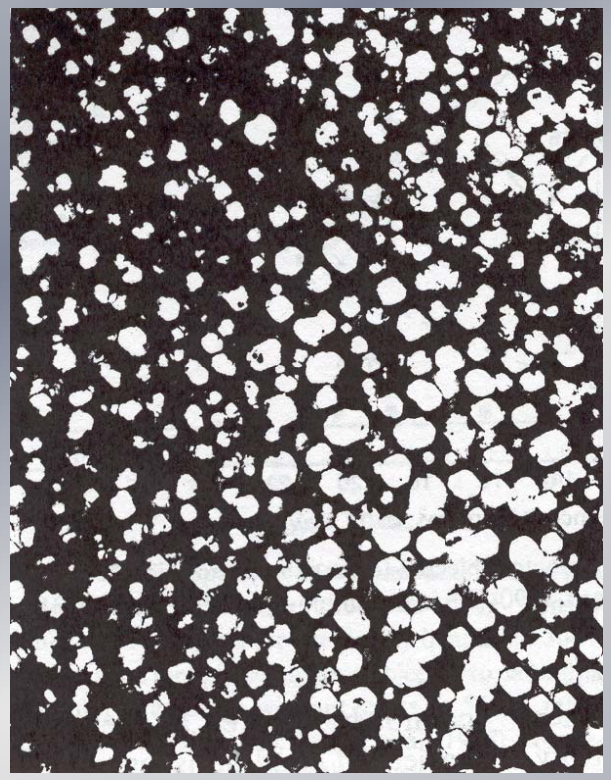

Swelling of Fe-Cr binary alloys and F/M steels in EBR-II and FFTF at 420-450°C (Garner, Romaneev, 1998)

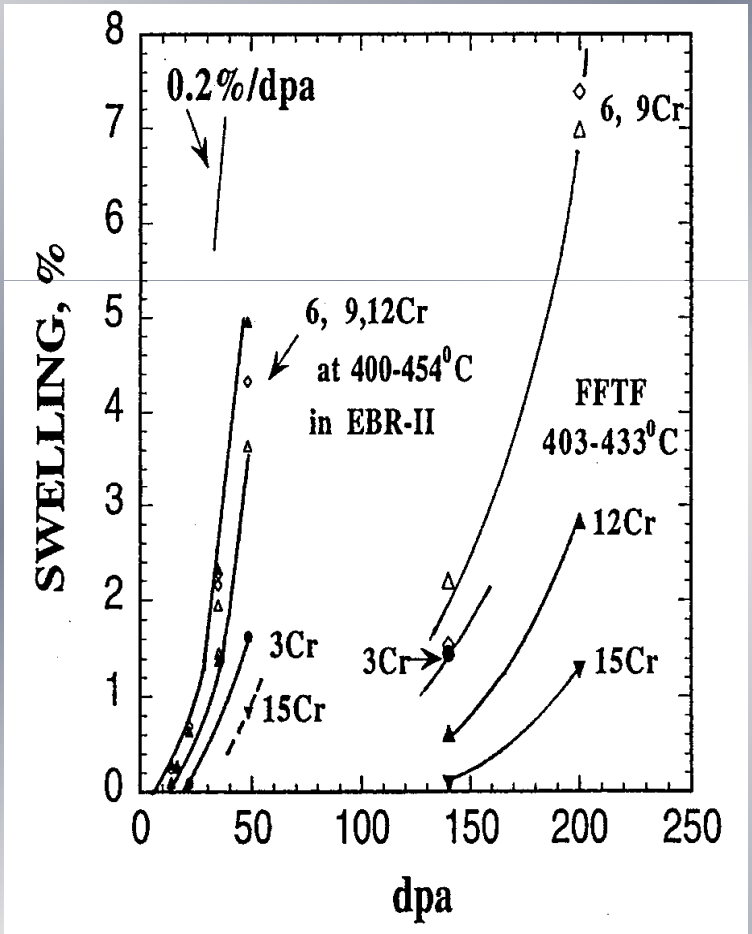

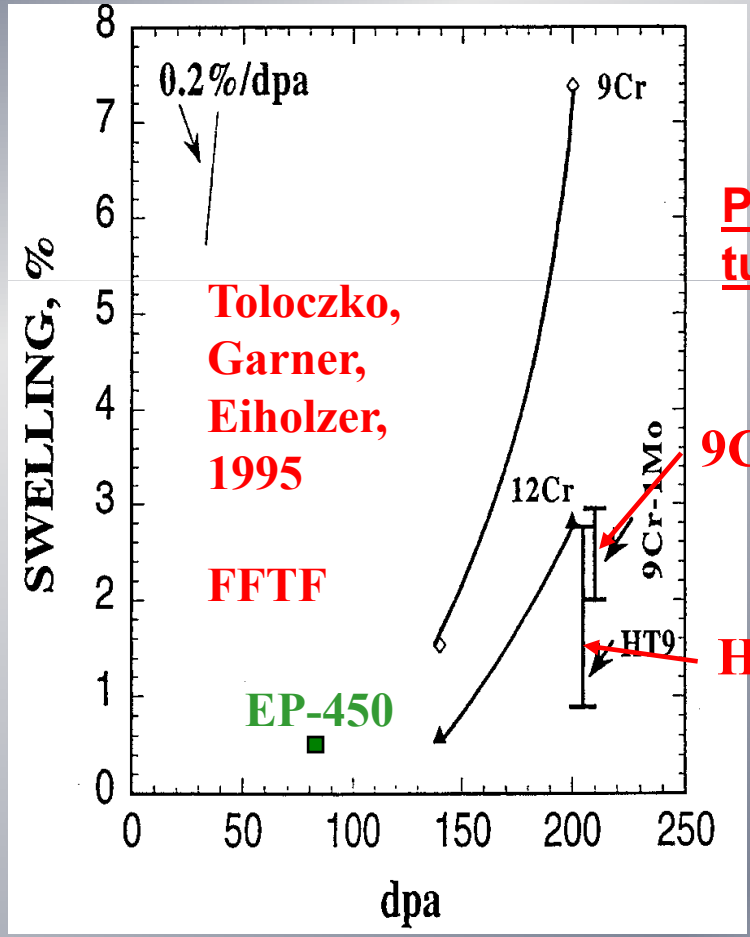

Pressurized tubes

9Cr-1Mo

HT9

Influence of helium generation rate to accelerate swelling of ferritic-martensitic steels (F. Garner, 1997)

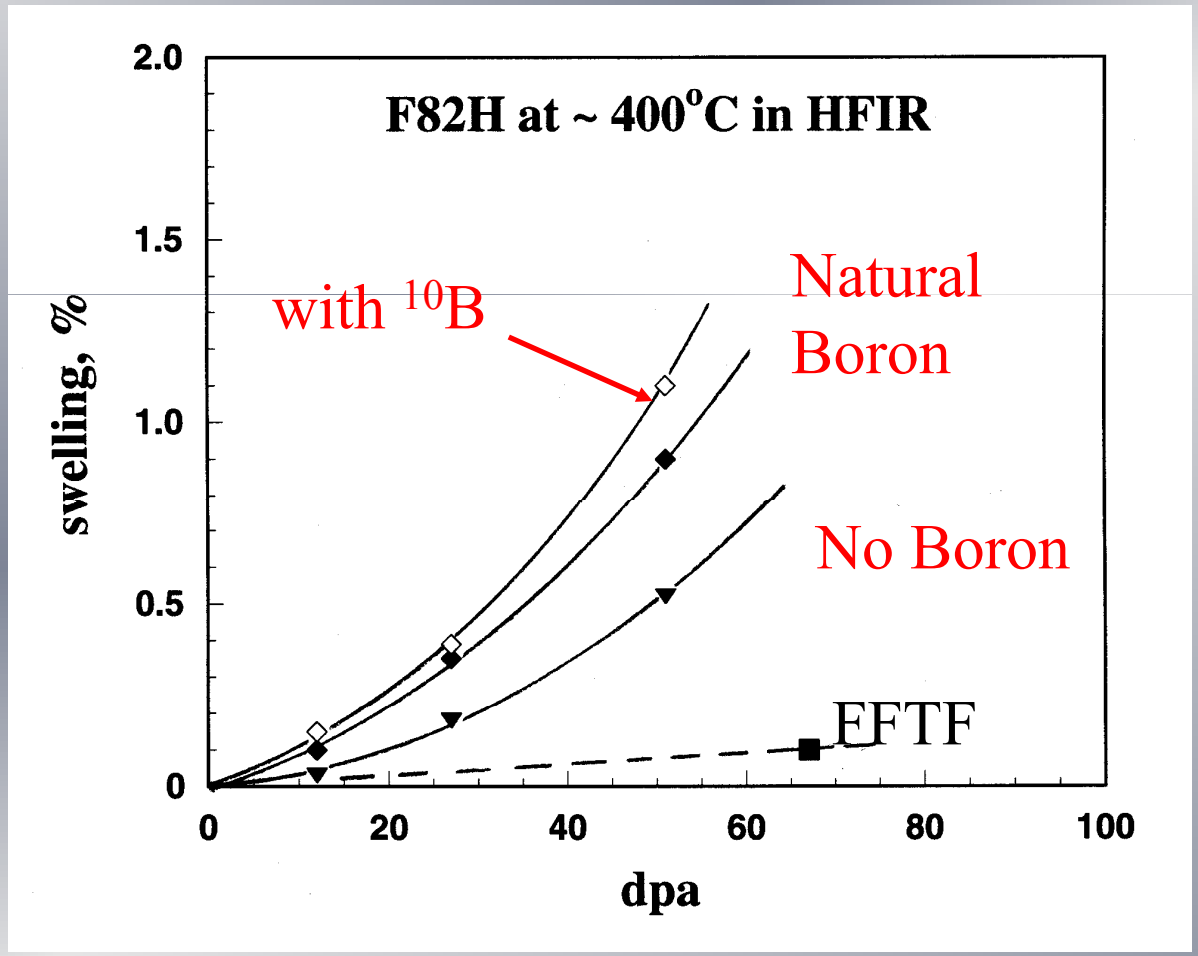

Compilation of data from Morimura, Miwa and Wakai

FFTF operated at higher dpa rates and lower gas generation rates compared to HFIR.

Normalized temperatures of swelling dependence of BCC materials and austenitic stainless steel (FCC): 1 – Cr alloy, 2 – ferritic steel with 13% of Cr; 3 – Nb; 4 – V; 5 – EI – 847.

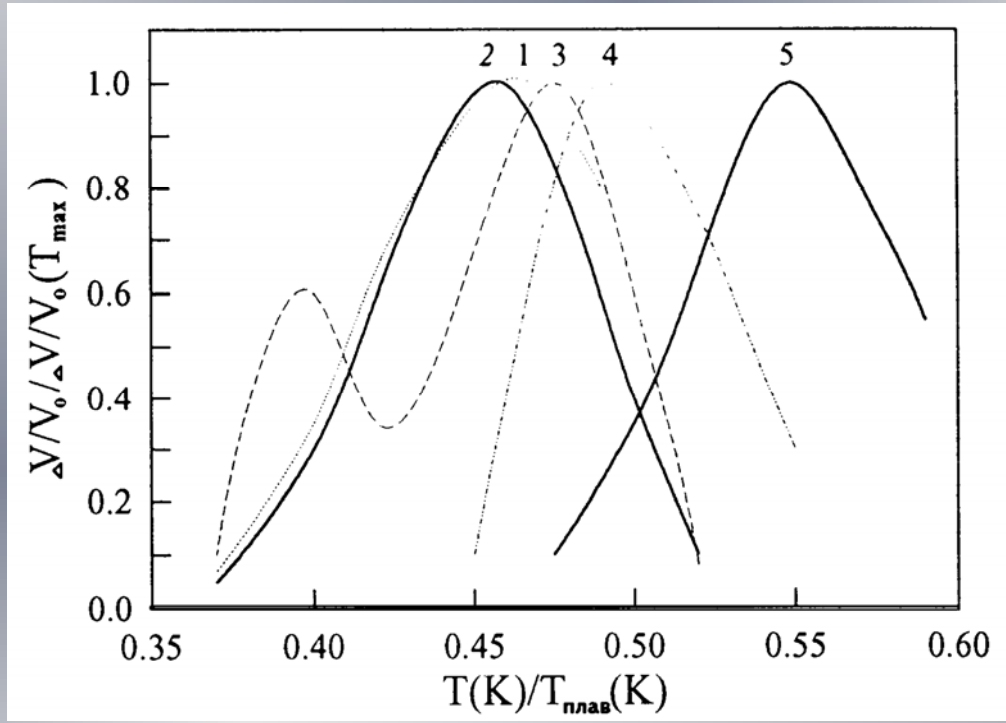

As it is seen from summarized data of temperature and dose dependencies of investigated materials swelling and from data of other authors the main characteristic properties of materials with FCC and BCC-lattice are:

-different temperature ranges of maximum swelling;

-for BCC-metals the process of void nucleation starts at lower temperatures;

-doses for start of void nucleation for BCC-metals are lower in comparison with materials with FCC-lattice.

Swelling dependence versus nickel concentration in matrix

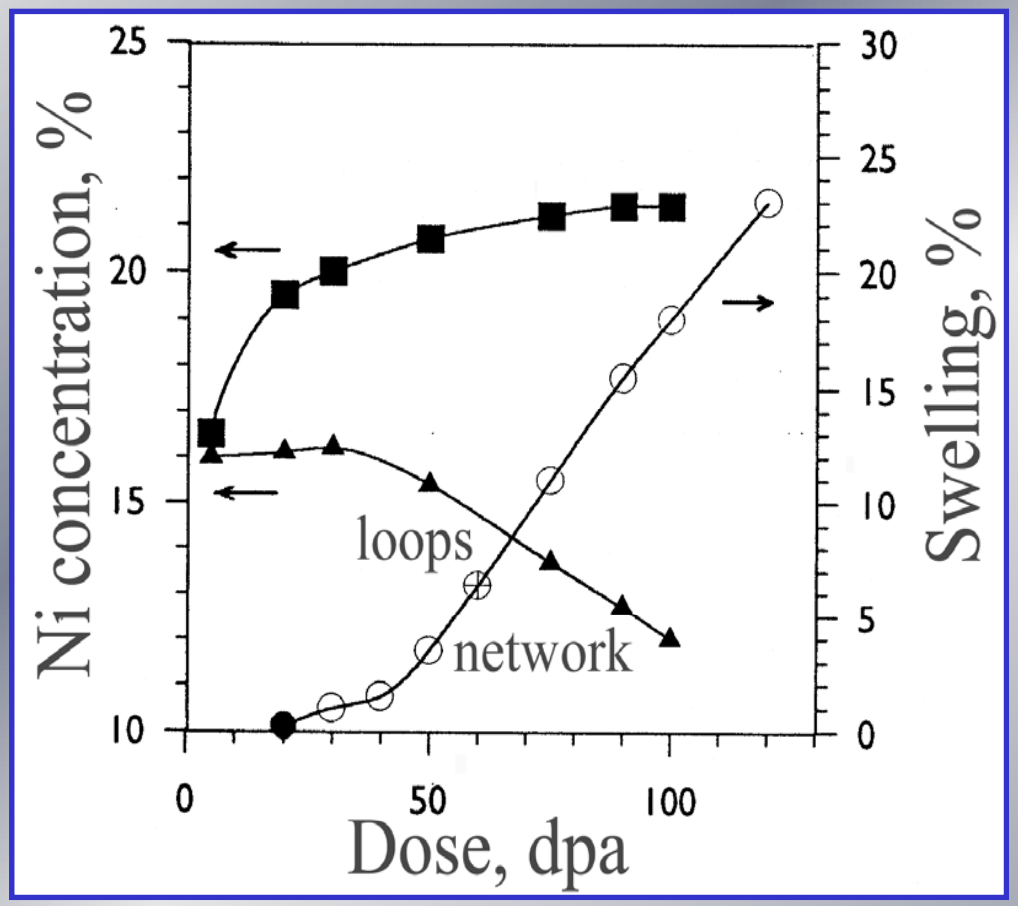

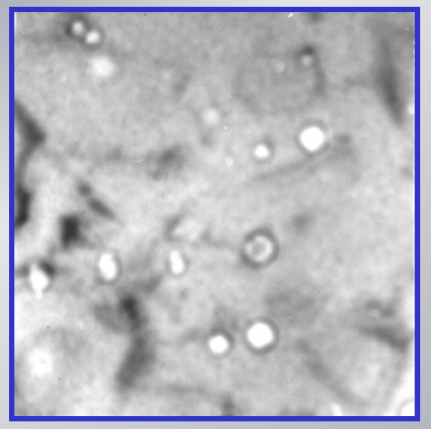

a)

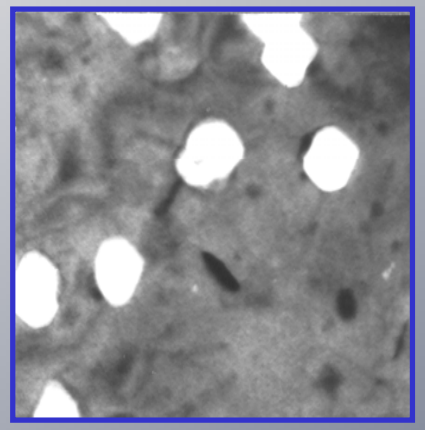

b)

(EI-847, Cr^{3+}, T_{irr}=625^{O}C):

▲- Ni in matrix; ■ - Ni in voids and loops; ● - D=20dpa; ○ - D=60dpa

a) – 20 dpa; b) – 60 dpa

Elements concentration change in solid solution of irradiated PNC 316 steel (Ukai S., Voyevodin V. et al, 2002)

- Formation of precipitates of different kinds (G- and M_6C-phases, phosphides etc.) leads to depletion of solid solution with important solution elements

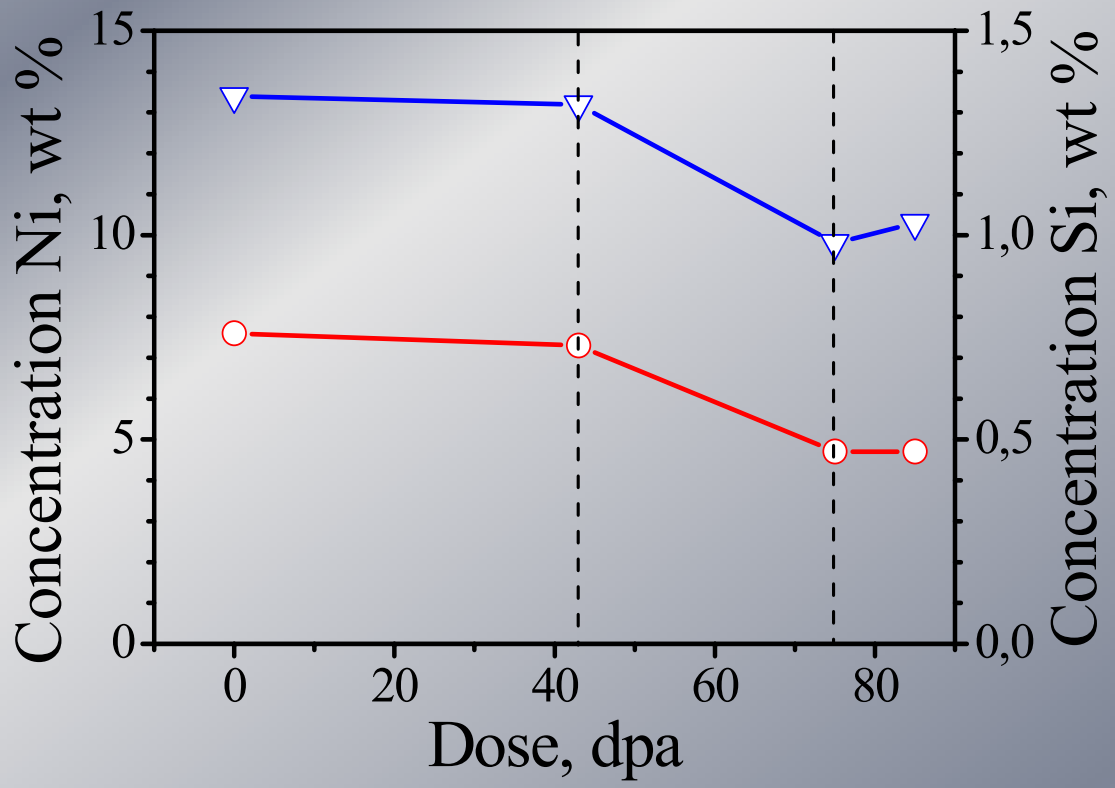

Microchemical influence of composition on void swelling

The change of matrix composition in the result of RIS causes the variation of main parameters determining the radiation swelling;

-energy and geometry characteristics of point defects and their complexes;

-concentration and strength of point defects sinks.

Evolution of porosity in each local area of irradiated material may proceed in his way.

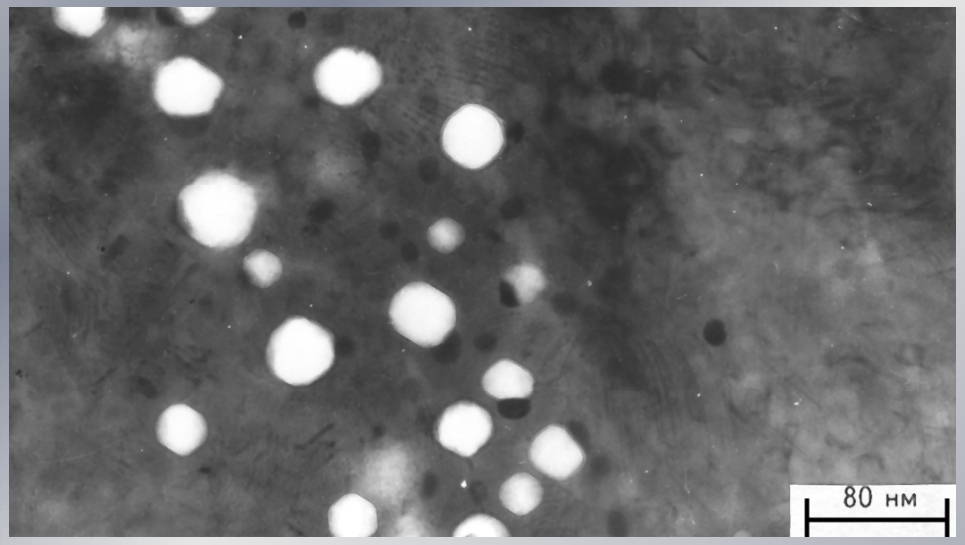

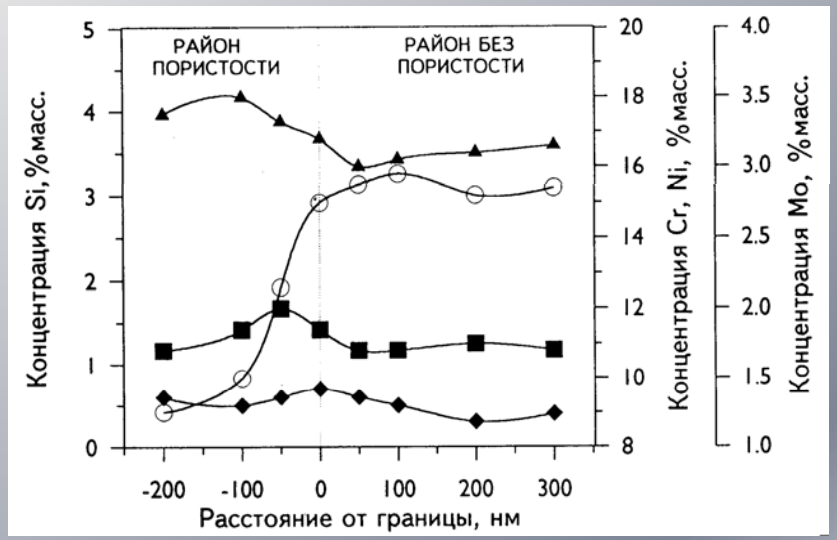

Local chemical composition in irradiated steel EI-847 (a) on area with high swelling, (b) on area with low swelling (Cr^{3+}, E=3 MeV, D=80 dpa, Tirr=650^{0}C).

Precipitates behaviour

Behaviour of precipitates during irradiation and their phase stability are determined by dynamic balance between the radiation dissolution of precipitates and their growth by irradiation enhanced and thermal diffusion, radiation-induced segregation.

Two mechanisms are suggested to be mainly responsible for precipitates stability during irradiation:

1) Displacement dissolution in cascades. This effect is unique and very often it is main destabilizing factor for precipitation occurring in irradiation environment.

Cascades can destroy crystallinity in the unstructured regions of their cores and cause disorder or mixing and stirring in the larger recombination zones surrounding the core. At higher temperatures, small particles can re-form in the solute-rich region following dissolution, and large particles can repair their cascade damage either by re-forming the original particles or by redistribution them as much smaller particles.

2) Radiation- induced solute segregation (RIS) . This effect is principal because it can be the basic reason of radiation-modified or radiation-induced precipitation in austenitic stainless steels. RIS of main segregants takes place at sinks of point defects and triggers precipitation when the local solubility limit is exceeded. As was described earlier, fot stainless steels the more important it seems inversal Kirkendall effect.

A possibly large difference in transmutation between sodium and water cooled reactors

- In sodium-cooled reactors very little hydrogen is retained in stainless steels.
- In water-cooled reactors large amounts of hydrogen can be retained when helium forms cavities.
- Much more helium and hydrogen form in water-cooled reactors.
- Are there possible consequences on swelling, mechanical properties and corrosion/cracking?

Temperature-dependent swelling observed in annealed steel 18Cr-10Ni-Ti at 50 dpa produced with a damage rate of 10^{-2} dpa/s.

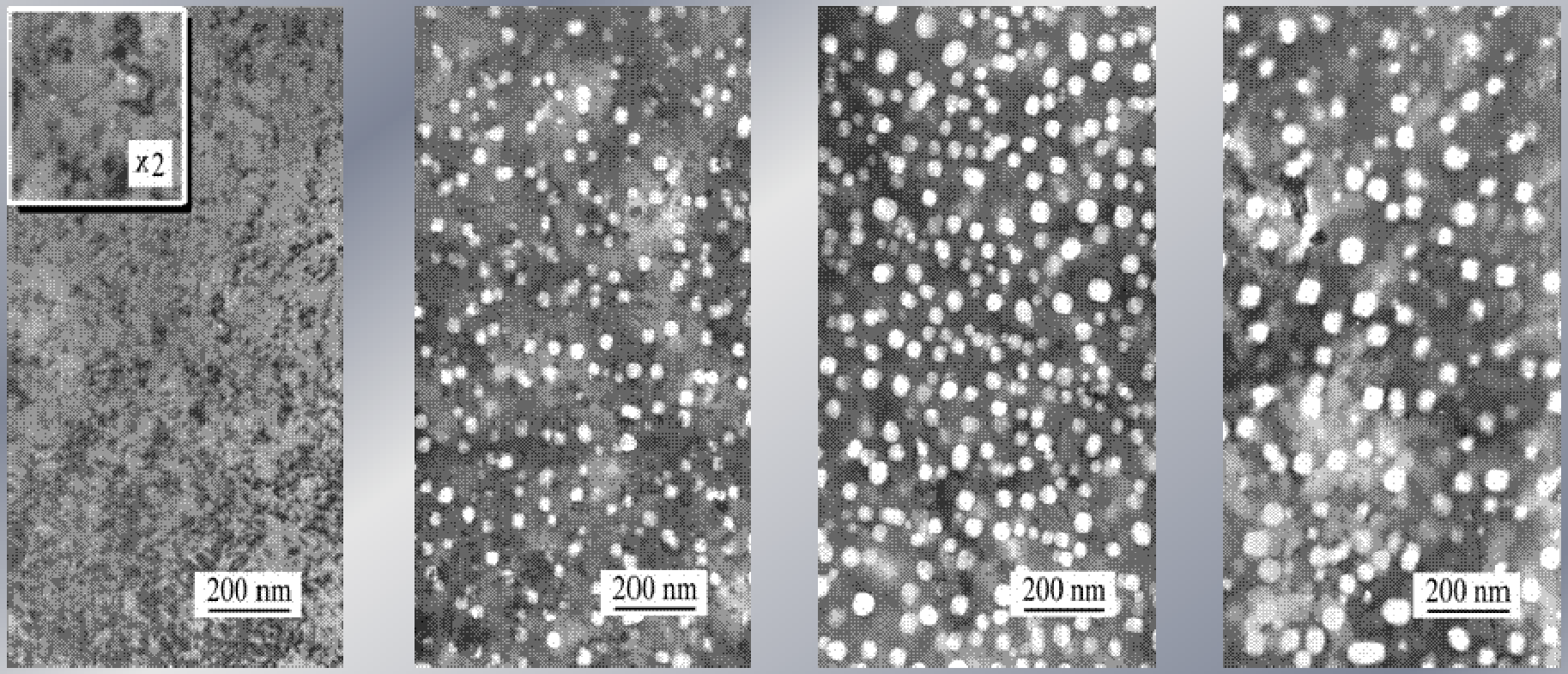

590°C 600°C 615°C 635°C

Dose-dependent swelling observed in annealed steel 18Cr-10Ni-Ti at 635°C produced with a damage rate of 10^{-2} dpa/s.

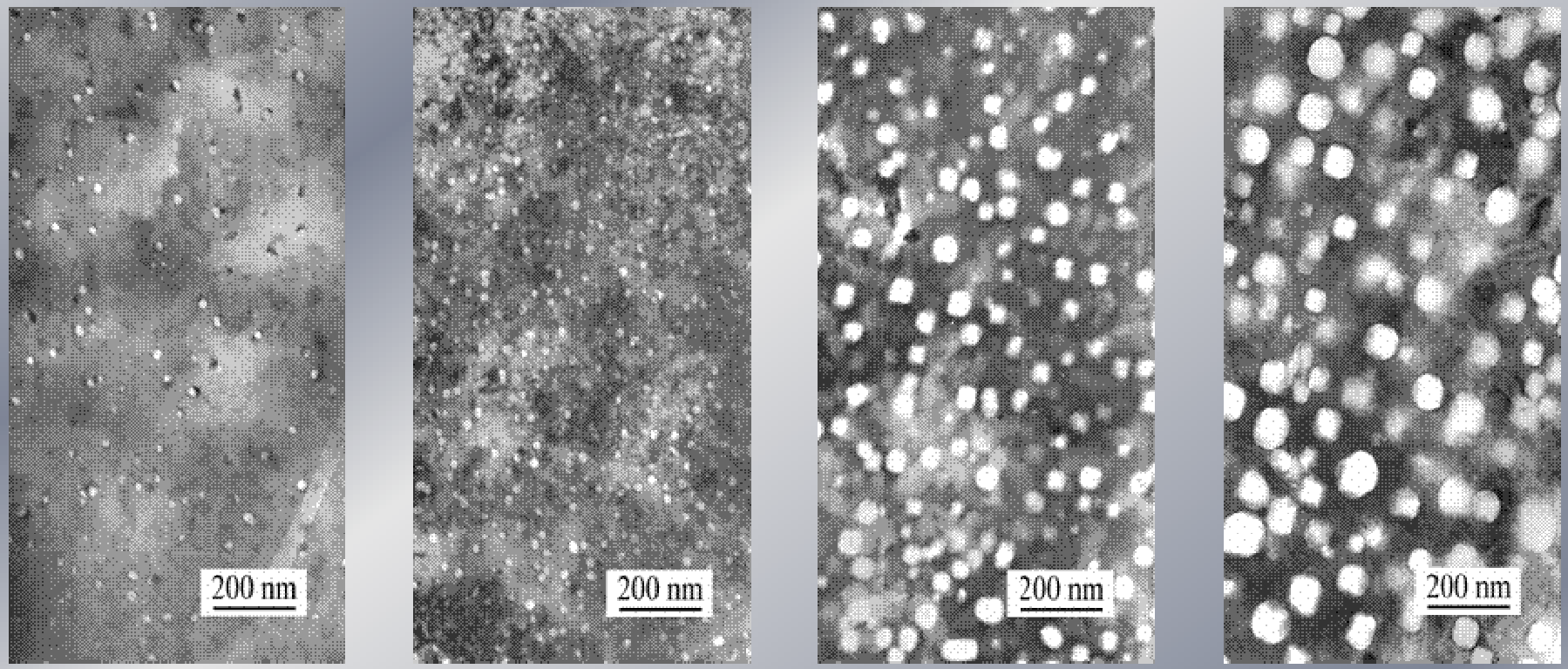

5 dpa 20 dpa 50 dpa 100 dpa

Improved understanding and description of swelling at PWR-relevant temperatures and dpa rates

- Collection of actual PWR data on the actual steel, especially 304 SS, is the most important and also the most difficult activity.
- Collection of swelling data from other steels from other reactors, especially in Russia and Kazakhstan, provides some guidance but no confident predictive capability.
- Charged particles can be used to test some issues at PWR-relevant temperatures.
- Generally, we can expect that SA 304 will swell before CW 316, with voids occurring at temperatures >300°C, with relatively low steady-state swelling rates below at least 350°C, accelerating with lower dpa rate.
- Swelling/stress/creep feedback effects in thick, constrained components will be very important in predicting strains arising from gradients in radiation conditions and thereby swelling.

Distribution of dose and temperature in baffle rings of VVER-1000 power reactors

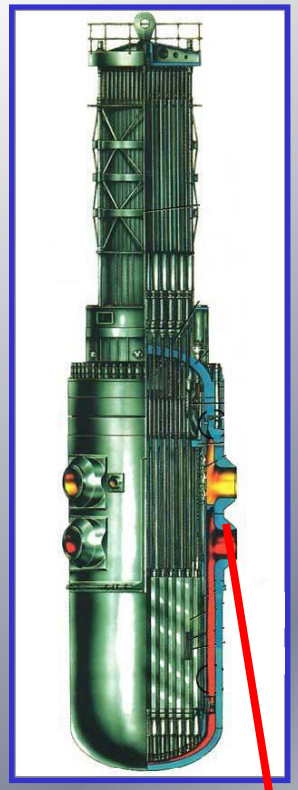

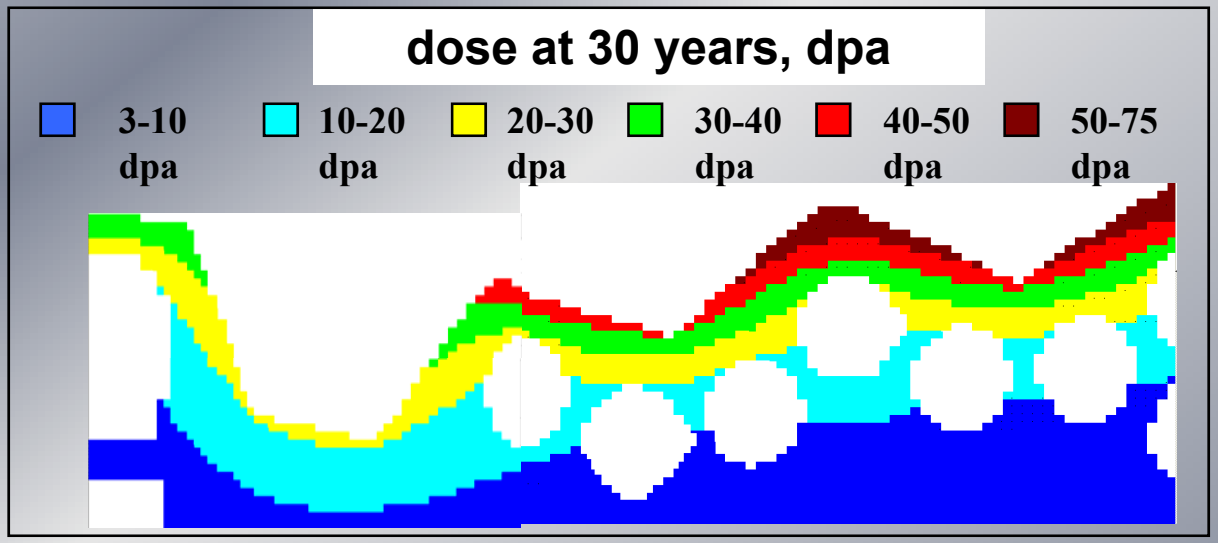

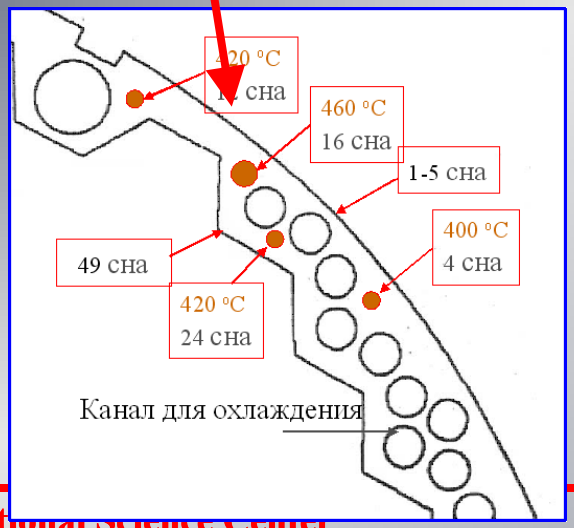

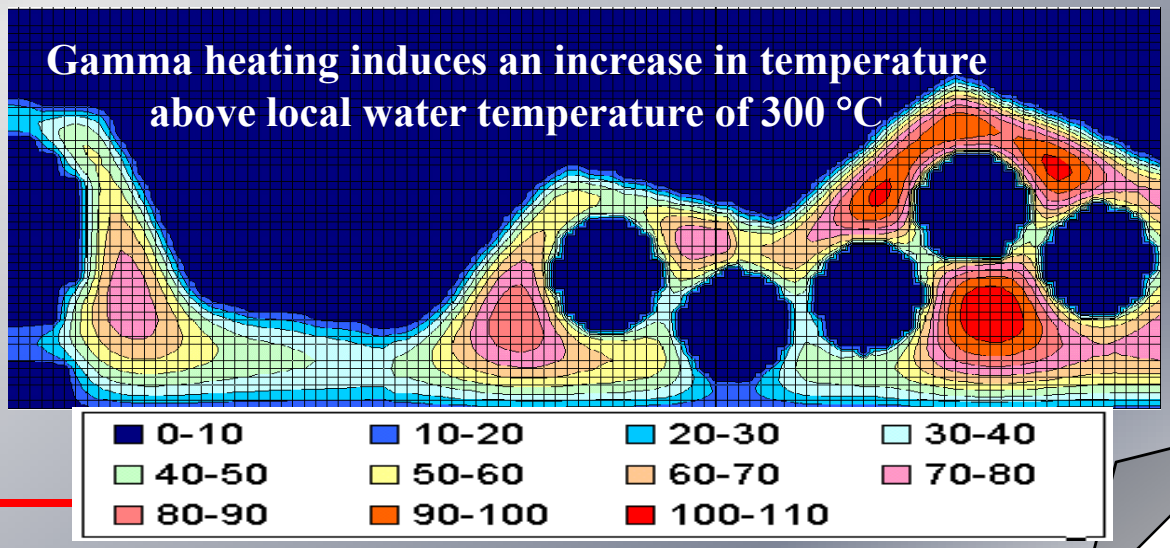

Schematic of reactor vessel, core and baffle-former assembly

Baffle-former assembly surrounds the core and is exposed to neutron flux and gamma heating

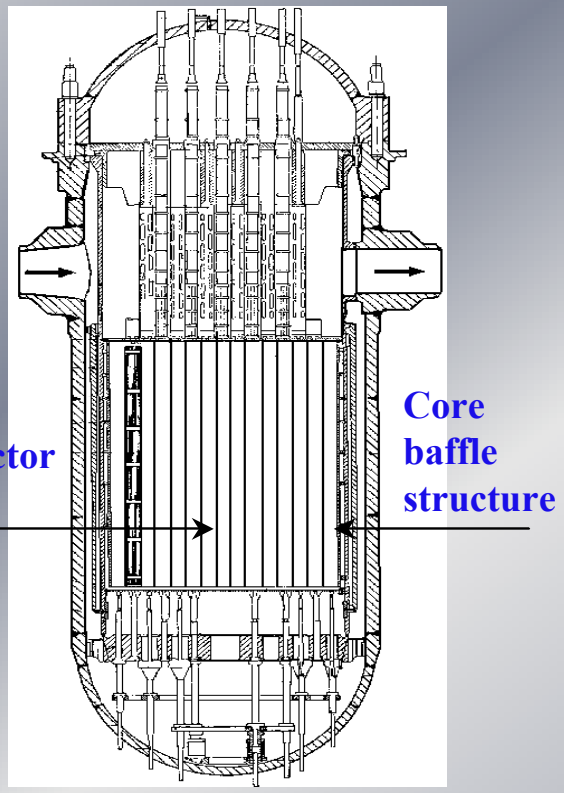

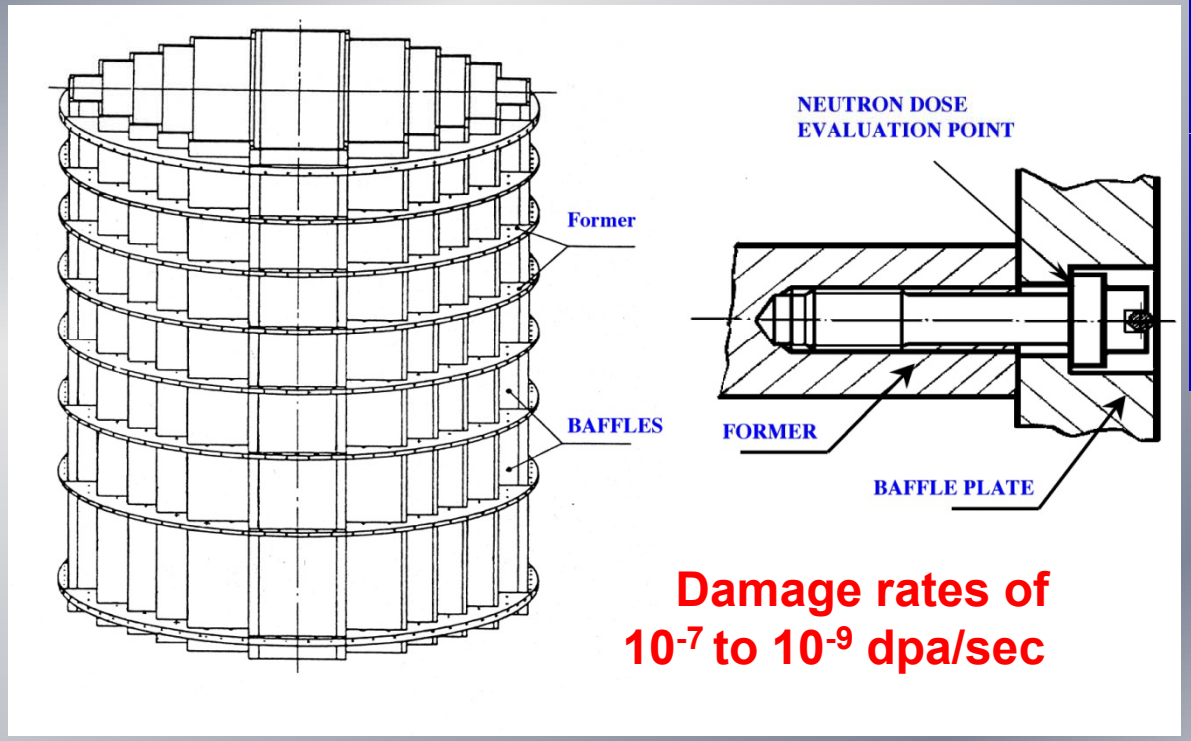

Damage rates of 10^{-7} to 10^{-9} dpa/sec

SA 304 plates and CW 316 bolts

Modeling of bolt behavior by the method of final elements

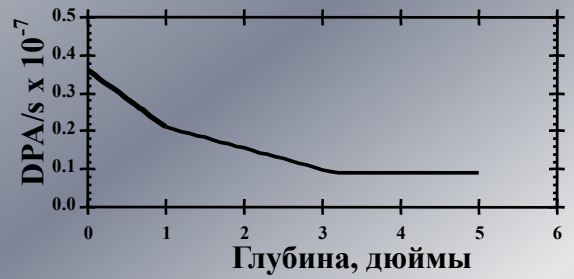

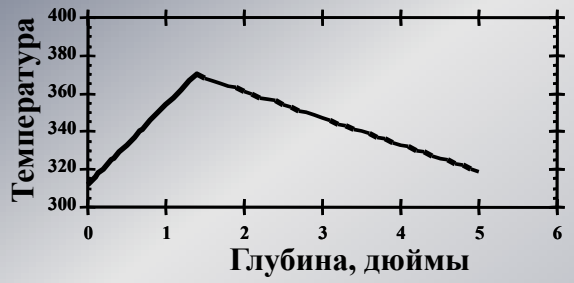

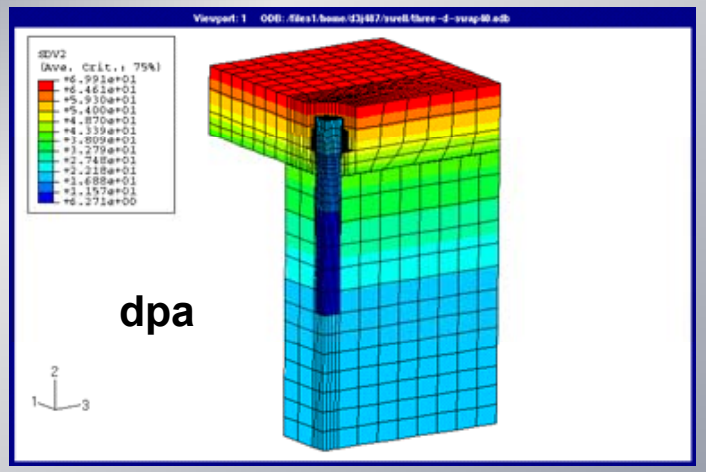

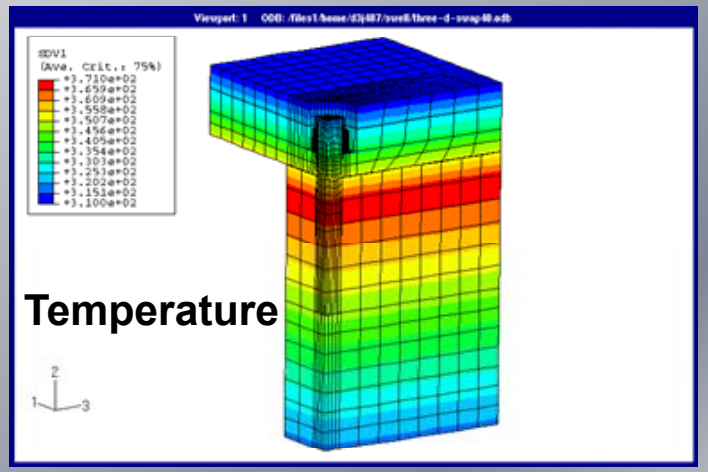

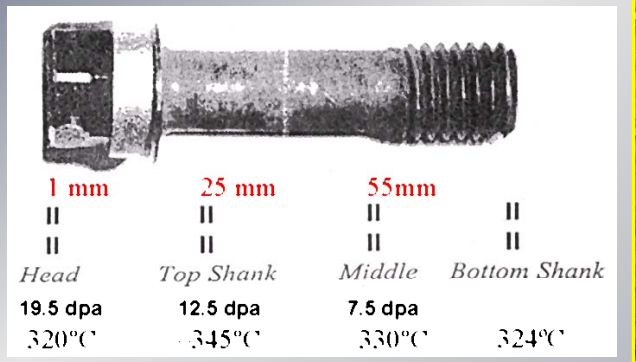

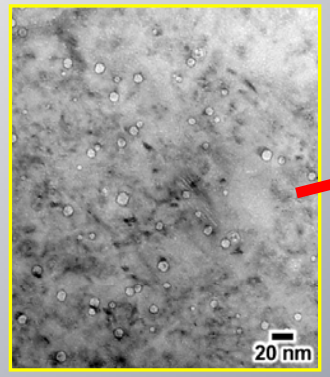

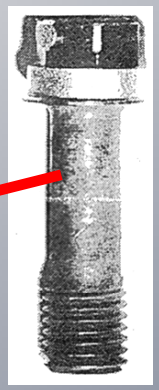

Voids in channel tube from Fe-0.06C-18Cr-10Ni-Ti, WWER-1000, Rovno-3 (Neustroev and others, 2002)

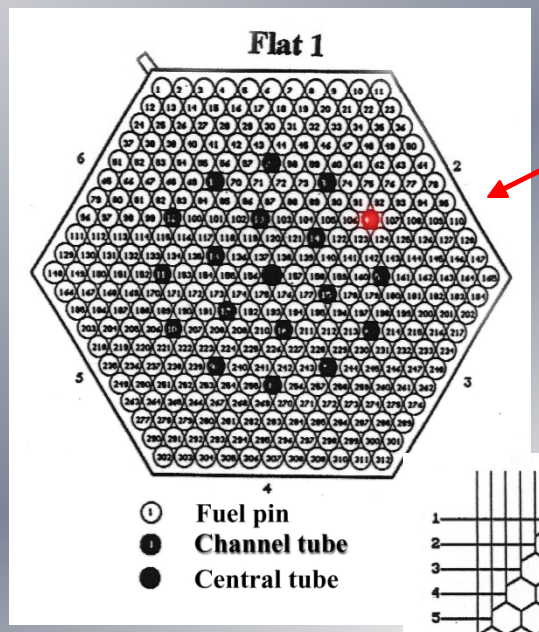

FA

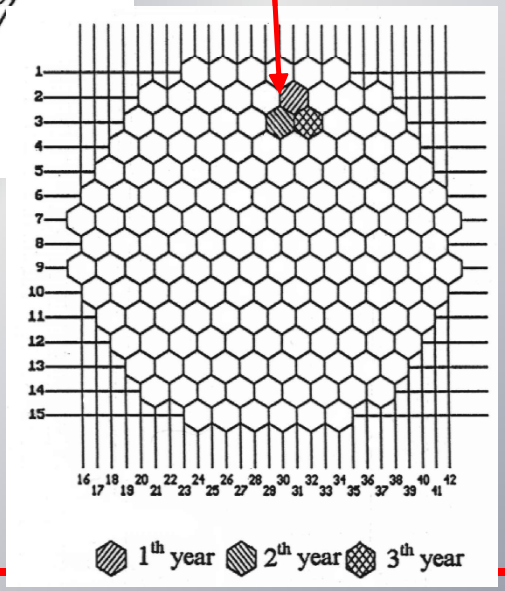

Cladding

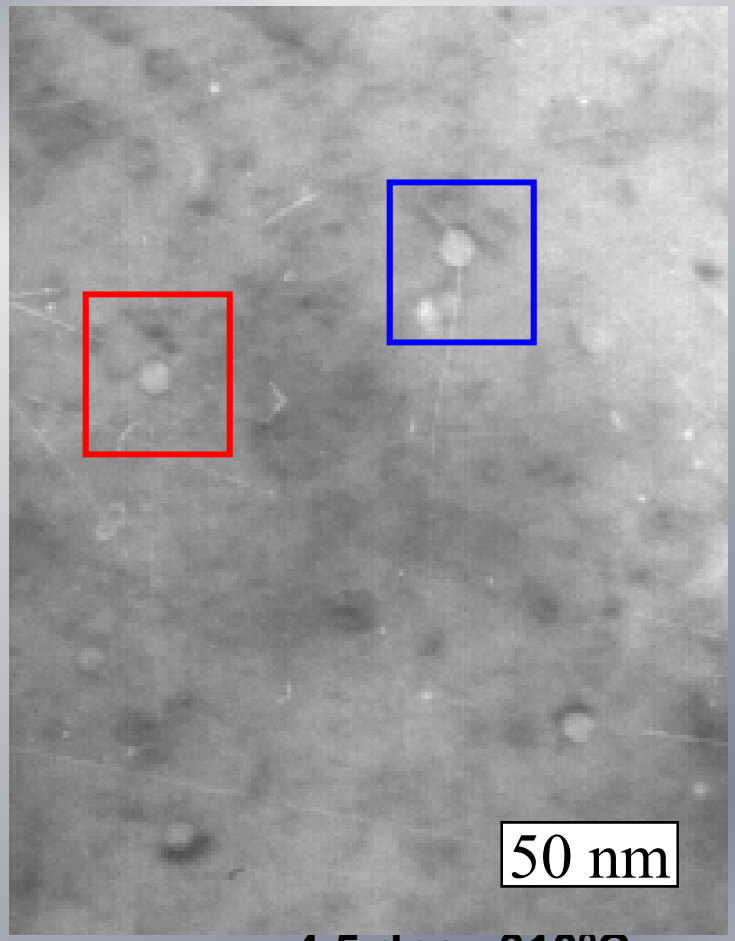

4.5 dpa, 310°C

Calculation of data of variation of thermal-elastic stresses, of swelling and of shroud diameter during reactor operation

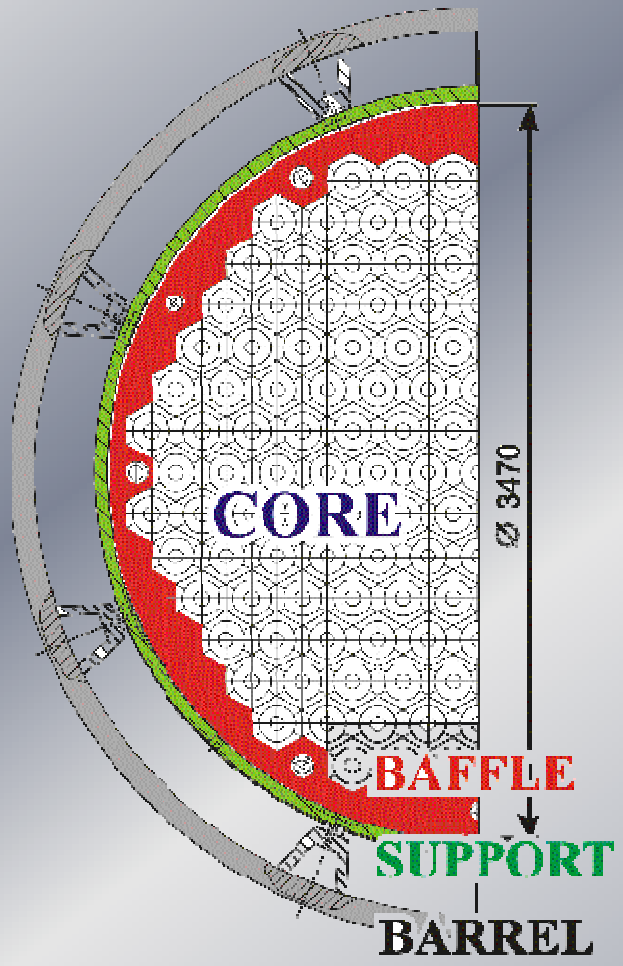

t, years	σ, MPa	ΔV/V%	Δd, mm
17	270	0,5–3	3,0
30	340	1–49	5,0
50	450	?	8,2

Localization of plastic deformation in material of PVI (ε≈ 7%)

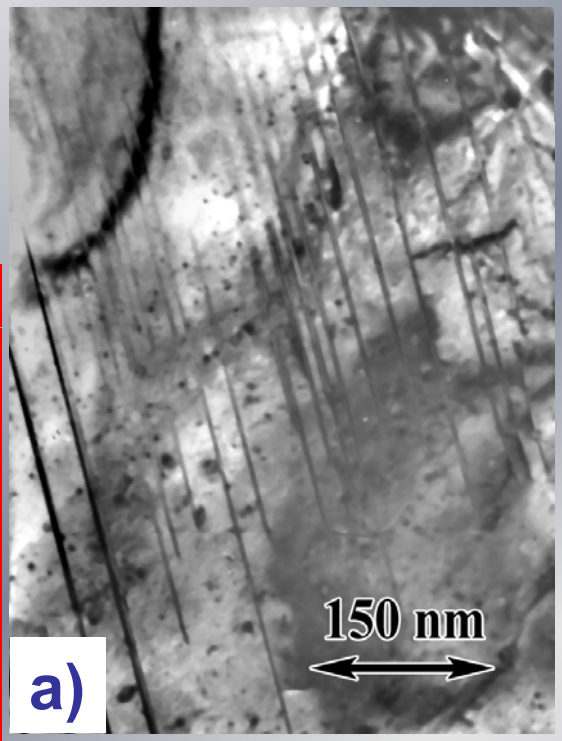

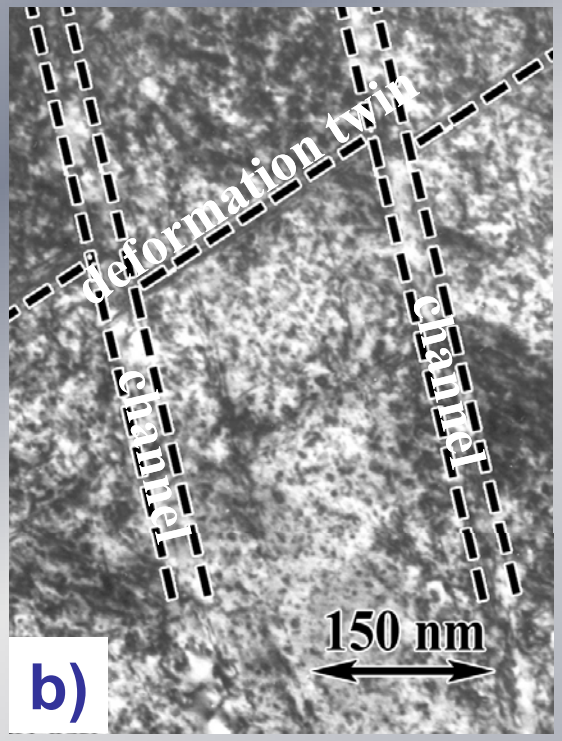

At room temperature the main deformation mechanism is twinning (fig. a).

At 300°C the main mechanism of deformation is localization of plastic flow in narrow (~50-60nm) dislocation channels (fig. b)

a) dose 1 dpa and deformation at 20°C;
b) dose 5 dpa and deformation at 30°C.

Failure of material of PVI due to the high swelling (100 dpa, 600°C, ε=7%)

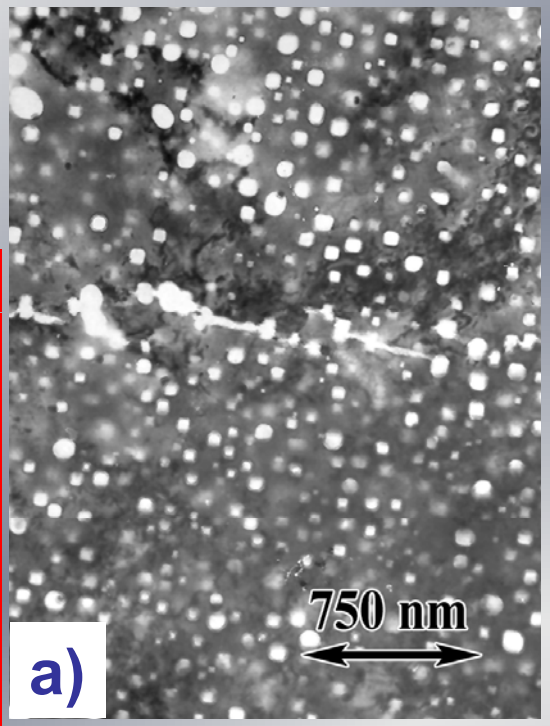

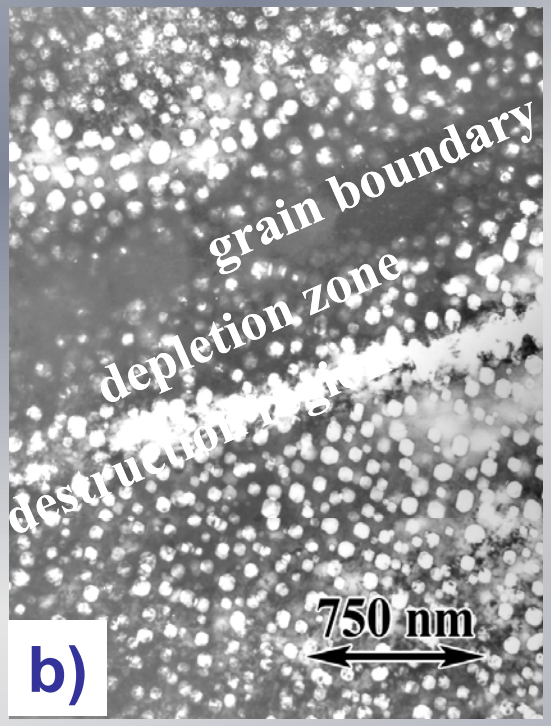

In the grain body the cracking proceeds due to the localization of sliding on void network (fig. a).

In near boundary sites the failure proceeds on the distance of 0.4-0.5 mkm from boundary due to the presence of increased concentration of voids in these sites (fig. b).

a) cracks in matrix b) failure along the grain boundaries

Hardening and ductility loss observed in two stainless steels irradiated in the HFIR, HFR, and R2 mixed spectrum reactors at 250°C at helium/dpa ratios ranging from 10 to 35 appm/dpa (after Elen and Fenici, 1992)

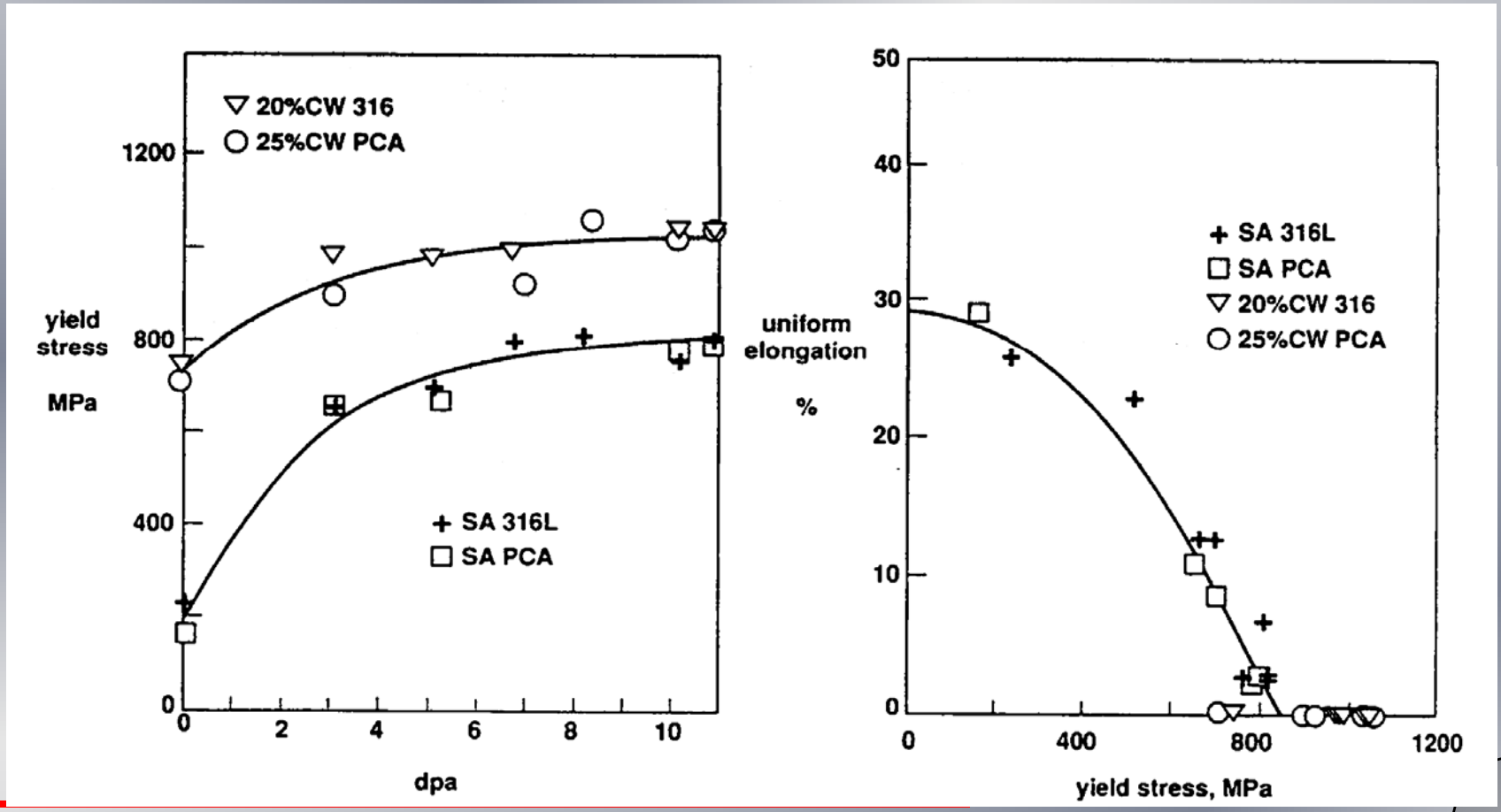

Examples of some environmental changes at structural materials of FBR under irradiation

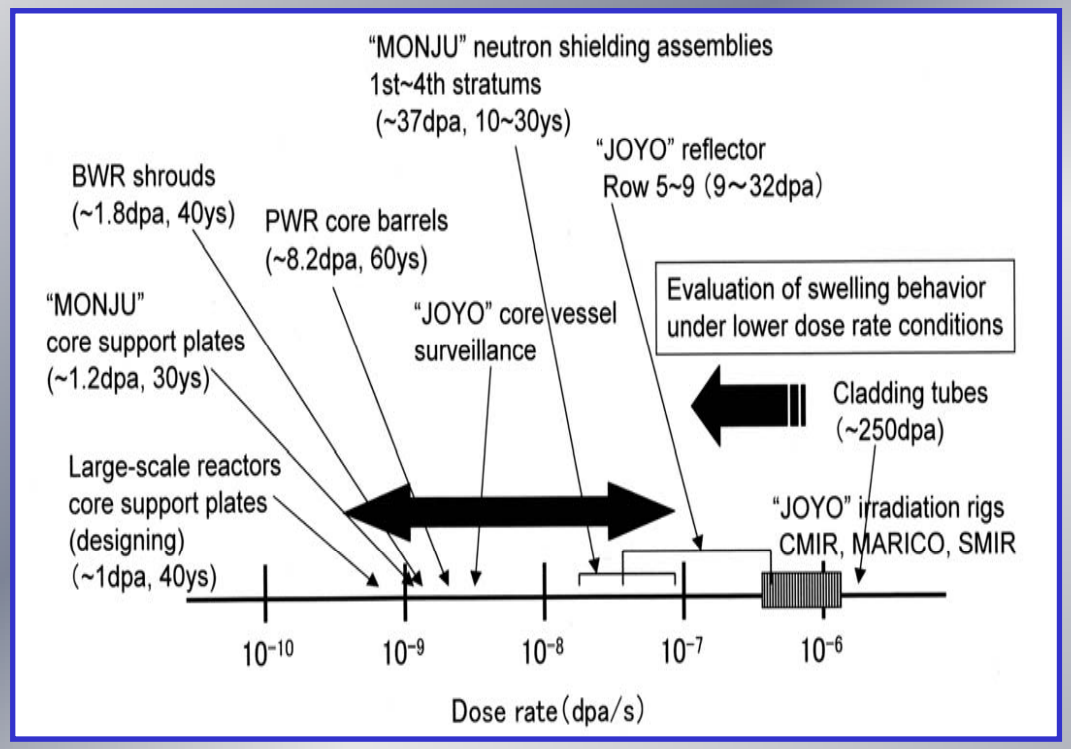

Temperature change

1-$T_1^{irr} < T_{max}$ sw $< T_2^{irr}$

2-$T_1^{irr} < T_{max}$ sw $> T_2^{irr}$

$T_1^{irr} > T_{max}$ sw $< T_2^{ir\ r}$

$T_1^{irr} > T_{max}$ sw $> T_2^{ir\ r}$

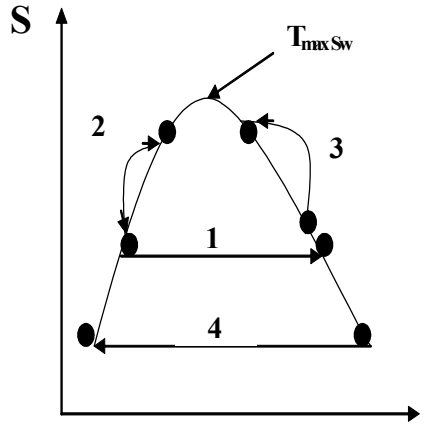

Scheme of T changes

Stress-level of residual stress due to final cold working of cladding and gas pressure in fuel pins due to fission products release under irradiation is estimated as 50-200 MPa.

General tendency of dpa rate influence on swelling in austenitic steels

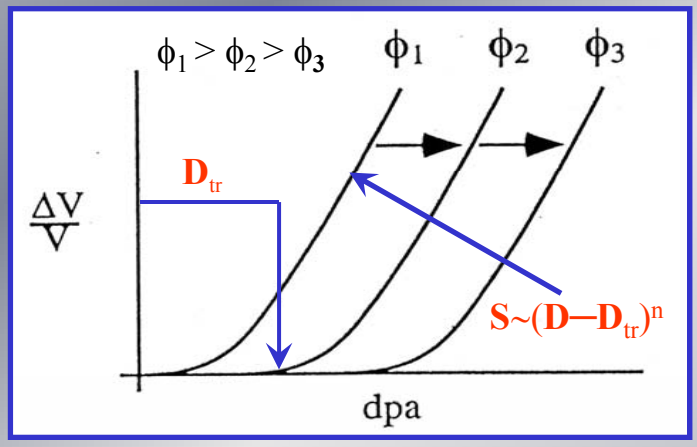

- Dpa rate effects always takes place during irradiation as a result of spatial flux gradients across fuel pin and irradiation at different rows of active zone.This effect is very important under comparison of swelling data from different reactors.
- The most of experimental results clearly demonstrate one common tendency in changing of neutron flux or dpa rate on swelling of ASS :
- Swelling increases with decreasing dose rate.
- This tendency keeping at all relevant reactor temperatures.
- Last time it was realized that differences in dose rate at most temperatures could mainly exert their influence on duration of transient regime of swelling. Discussion about influence on steady state swelling now is in progress.
- During the transient period few several rate-dependent phenomena take place- loops nucleation and growth, dislocation network development, solute redistribution,voids nucleation.The properties of the incubation period are certainly controlled by the coupling between these events.

Agreement between rate theory and void swelling data in pure Ni

$$\frac{dS}{d\phi_0 t} = -\frac{B}{\rho_i + n + b}\frac{\varepsilon D_v}{\phi_0}\left[(\rho_i - \rho_v)\overline{C}_v - (\rho_i + n)C_v^b + (\rho_v + n)C_v^0\right]$$

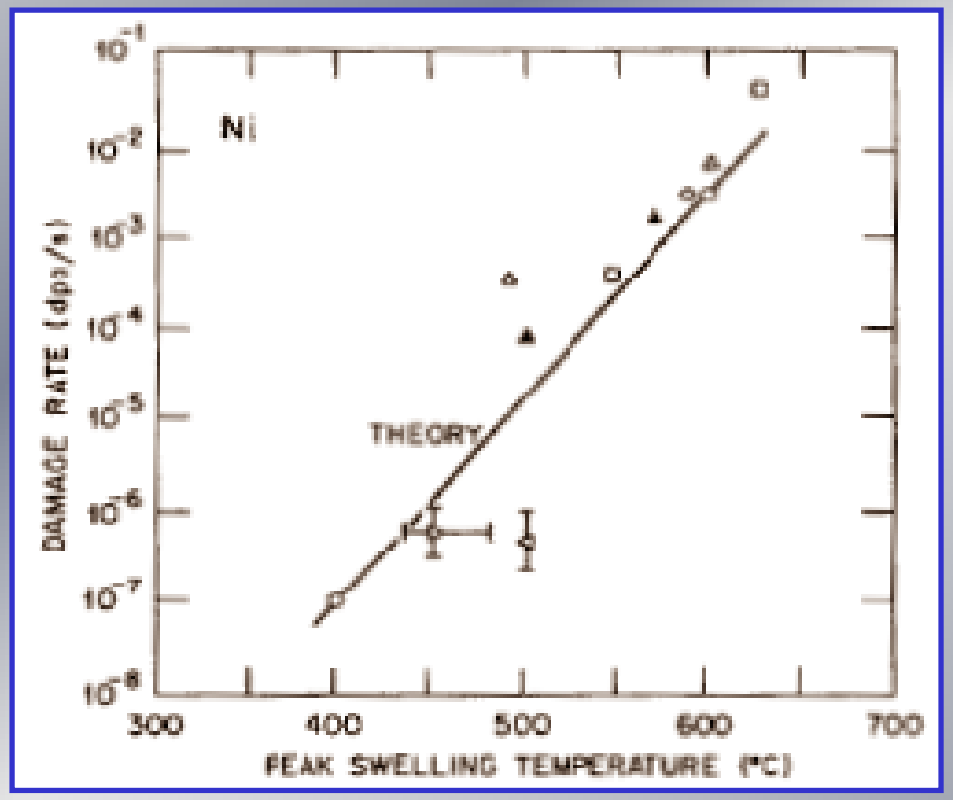

$$T_2 - T_1 = \frac{\left(\frac{kT_1^2}{E_m^v}\right)\ln\left(\frac{\phi_2}{\phi_1}\right)}{1 - \left(\frac{kT_1}{E_m^v}\right)\ln\left(\frac{\phi_2}{\phi_1}\right)}$$

Mansur, JNM 216 (1994) 97

Effect of dpa rate on swelling in commercial steels

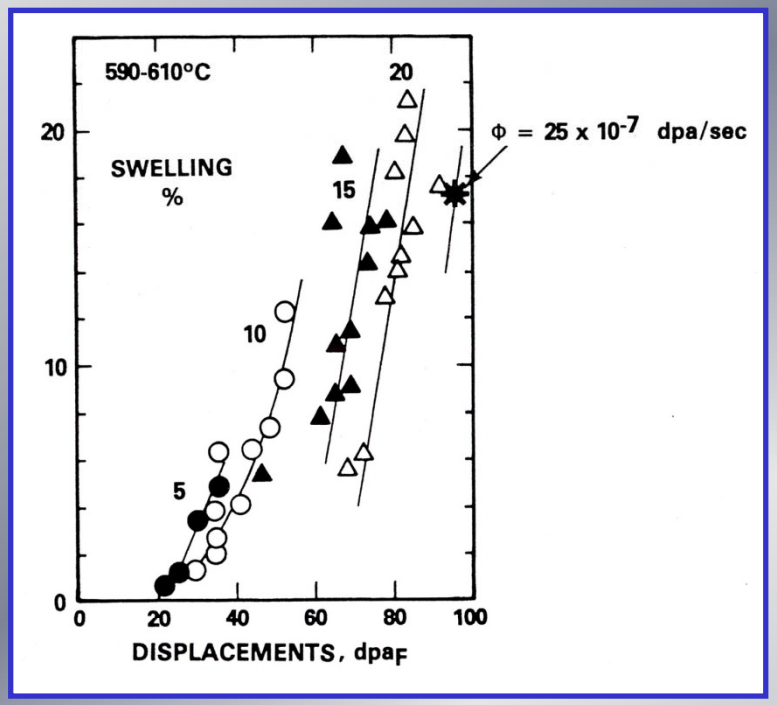

Dpa rate influence on swelling in 20% CW AISI 316 in PHENIX fuel cladding (dpa F=2/3dpaNRT) [Seran,1982].

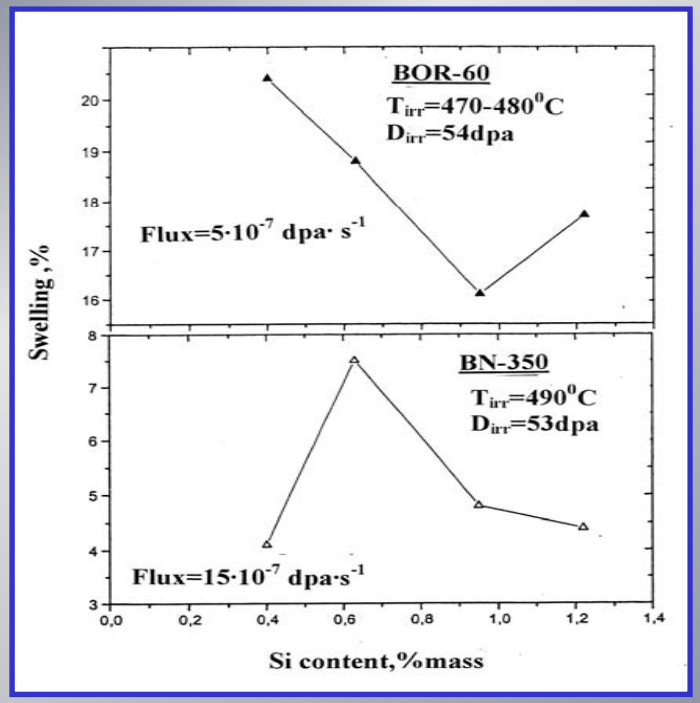

Swelling versus Si content (Steel 16Cr15Ni3MoNbB, irradiation in reactors BOR-60 and BN-350 with different dpa rate) [Budylkin, 2001].

Swelling in all commercial austenitic steels seems to be very sensitive to effect of dpa rate due to its influence on all components of microstructure evolution during irradiation.Comparison of swelling data received on different reactors (ever at the same dose and temperature) must take into account dpa rate.

Effect of dose rate on dislocation evolution during neutron irradiation ~at 426°C in Fe-15Cr-16Ni [Sekimura, 1991]

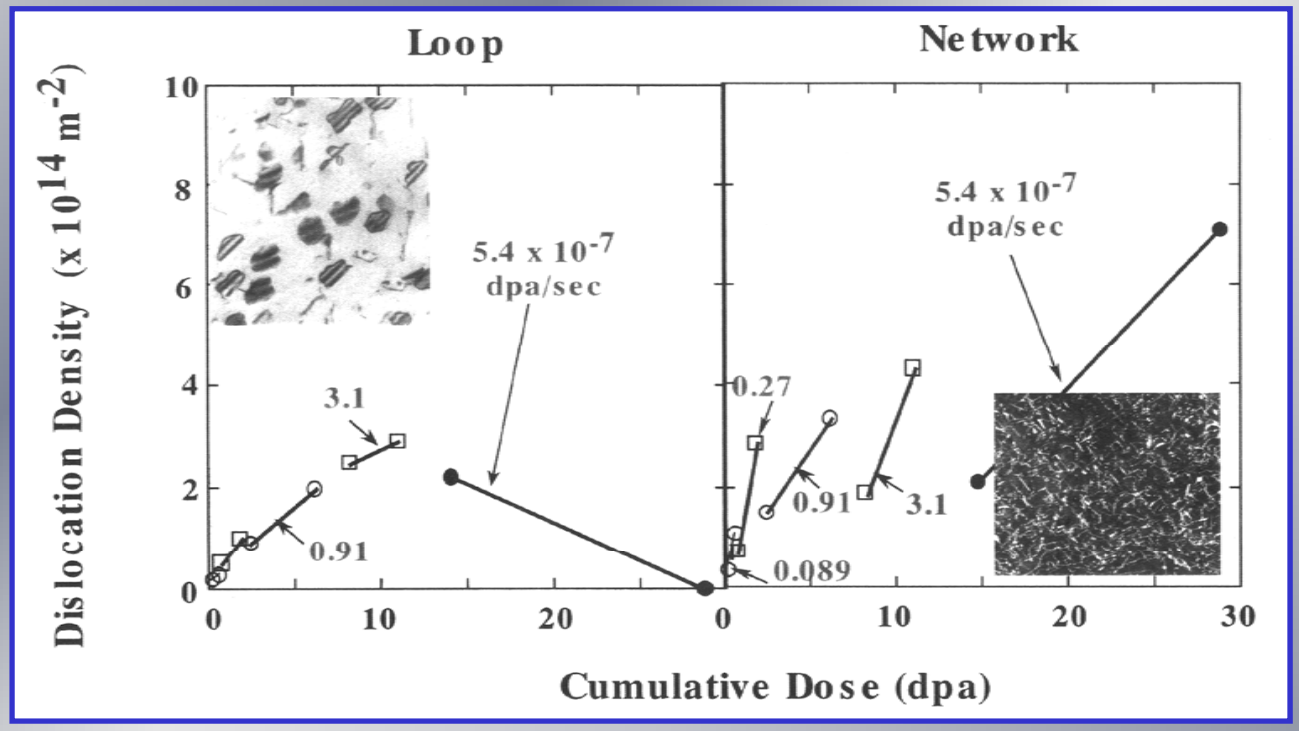

- Network formation is proceeded by unfaulting and interaction of dislocation loops, whose size and density are flux sensitive
- Swelling transient regime correlates well with dose required to form a dislocation network.
- Accelerated evolution of dislocation loops enhances cavity nucleation at low dose rate.

Dependence of loop density on dpa rate

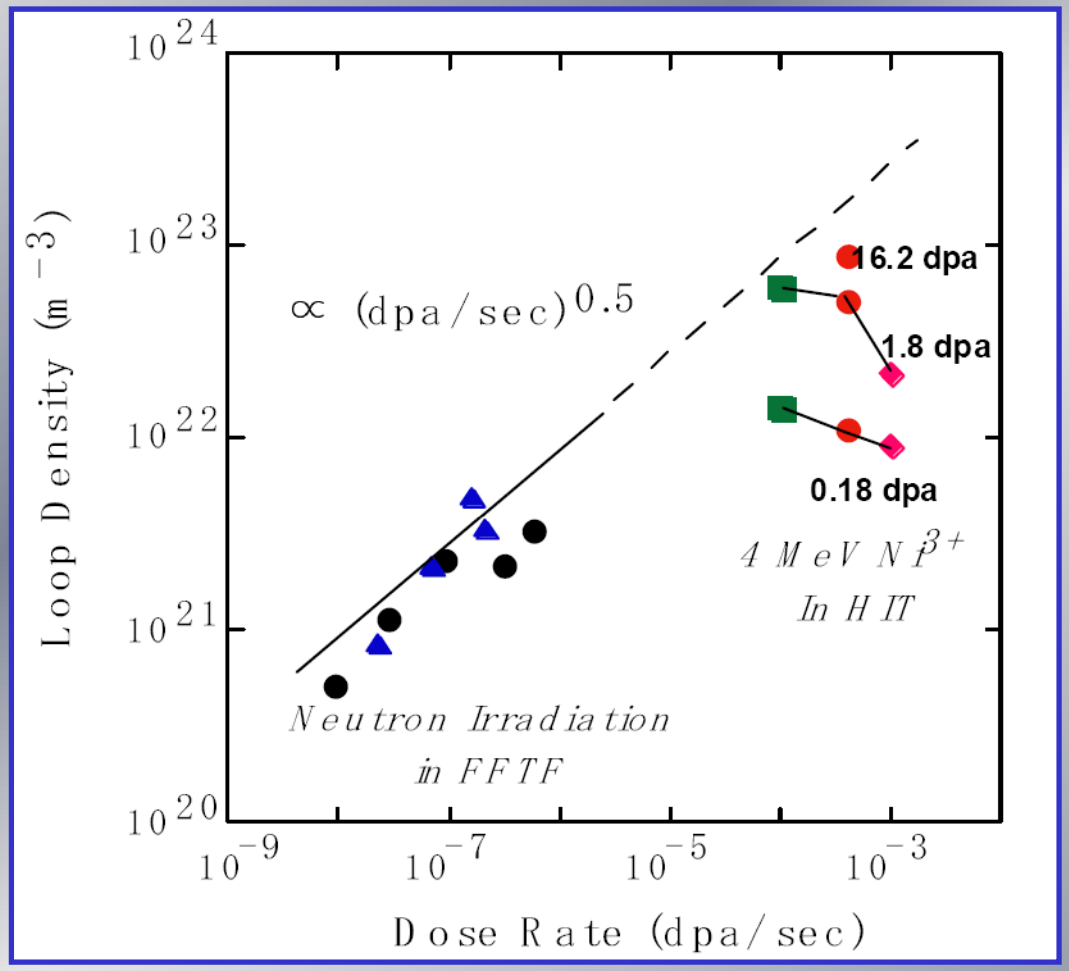

(T. Okita, N. Sekimura,

T. Iwai, F. A. Garner, 2001)

Damage dose rate effect on AISI 304L and Fe-18Cr-10Ni-Ti steels swelling [V.S. Neustroev et al.]

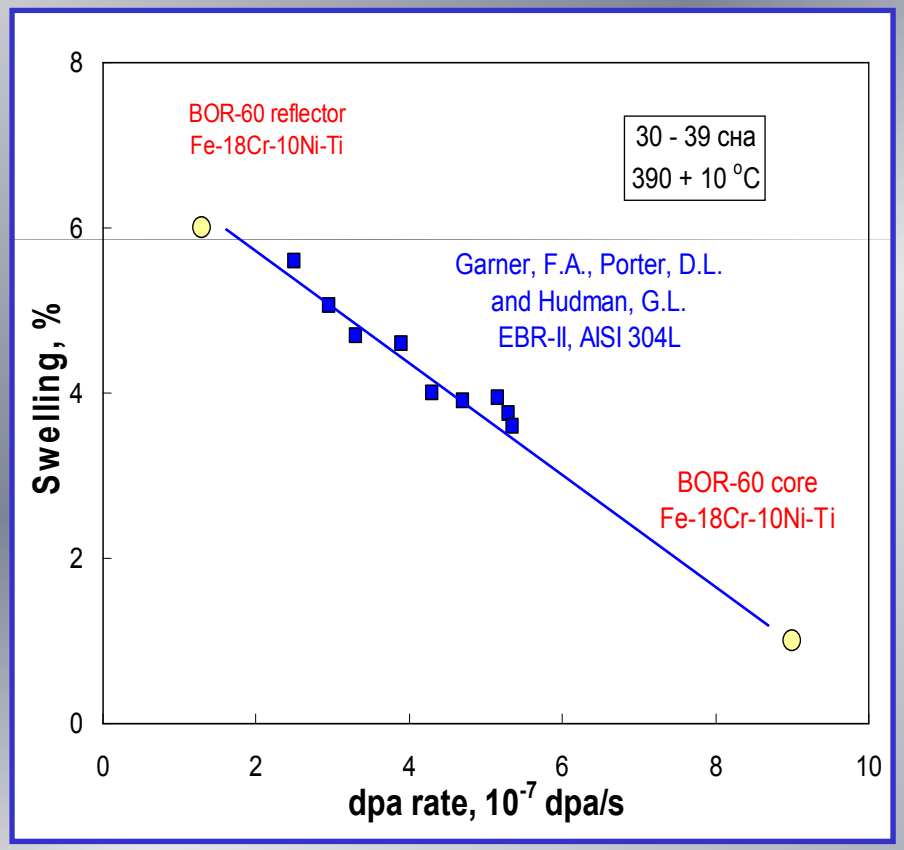

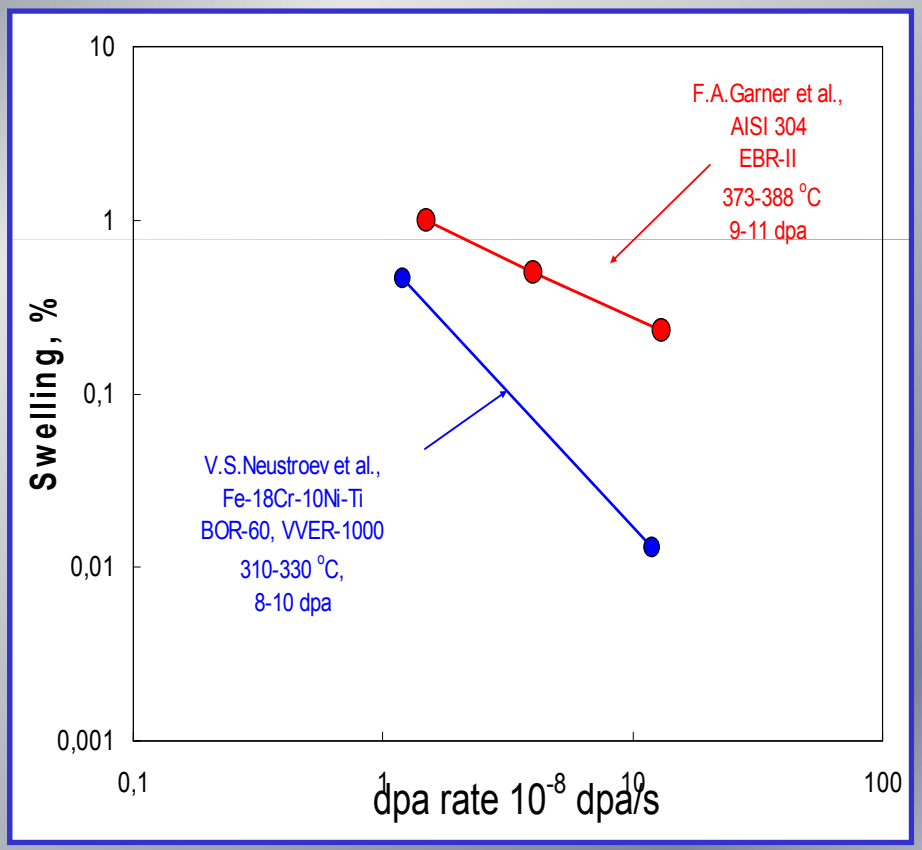

Temperature (D=50 dpa) and dose (T_{irr}=615 °C) swelling dependences for steel 18Cr-10Ni-Ti at different initial states (● – ST at 1050°C, 30 min., ▲ – 5.5% CW).

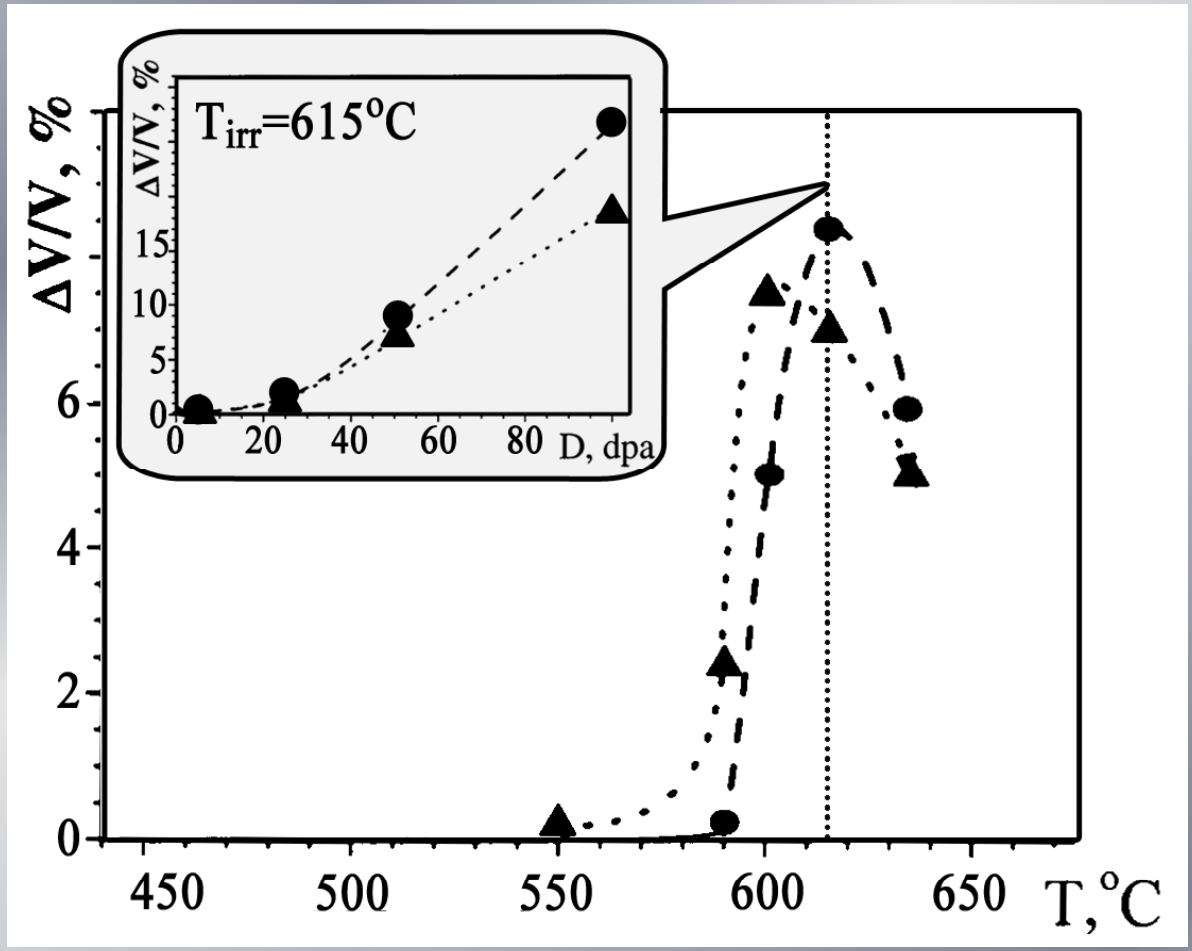

Influence of dpa rate on: a) swelling transient regime (D_0) b) swelling rate ($\dot{S}$) in maximum irradiation temperature

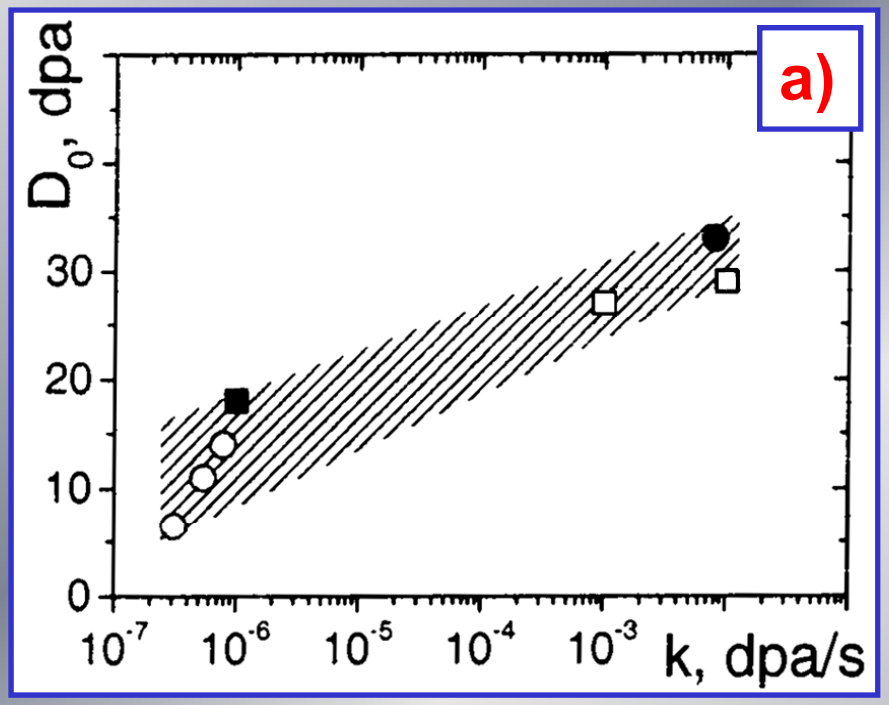

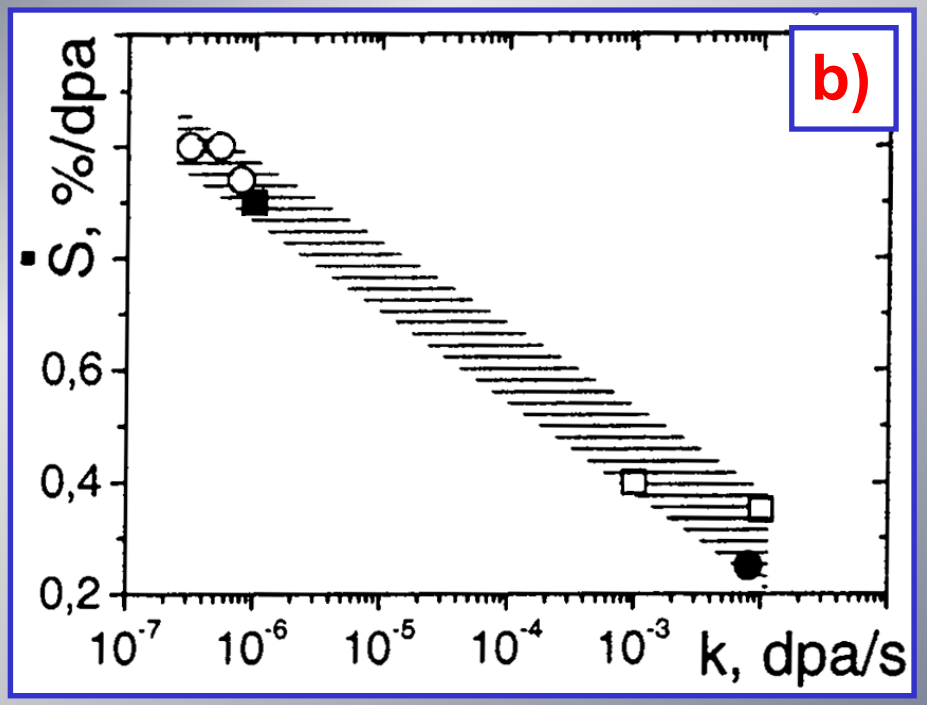

(□) – 18Cr-10Ni-Ti T_{irr} = 615°C and 590°C for 10^{-2} and 10^{-3} dpa/s respectively;
(■) – 18Cr-10Ni-Ti $T_{irr} \approx$ 480°C (BOR-60) [Neustroev V.S. et al, 2000];
(○) – Fe-15Cr-16Ni $T_{irr} \approx$ 410°C (FFTF) [Okita T. et al, 2002];
(●) – 15Cr-16Ni-3Mo-Nb T_{irr} = 650°C (high ions) [Voyevodin V.N. et al].

RIS sensitivity to dpa rate

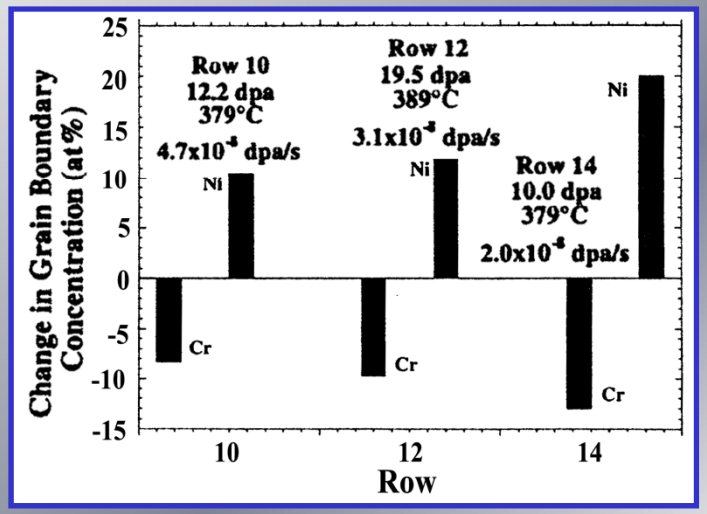

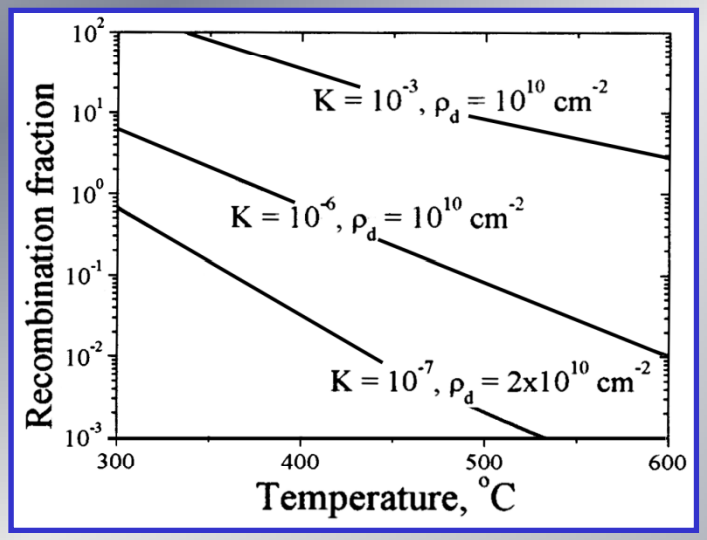

♦As the dpa rate decreases, the amount of Ni enrichment and chromium depletion in steel 304 increases. In all cases the segregation is larger in the lower dose rate samples. (Irradiation in EBR-II) [Allen et al, 2001](a)

♦Ni (and Si) segregate on loops faster at low dose rate [V.Voyevodin, 1994]

♦ Calculations by rate theory for ratio of recombination point defects fraction to fraction of point defects disappearing on sinks: at relevant temperatures decreasing of dpa rate leads to decreasing recombination and increasing the segregation on sinks.

If Dpa rate↓ Recombination↓ Segregation↑.

It is obviously that recombination is important only for high dpa rates.

[N.Lazarev, V.Voyevodin, 2002] (b)

Influence of dpa rate on precipitates stability

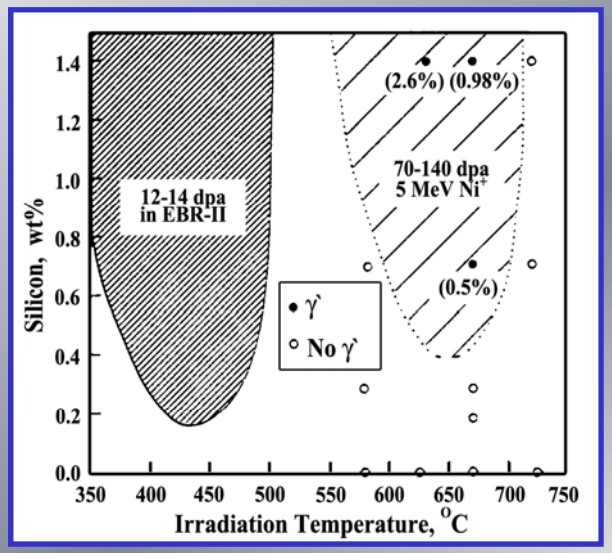

γ'-phase (Ni_3Si) formation in alloys Fe-15Cr-20Ni-Si at different dpa rate ~ 10^{-6} dpa/s in EBR-II, 2×10^{-3}dpa/s for ions

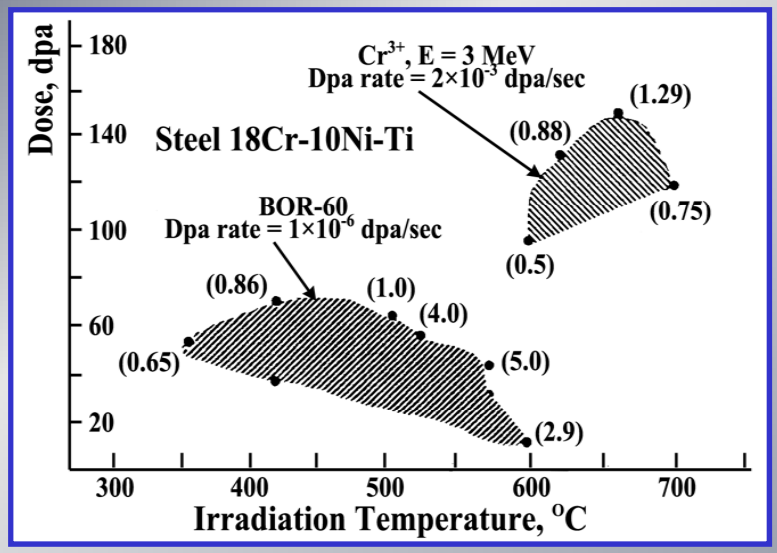

G-phase ($Ti6Ni16Si7$) stability during irradiation in alloys Fe-18Cr-10Ni-Ti at ~10^{-6} dpa/s in BOR-60 and 2×10^{-2}dpa/s for ions

G-phase($Ti_6Ni_{16}Si_7$) stability during irradiation depends from dpa rate. Volume fractions of G-phase are shown in parentheses. [Voyevodin, 1996]. It is obviously that decreasing of dpa rate leads to more intensive precipitation of Ni and Si- content phases (γ"and G - phase). As a result Ni and Si content at matrix decreases and create possibilities for intensive swelling.

Stress influence on swelling parameters

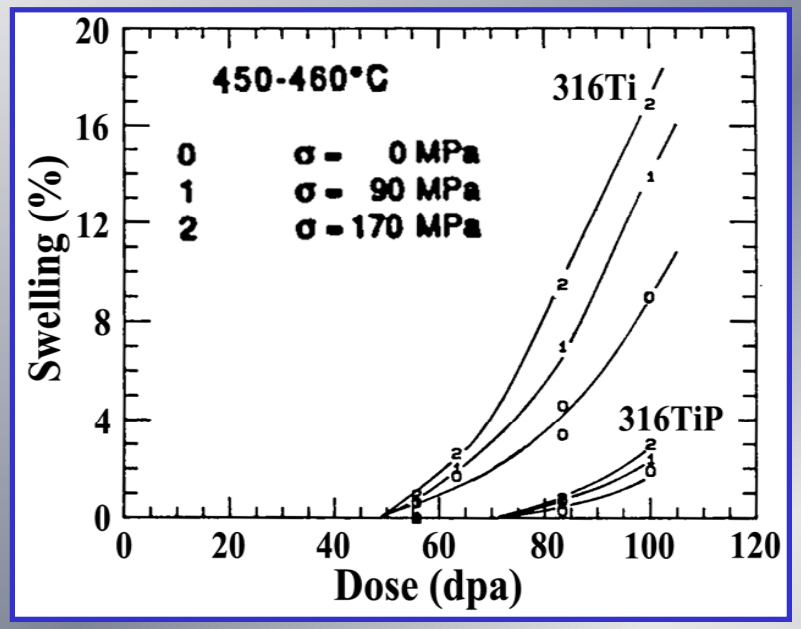

Stress effect on swelling of 316 SS irradiated in PHENIX [Dubuisson et al, 1992].

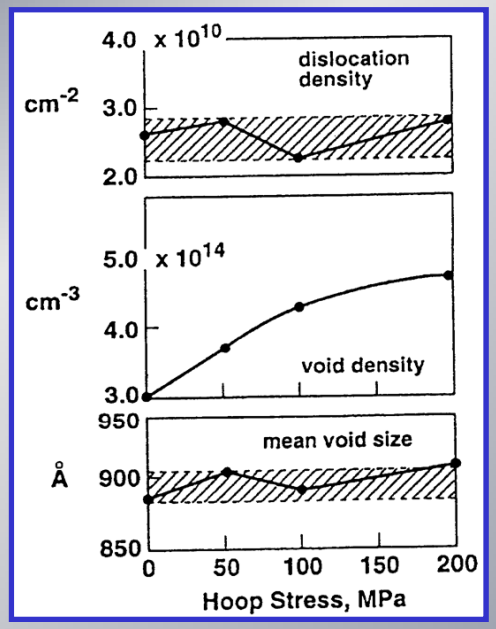

Microstructural data for 16Cr15Ni3MoNbB steel (irradiation at BOR-60, 480^{0}C, 60dpa) [Porollo,1999].

Mathematically stress effects can be described as follows: the swelling level can be determined as :

$\Delta V/V_0(\sigma_{hy})=\Delta V/V_0(\sigma_{hy}=0)\times(1+A\times\sigma_{hy})$ – for incubation period

$\Delta V/V_0(\sigma_{hy})=\Delta V/V_0(\sigma_{hy}=0)+B\times\sigma_{hy}$ – for steady state swelling rate

where $\Delta V/V_0$ – stress free volume change, σ_{hy} – hydrostatic stress, $\sigma_{hy}=1/3(\sigma_1+\sigma_2+\sigma_3)=1/2\sigma_\theta$

$\sigma_{1,2,3}$ – axial, σ_θ – shear stresses, A and B – material constants.

Mechanisms of stress influence on swelling

- Stress accelerate processes of microstructural evolution-influence on diffusion, dislocation structure evolution and microchemical changes.
- Stress influence is much more effective at high irradiation temperatures.

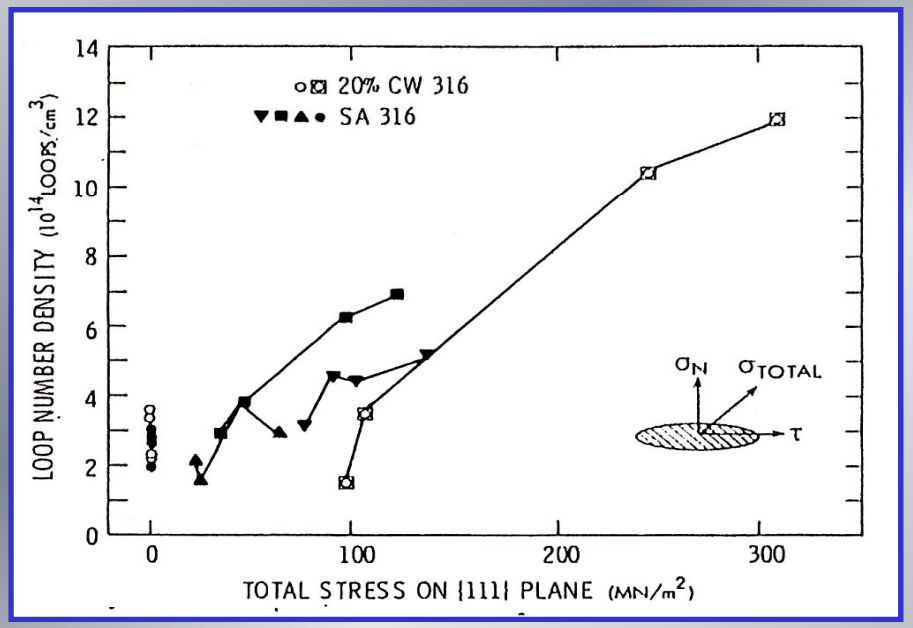

Stress enhances Frank loops number density on close-packed planes and accelerate network formation (EBR-II, 500^{0}C, 15 dpa [Brager, 1977]

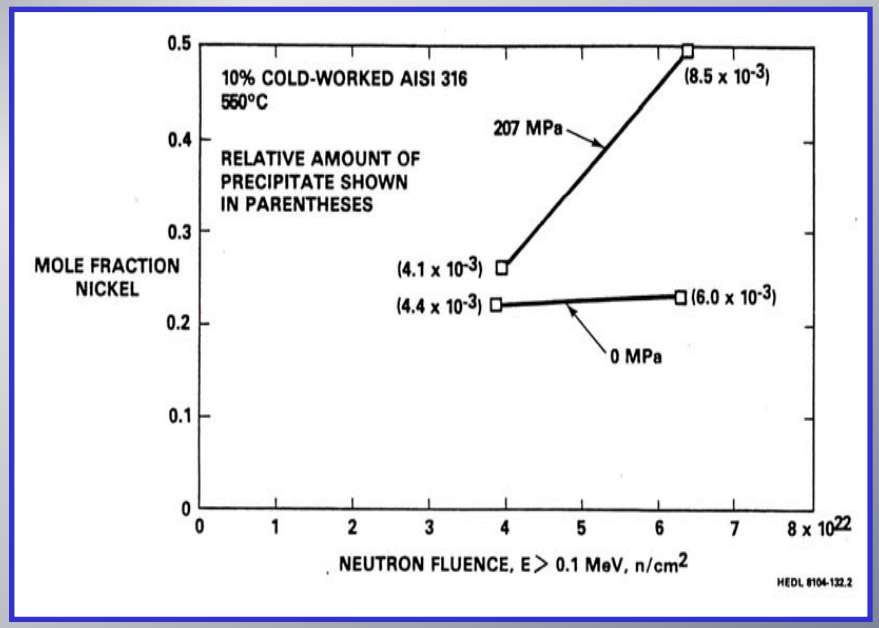

Effect of stress on nickel segregation in AISI 316. Stress provoke a more intensive nickel removing from matrix and precipitation (EBR-II, T_{irr}=550^{0}C) [Garner, 1982]

Dependence of nickel swelling on damaging dose at different temperature regimes

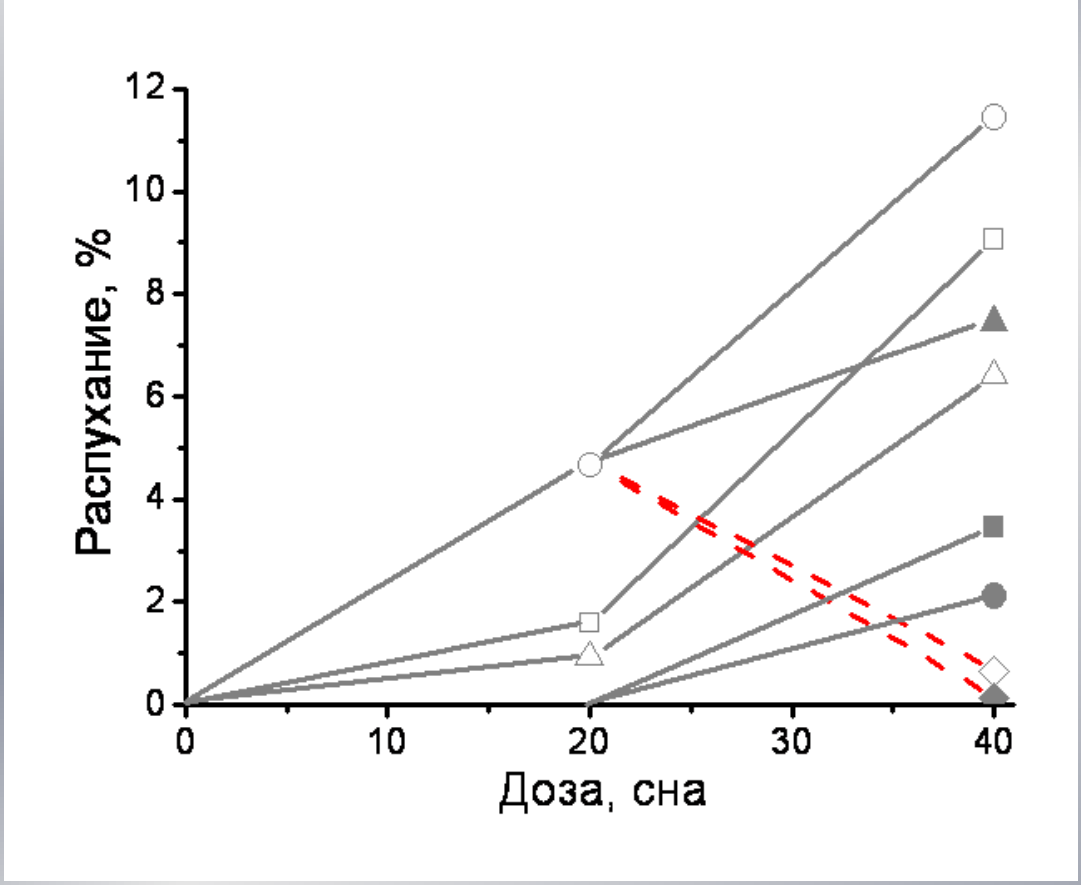

○ - 550–450°C
● - 50–550°C
□ - 450–550°C
■ - 300–550°C
△ - 650–550°C
▲ - 550–650°C
◊ - 550–300°C
◆ - 550–50°C

Lebedev S.Ya., Panin S.D., Rudnev S.I. Influence of variable temperature regime of irradiation on void formation in nickel// VANT. Ser.PhRD and RMS. – 1980. –Issue 3.-p.30-33

Temperature history influence on swelling

Temperature change in reactor core components-result of temperature excursions during power transient or scheduled relocations of fuel subassemblies, fuel burn up. Start up and shut down are especially important. A complex relationship exists between the peak swelling rate temperature, the nature of temperature change(increase or decrease from initial temperature) and the metallurgical conditions of the alloy.

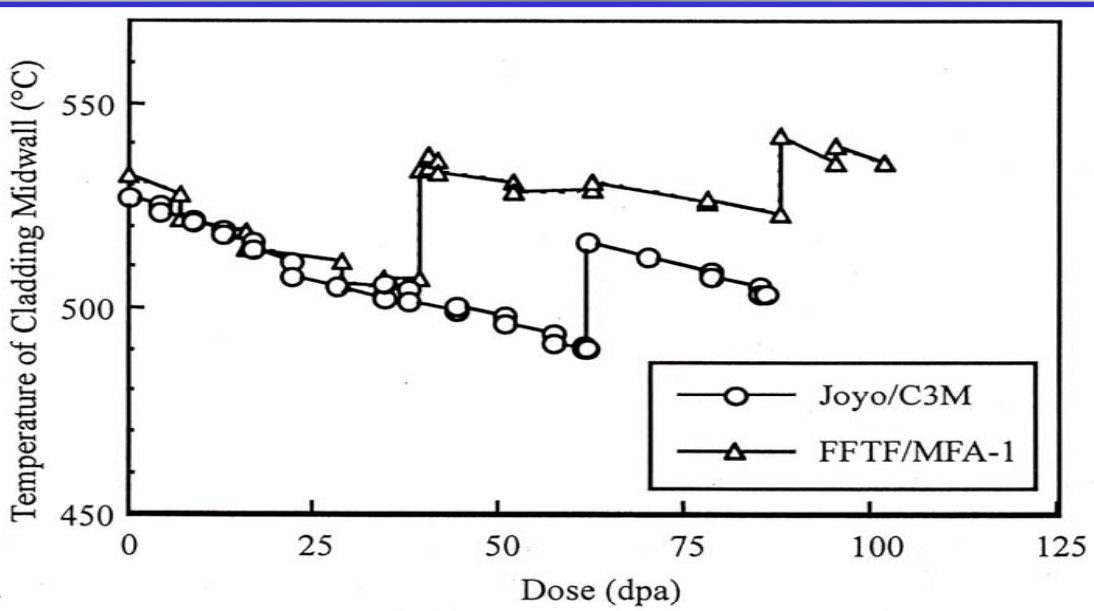

The microstructural evolution of cladding irradiated with temperature decreases is similar to the microstructural evolution of sample which has low dislocation density.It can effect void nucleation and in influence swelling level at this samples.

Temperature history of cladding due to gradually decreasing with burning of MOX fuel [Akasaka, 2001].

BR-5 (chanal tube steel 18Cr9NiTi) 1 – 300…400^{0}C, 2 – 400...450^{0}C, 3 - exploitation at 450…500^{0}C (Sw=0.1%)
Typically Sw of steel 18Cr9NiTi at 460^{0}C, 40 dpa ~12%.
First stage low temperature irradiation is equal to influence of CW deformation and swelling supress.

Effect of temperature history on segregation and precipitates behaviour

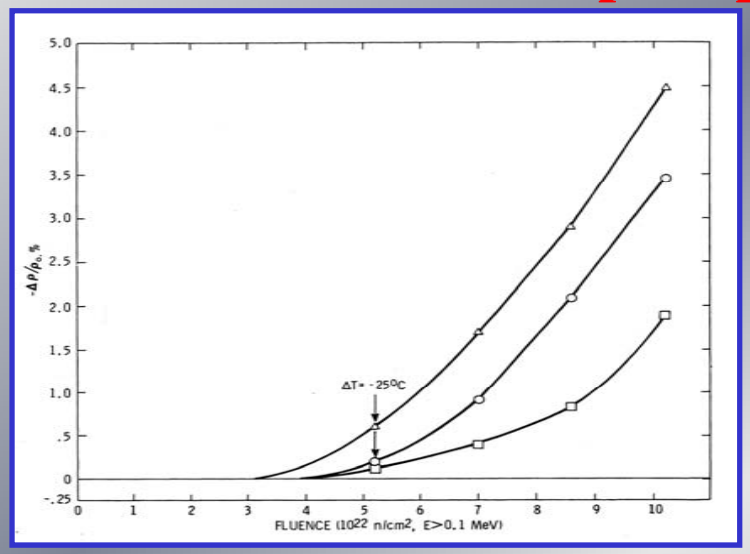

Swelling-fluence relationship for specimens of AISI 316 10% CW undergoing a - 25°C temperature change (EBR-II) [Bates, 1981]

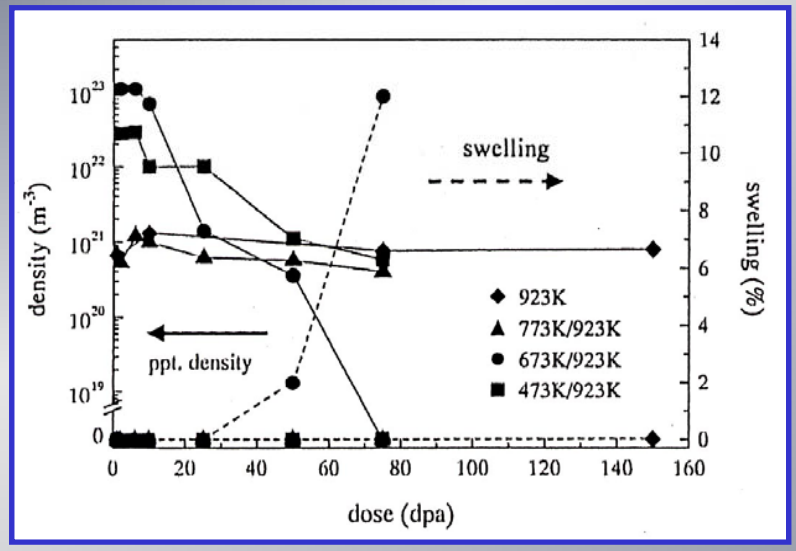

Phosphide density and swelling at temperature changes (Fe-Cr-Ni+P alloy, 2.4MeVCu) [Watanabe, 1999]

The temperature change data always lie above the isothermal results of both the starting and final temperature. Typically Ni segregate at high T, Si - at low T. Changing of temperature provide a conditions for simultaneous segregation of Ni and Si and possible γ′-phase formation. It change diffusion parameters of vacancies and leads to more easy voids formation.

Temperature changes under irradiation (673/923K) leads to phosphides instability (under constant temperature they exist up to higher doses), formation of dislocation loops system and swelling increasing compare with irradiation at constant temperature.

Average swelling rates measured in Russian F/M steel EP-450

Dvoriashin, Porollo, Konobeev and Garner, ICFRM-11

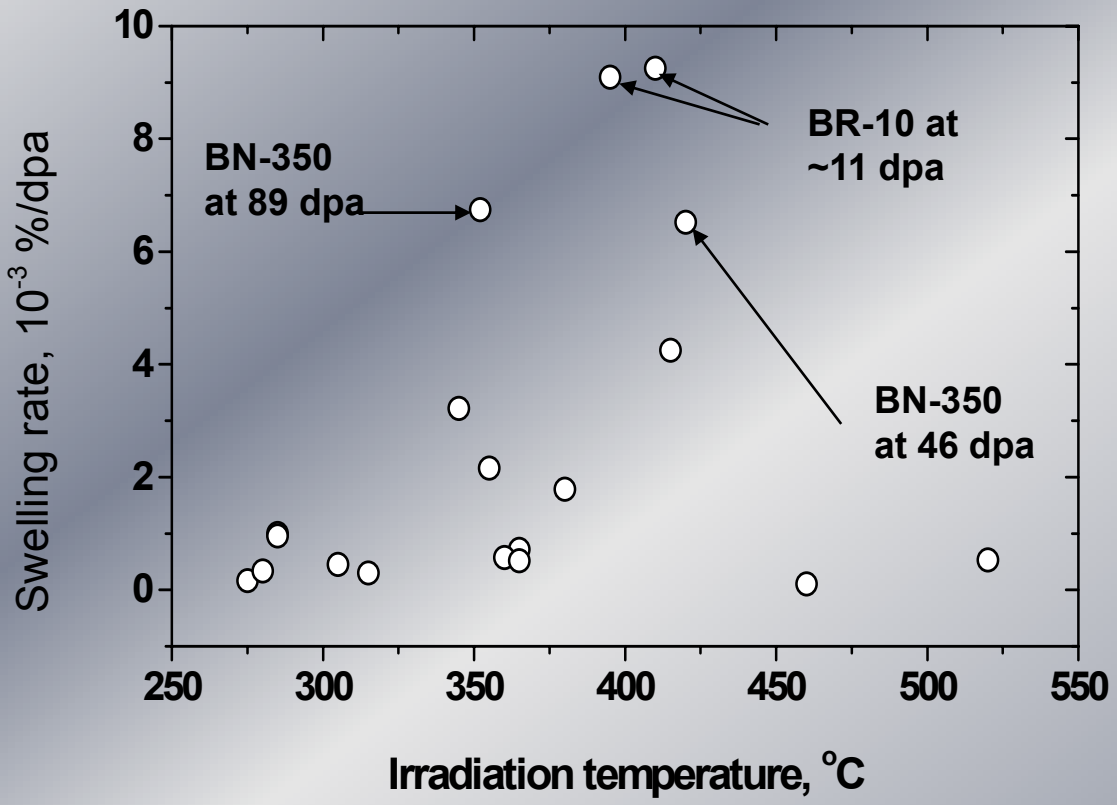

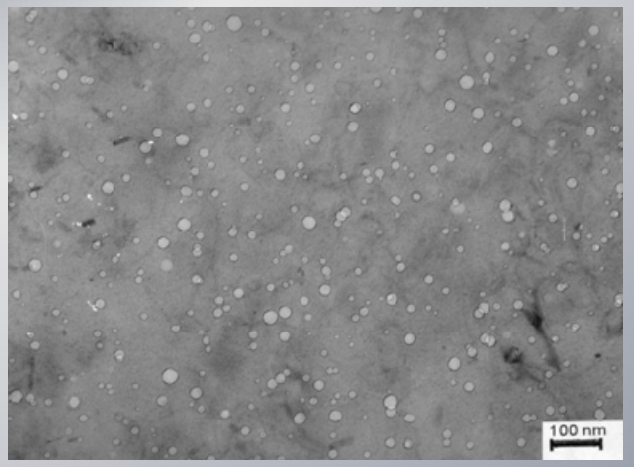

89 dpa, 352ºC

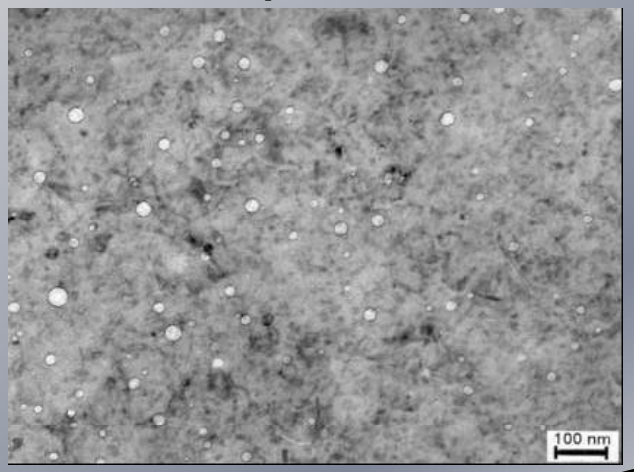

46 dpa, 420ºC

dpa rate in BR-10: 7×10^{-8} dpa/sec

dpa rate in BN-350: $1\text{-}2 \times 10^{-6}$ dpa/sec

Swelling is accelerated at lower dpa rates

Effect of neutron spectra on properties of construction steels can be more complicated!

- The dpa concept is valid for comparison of data from various spectral environments only if no other process is acting strongly.
- Transmutation is a process that is very sensitive to neutron spectra. Some materials of interest will transmute strongly.
- Ni, Mn, Cu, B, W and Re are good examples.
- If the transmutant affects the property of interest, the use of dpa is insufficient by itself to correlate data.
- For most purposes, stainless steels and ferritic-martensitic steels are relatively insensitive to transmutation, except for He, H, Mn, and V.

Sources of helium and of hydrogen

Sources of helium and hydrogen in nuclear reactors are the nuclear reactions in nickel containing materials under neutron influence:

$$\left.\begin{array}{l} {}^{58}_{28}Ni + {}^{1}_{0}n \rightarrow {}^{59}_{28}Ni \\ {}^{59}_{28}Ni + {}^{1}_{0}n \rightarrow {}^{4}_{2}He + {}^{56}_{26}Fe \end{array}\right\} \left(E < 0.1MeV\right)$$

$${}^{58}_{28}Ni + {}^{1}_{0}n \rightarrow {}^{4}_{2}He + {}^{55}_{26}Fe \quad \left(E > 0.1MeV\right)$$

$${}^{59}_{28}Ni + {}^{1}_{0}n \rightarrow {}^{1}_{1}H + {}^{59}_{27}Co \quad \left(E < 0.1MeV\right)$$

$${}^{58}_{28}Ni + {}^{1}_{0}n \rightarrow {}^{1}_{1}H + {}^{58}_{27}Co \quad \left(E > 0.1MeV\right)$$

$$3Fe + 4H_2O \rightarrow Fe_3O_4 + 4H_2 + 1.7kJ$$ - ***reaction of corrosion***

Concentration of clusters and atoms of helium in the core of reactor WWER-1000

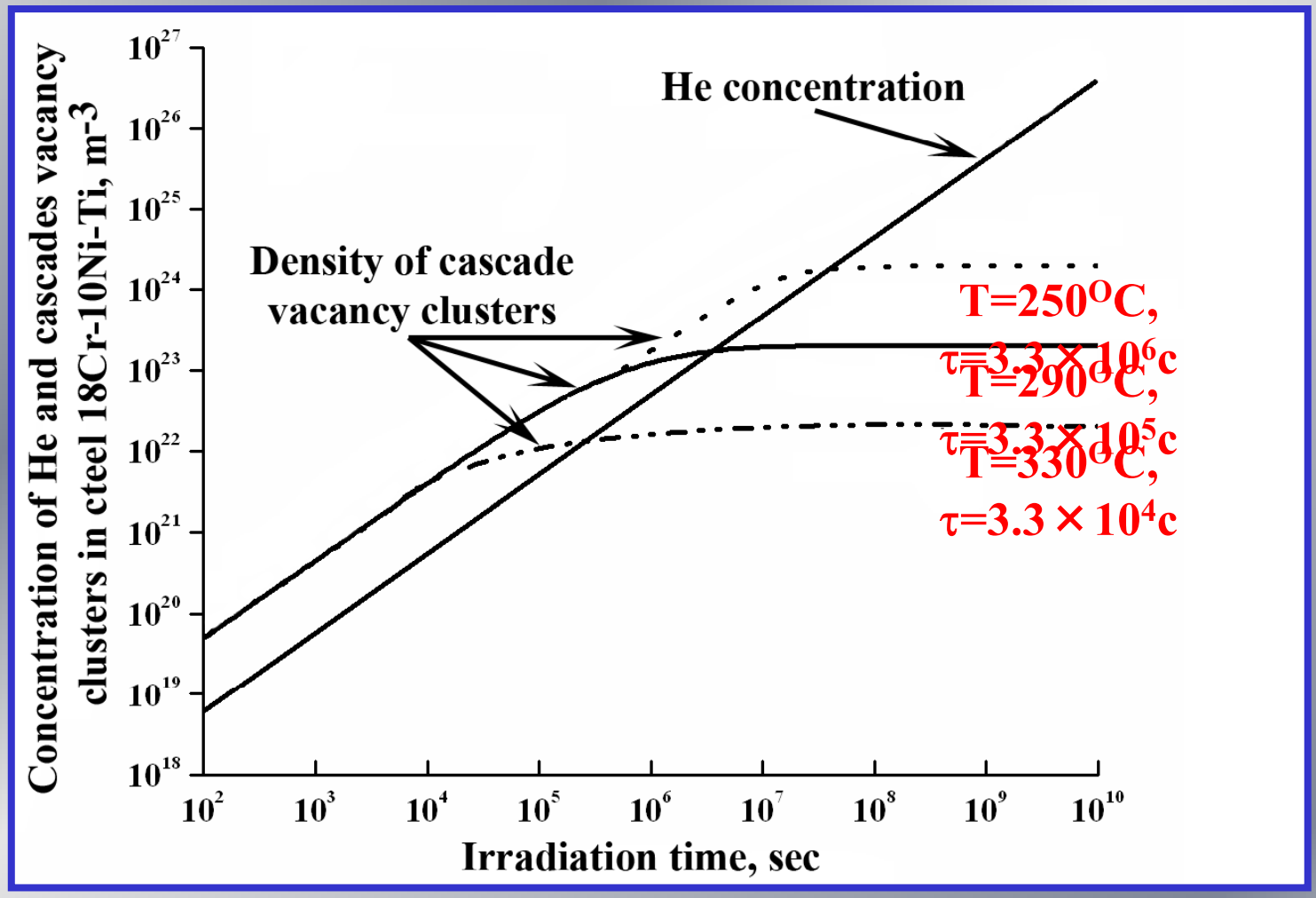

Vacancy clusters life time increases with increase of He atoms in his cluster.

Burn-up of Mn and its generation in nuclear reactions of transmutation in the core of reactor WWER-1000 in structure produced from steel 18Cr-10Ni-Ti

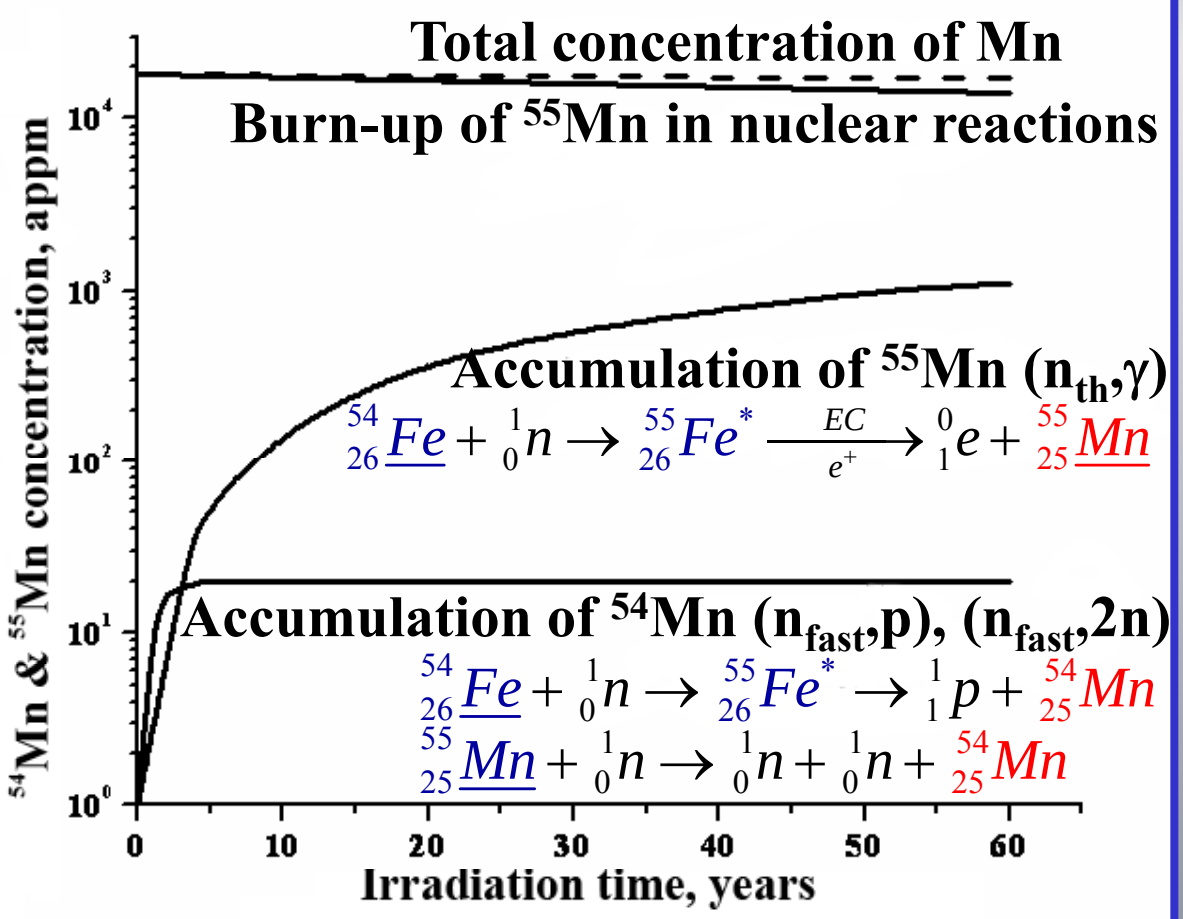

The general concentration of manganese decreases as a result of transmutation reactions.

Mn generated from nuclear reaction does not come into the matrix but is situated in the interstitial space and influences on the microstructural evolution.

Joint influence of helium and deuterium on the processes of accumulation and release of gaseous transmutants in materials of PVI of nuclear reactors

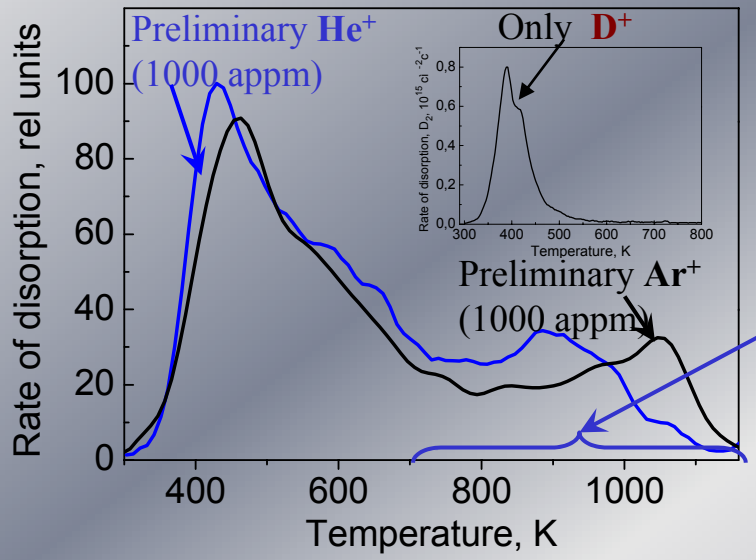

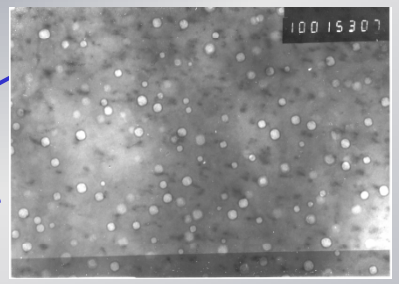

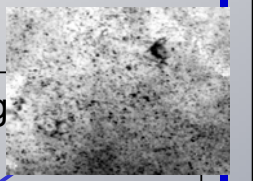

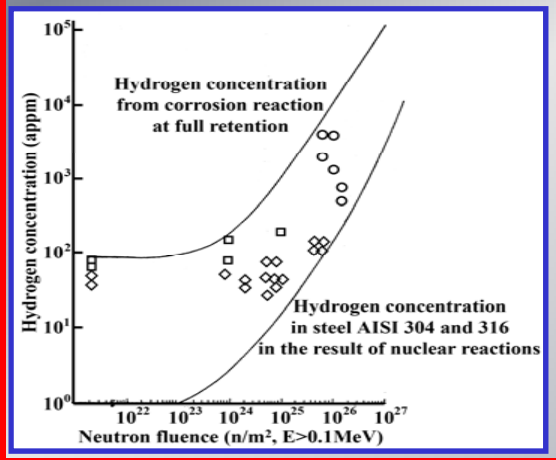

-One order increase of trapped hydrogen and broadening of temperature range of its release from structure materials on structures of radiation origin produced under irradiation with ions of inert gases (helium, argon)

-At damage higher 1 dpa accumulation of deuterium decreases at increase of titanium concentration.

Parameters of porosity in steel 18Cr-10N-iTi irradiated by different ions at T_{irr}=600 ^{o}C

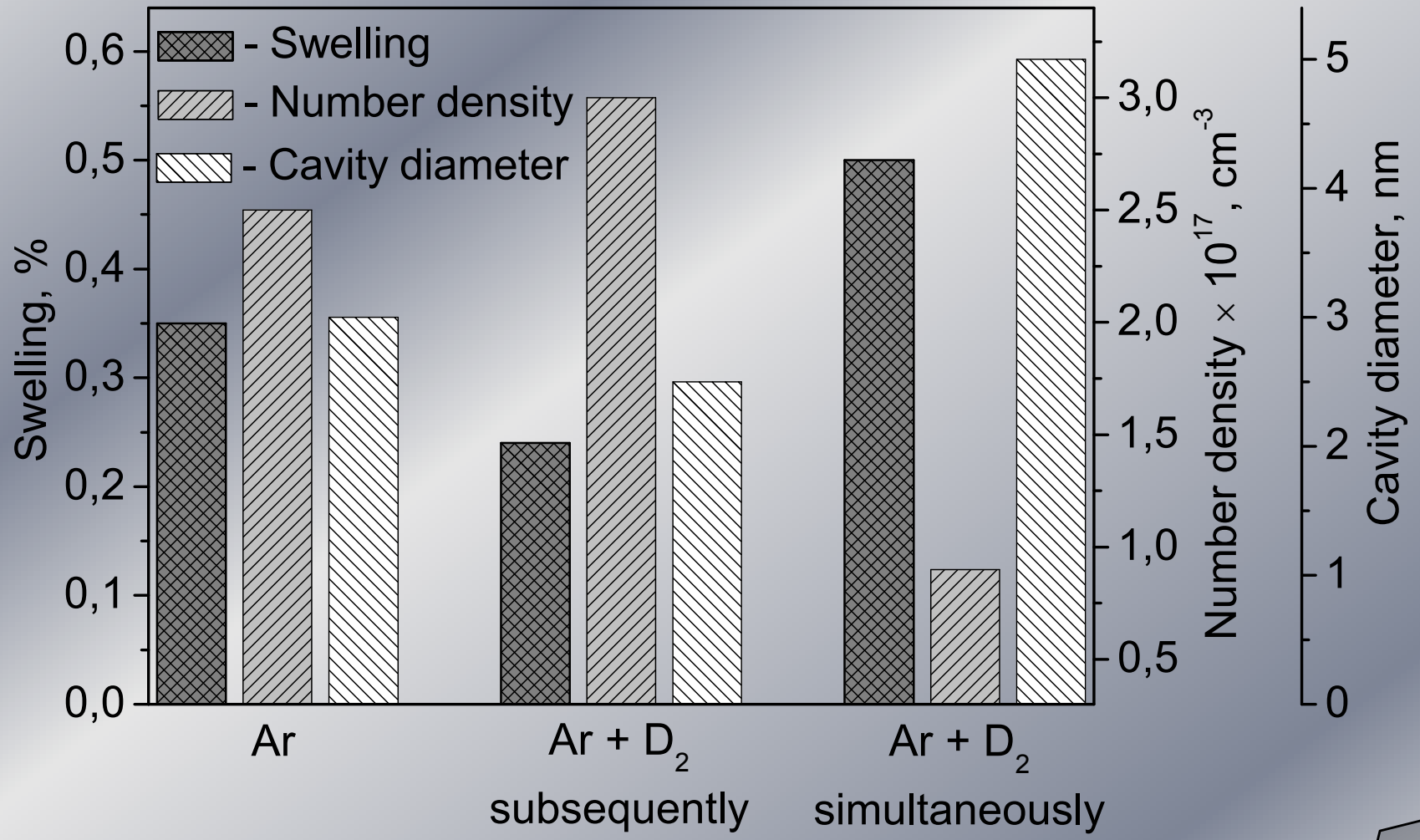

Influence of ion implanted helium on capture of deuterium in steel 18Cr10NiTi

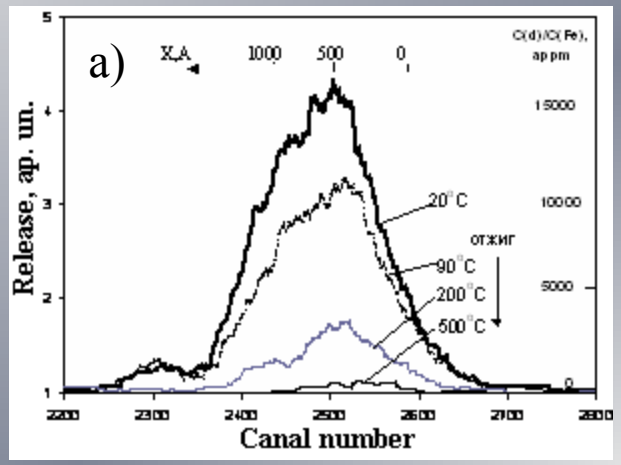

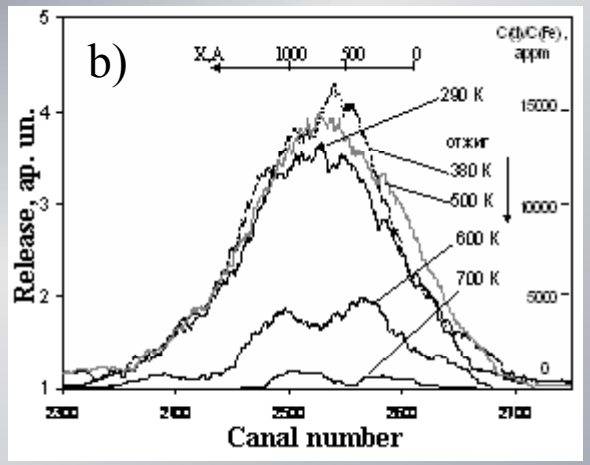

Profiles of deuterium distribution implanted at T to the dose 1.10^{16}cm^{-2} and after annealing in specimen with preliminary implanted to dose 5.10^{15}cm^{-2} (a) and 5.10^{14}cm^{-2} (b) helium

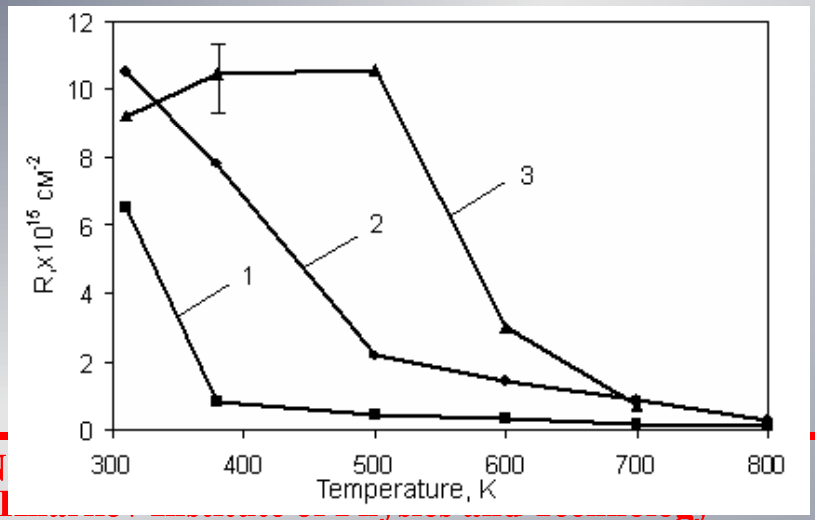

Quantity of deuterium retained in steel 18Cr10NiTi implanted to dose 1.10^{16}cm^{-2} without helium (1) and with preliminary implanted helium to dose 5.10^{15}cm^{-2} (2) and 5.10^{16}cm^{-2} (3)

Influence of helium on deuterium retention in steel 18Cr10NiTi and displacement of the curve of gas release towards high temperatures

He+D

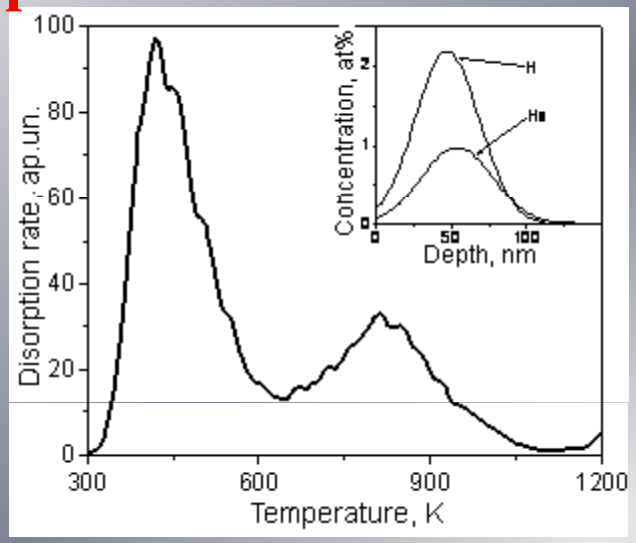

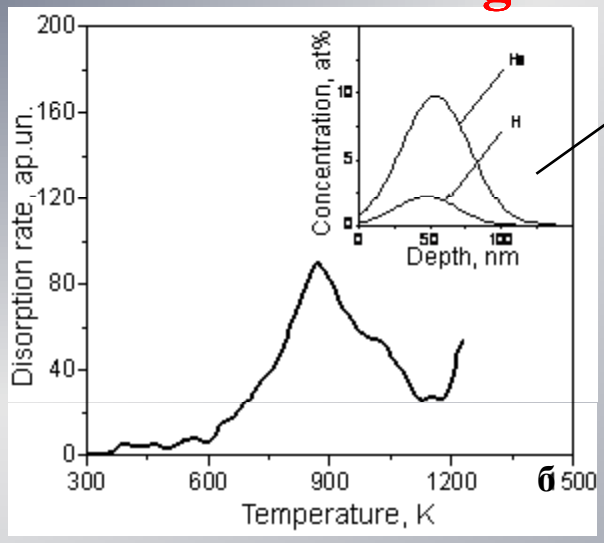

Insertions illustrate the relationship of profiles of helium and of hydrogen (SRIM)

Spectra of hydrogen thermal desorption from steel 18Cr10NiTi irradiated by ions of H_2^+ at T=300 K to the dose $1.10^{16}H^+/cm^2$ after preliminary implantation of helium to dose $5.10^{15}He^+/cm^2$ (a) and $5.10^{16}He^+cm^2$ (b). Heating rate 4°/s

D

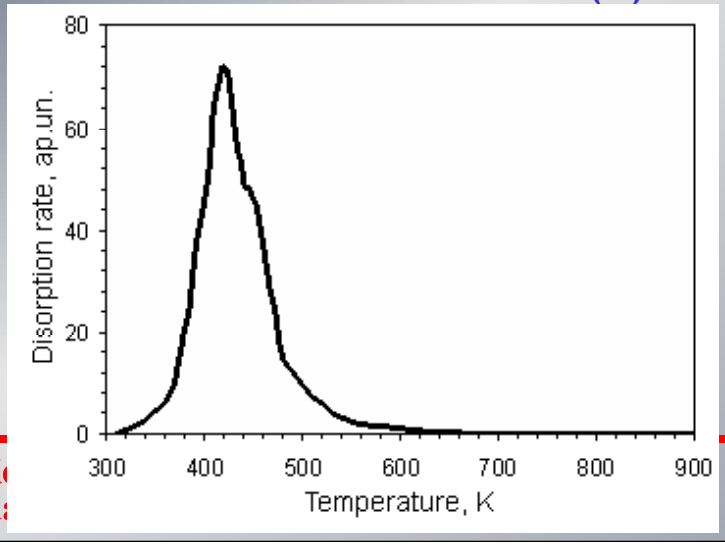

Spectrum of thermal desorption of deuterium from steel 18Cr10NiTi irradiated by ions of D_2^+ at T=300K to dose $1.10^{16}D^+/cm^2$. Rate of heating 4°/s

Mechanisms of deuterium retention in steel 18Cr10NiTi on helium bubbles

Steel microstructure development in steel under irradiation by ions of helium and hydrogen and post implantation annealing

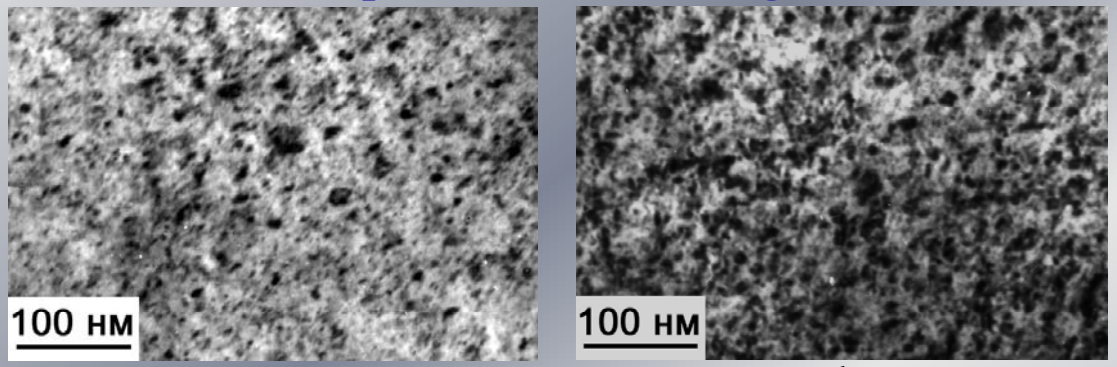

a b

Microstructure of steel 18Cr10NiTi irradiated by helium ions with energy 12 KeV at T_{irr} up to the dose $5.10^{15}cm^{-2}$ (a) and $5.10^{16}cm^{-2}$ (b)

Helium thermal desorption

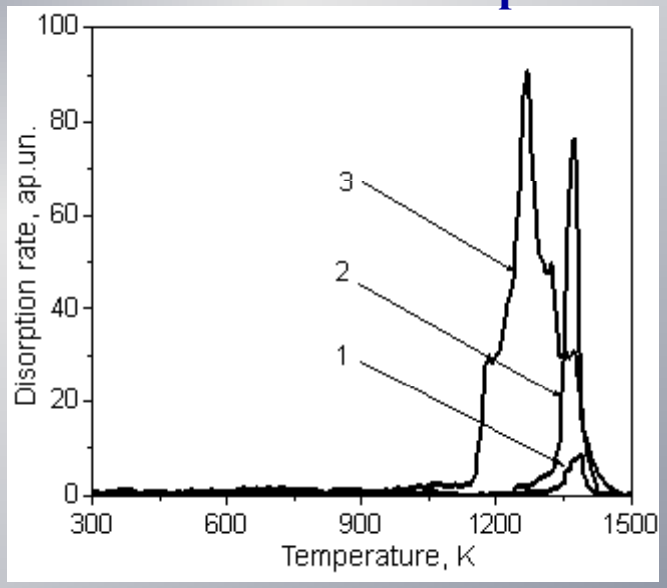

Dose dependence of helium release from steel 18Cr10NiTi irradiated by ions of He^+ at T=290 K up to the doses 5.10^{14} (1), 5.10^{15} (2) and 5.10^{16} (3) ions/cm^2. Rate of heating 4°/s

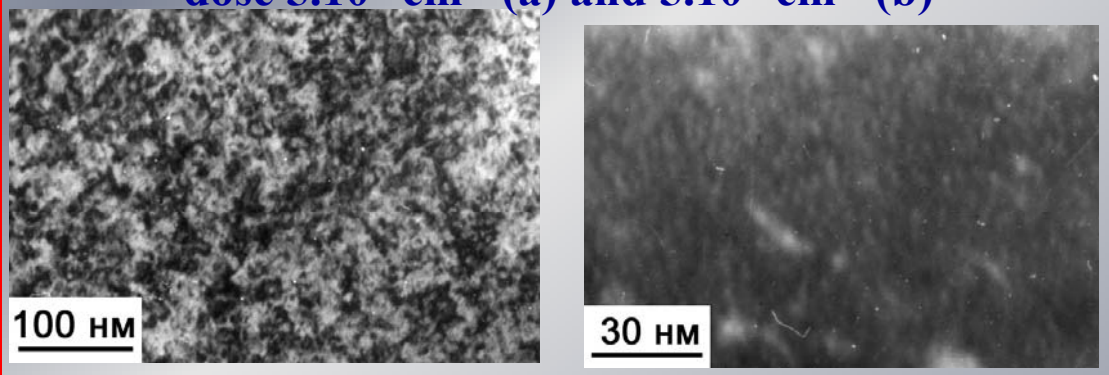

a b

Microstructure of steel 18Cr10NiTi after irradiation at T by helium ions up to the dose $5.10^{15}cm^{-2}$ (a) and $5.10^{16}cm^{-2}$ (b) and by hydrogen ions up to the dose $1.10^{16}cm^{-2}$ and subsequent annealing at 600 K.

Degradation of physical-mechanical properties of materials under irradiation
O.V. Borodin, V.V. Bryk, A.S. Kalchenko, G.D. Tolstolutskaya, V.N. Voyevodin

Radiation effects

Helium

$$\left.\begin{array}{l} {}^{58}_{28}Ni + {}^{1}_{0}n \rightarrow {}^{59}_{28}Ni \\ {}^{59}_{28}Ni + {}^{1}_{0}n \rightarrow {}^{4}_{2}He + {}^{56}_{26}Fe \end{array}\right\} (E < 0.1MeV)$$

$${}^{58}_{28}Ni + {}^{1}_{0}n \rightarrow {}^{4}_{2}He + {}^{55}_{26}Fe\,(E > 0.1MeV)$$

Hydrogen

$${}^{59}_{28}Ni + {}^{1}_{0}n \rightarrow {}^{1}_{1}H + {}^{59}_{27}Co\,(E < 0.1MeV)$$

$${}^{58}_{28}Ni + {}^{1}_{0}n \rightarrow {}^{1}_{1}H + {}^{58}_{27}Co\,(E > 0.1MeV)$$

$$3Fe + 4H_2O \rightarrow Fe_3O_4 + 4H_2 + 1.7kJ$$

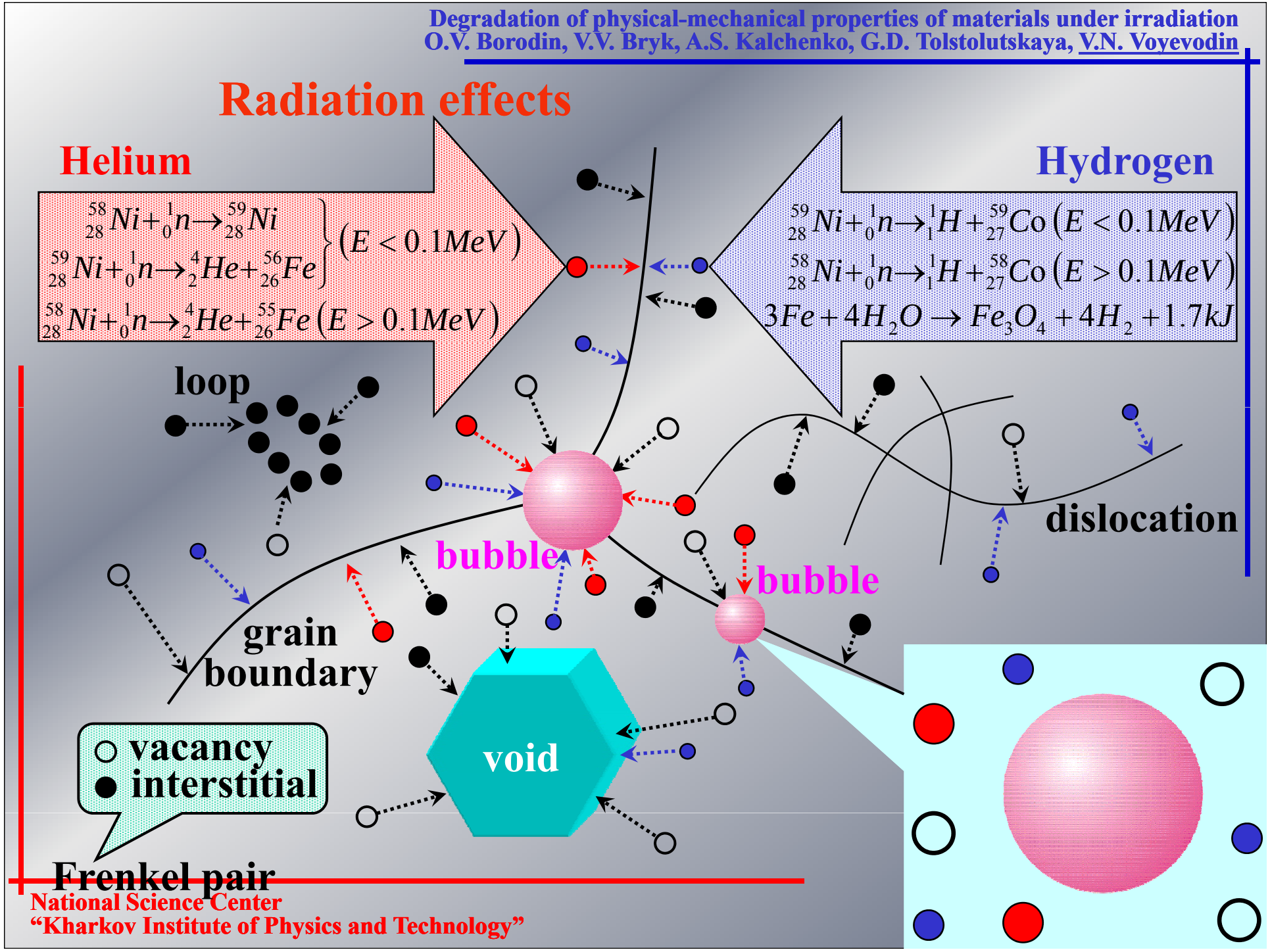

National Science Center
"Kharkov Institute of Physics and Technology"

Degradation of physical-mechanical properties of materials under irradiation
O.V. Borodin, V.V. Bryk, A.S. Kalchenko, G.D. Tolstolutskaya, V.N. Voyevodin

Radiation effects

Helium

$$\left.\begin{array}{l} {}^{58}_{28}Ni + {}^{1}_{0}n \rightarrow {}^{59}_{28}Ni \\ {}^{59}_{28}Ni + {}^{1}_{0}n \rightarrow {}^{4}_{2}He + {}^{56}_{26}Fe \end{array}\right\} (E < 0.1MeV)$$

$${}^{58}_{28}Ni + {}^{1}_{0}n \rightarrow {}^{4}_{2}He + {}^{55}_{26}Fe\,(E > 0.1MeV)$$

Hydrogen

$${}^{59}_{28}Ni + {}^{1}_{0}n \rightarrow {}^{1}_{1}H + {}^{59}_{27}Co\,(E < 0.1MeV)$$

$${}^{58}_{28}Ni + {}^{1}_{0}n \rightarrow {}^{1}_{1}H + {}^{58}_{27}Co\,(E > 0.1MeV)$$

$$3Fe + 4H_2O \rightarrow Fe_3O_4 + 4H_2 + 1.7kJ$$

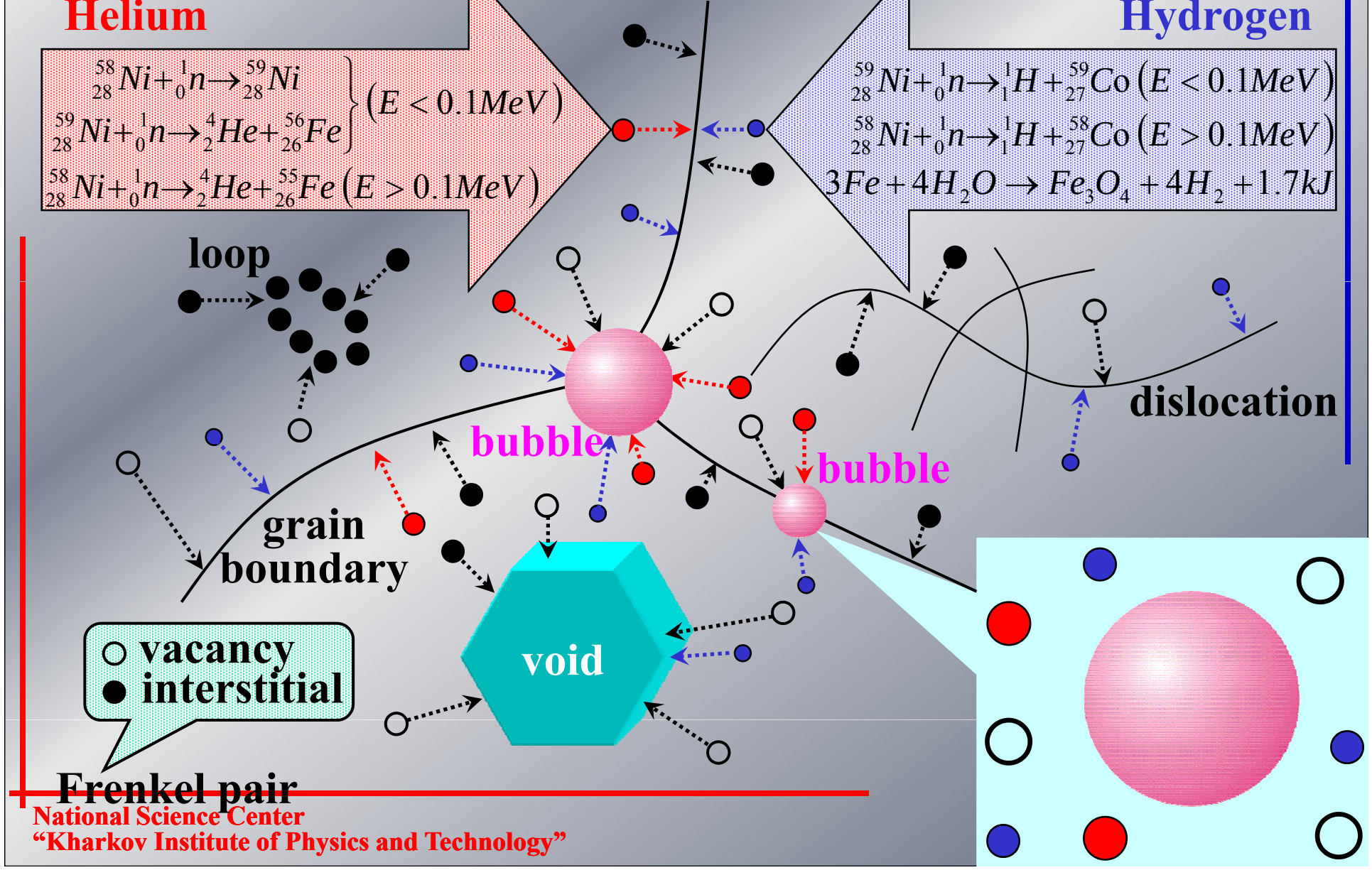

National Science Center
"Kharkov Institute of Physics and Technology"

Phase transformation at "spallation" irradiation in alloy AI 5052 (Al-3%Mg) (J.Stubbins,V.Voyevodin.unpublished work

Unirradiated

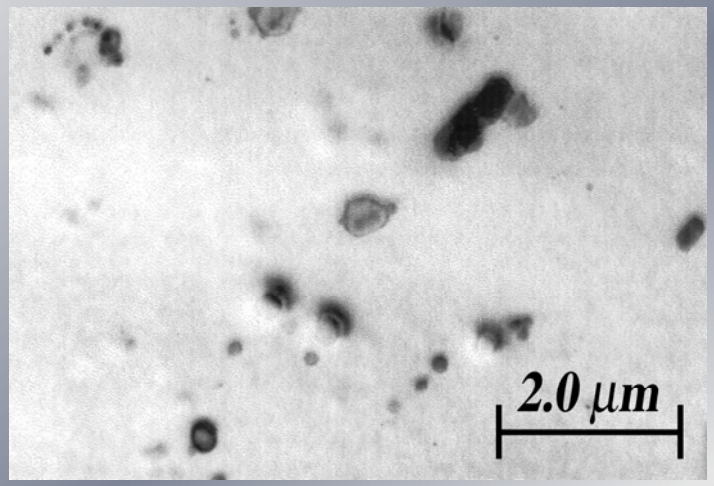

Irradiated

LASREF (D=0.35dpa, $T_{irr}=55^0C$)

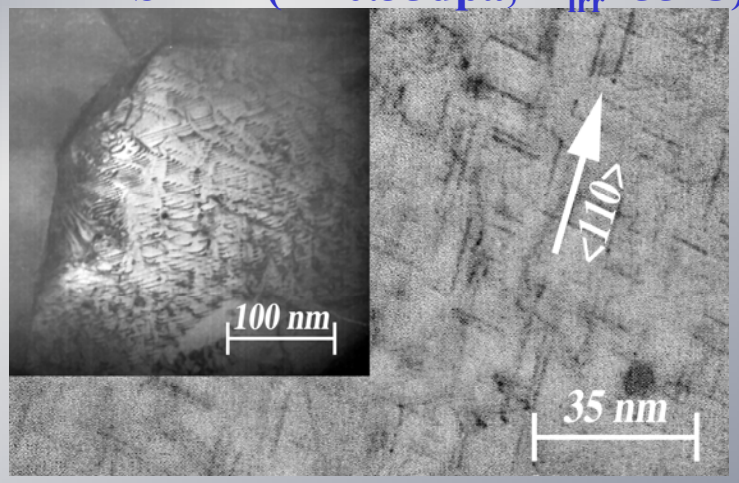

$^{27}Al\ (n,\gamma) \rightarrow ^{28}Al\ \ Al \rightarrow ^{28}Si + \beta$

$2\ Mg + Si \rightarrow Mg_2Si$

Homologous temperatures of physical-mechanical properties manifestation for austenitic (solid line), of martensitic stainless steels (dotted line).

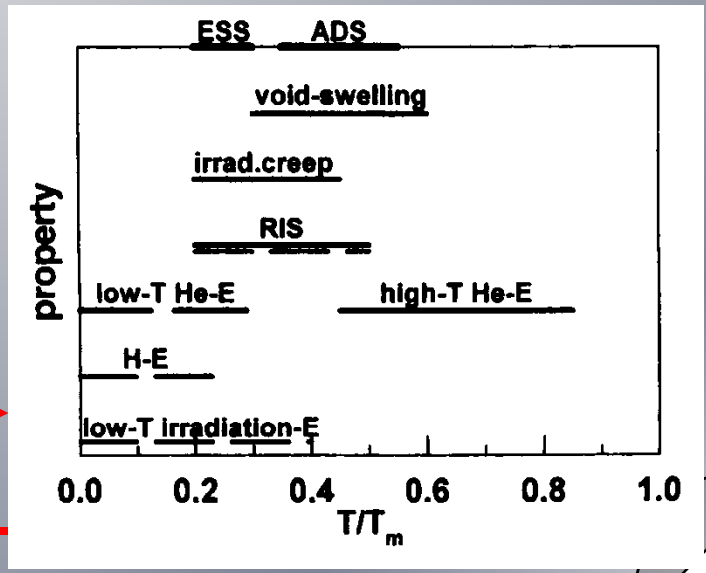

Structural Evolution During Irradiation

ODS Martensitic Steel (M93)

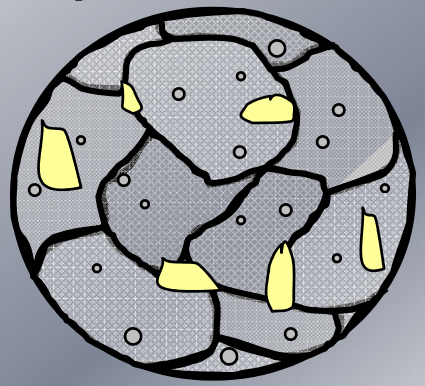

$M_{23}C_6$

Oxide Particle

Grain with a high dislocation density (network dislocation)

MC or M_2C

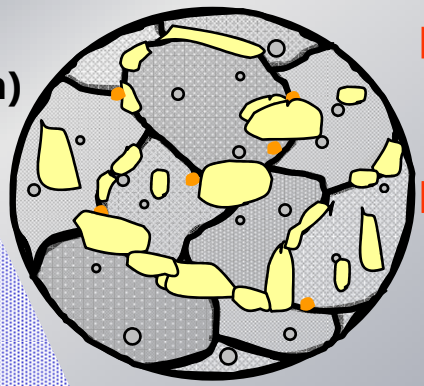

■ Low Temp. Irrad.
- Coarsening of $M_{23}C_6$

■ High Temp. Irrad.
- Coarsening of $M_{23}C_6$
- Formation of M_2C / MC

Neutron Irradiation
(Irradiation Effect + Thermal Aging Effect)

ODS Ferritic Steel (F94, F95)

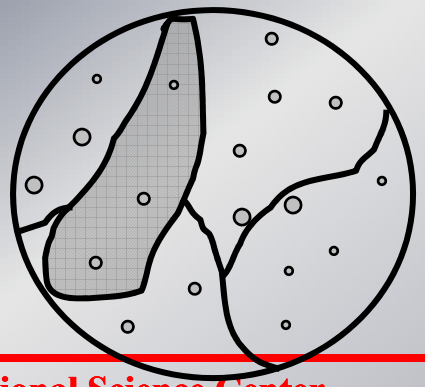

M_6C

Line dislocation

- Dislocation formation in recrystallized grain
- M_6C formation at G.B.
- Small amount of $M_{23}C_6$ formation at G.B.

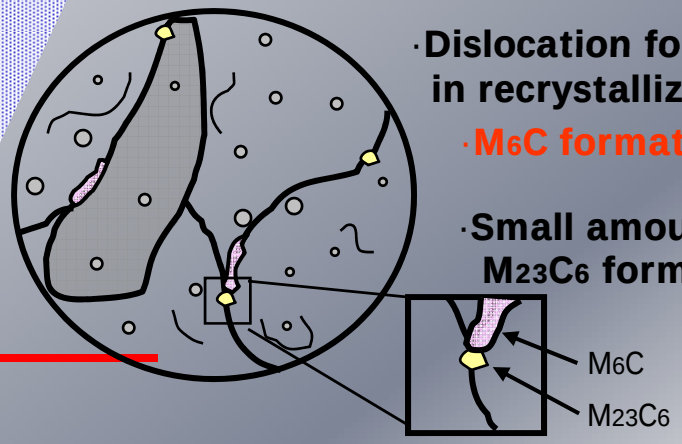

Grain with a low dislocation density

Summary to lecture 3.

- loss of radiation stability with changes in their structure and composition under irradiation. Changing and degradation of original physical-mechanical properties of materials during irradiation (particular, void swelling) are result of evolution of complicated structure-phase transformations.
- Possibility of the use of materials in nuclear power plants is determined by real conditions of irradiation – by energy spectrum of neutrons, by temperature of irradiation etc, because just these conditions determine the dynamical behavior of agglomerates of point defects and transmutants responsible for the mechanisms of degradation and dimensional instability.
- The key question of evolution of radiation-induced microstructure is the difference in the absorption of interstitial atoms and vacancies on different sinks, that causes the cooperative development of all microstructure components in irradiated material. There is the obvious relation between structure-phase state of irradiated material and its radiation resistance.